

2016

Distributed approaches for solving non-convex optimizations under strong duality

Xu Ma

Iowa State University

Follow this and additional works at: <https://lib.dr.iastate.edu/etd>

 Part of the [Electrical and Electronics Commons](#)

Recommended Citation

Ma, Xu, "Distributed approaches for solving non-convex optimizations under strong duality" (2016). *Graduate Theses and Dissertations*. 15769.

<https://lib.dr.iastate.edu/etd/15769>

This Dissertation is brought to you for free and open access by the Iowa State University Capstones, Theses and Dissertations at Iowa State University Digital Repository. It has been accepted for inclusion in Graduate Theses and Dissertations by an authorized administrator of Iowa State University Digital Repository. For more information, please contact digirep@iastate.edu.

Distributed approaches for solving non-convex optimizations under strong duality

by

Xu Ma

A dissertation submitted to the graduate faculty
in partial fulfillment of the requirements for the degree of
DOCTOR OF PHILOSOPHY

Major: Electrical Engineering

Program of Study Committee:

Nicola Elia, Major Professor

Wolfgang H. Kliemann

Umesh Vaidya

Venkataramana Ajarapu

Degang Chen

Iowa State University

Ames, Iowa

2016

Copyright © Xu Ma, 2016. All rights reserved.

DEDICATION

I would like to dedicate this dissertation to my beloved parents.

TABLE OF CONTENTS

LIST OF TABLES	vii
LIST OF FIGURES	viii
ACKNOWLEDGEMENTS	ix
ABSTRACT	x
CHAPTER 1. OVERVIEW	1
1.1 Introduction	1
1.1.1 The Continuous-Time Optimization Dynamics	2
1.1.2 A Control Perspective for the Optimization Dynamical System	4
1.1.3 Motivations for the Continuous-Time Optimization Dynamics	4
1.1.4 The Optimal Power Flow Problem	6
1.2 Organization of This Dissertation	8
1.3 The Main Contributions	10
CHAPTER 2. PRELIMINARIES	13
2.1 Notations	13
2.2 Basics Concepts in Graph Theory	13
2.3 Constrained Optimizations	15
2.4 Sum of Squares Relaxations	17
2.5 Continuous-Time Dynamical Systems	18
CHAPTER 3. THE CONTINUOUS-TIME OPTIMIZATION DYNAMICS .	21
3.1 Definition of the Optimization Dynamics	22
3.2 A Local Convergence Result	23

3.3	The Convergence Proof	23
3.3.1	Initialization	25
3.3.2	The R-S-T Systems	25
3.3.3	Existence and Uniqueness of the Solution	30
3.3.4	Locally Asymptotic Stability	30
3.4	Summary	31
CHAPTER 4. THE NON-CONVEX QCQP PROBLEMS		32
4.1	Global Optimality Conditions	33
4.2	Relations to the Convex Relaxations	36
4.2.1	The Lagrange Dual Relaxation	36
4.2.2	The SDP Relaxation	37
4.2.3	Relations to the Global Optimality Conditions	38
4.3	Issues in the Application of Traditional Primal-Dual Algorithms	39
4.3.1	The Sub-Gradient Method	40
4.3.2	The ADMM Algorithm	41
4.4	The Associated Optimization Dynamics	42
4.4.1	Convergence Analysis	42
4.4.2	Global Convergence Analysis for Equality-Constrained QCQPs	43
4.5	Partitioning and MAXCUT Problems	47
4.5.1	The Two-Way Partitioning Problem	47
4.5.2	The MAXCUT Problem	47
4.5.3	A MAXCUT Example	48
4.6	Phase Recovery Problems	51
4.6.1	Problem Formulation	51
4.6.2	The Augmented Lagrangian and Associated Optimization Dynamics	52
4.6.3	Simulations	54
4.7	The Convex SOCPs	56
4.7.1	Problem Formulation	56
4.7.2	Strong Duality	58

4.7.3	The Associated Optimization Dynamics	60
4.7.4	Simulations	61
4.8	Summary	62
CHAPTER 5. OPTIMAL POWER FLOW PROBLEMS		63
5.1	Formulation of the OPF Problem	64
5.1.1	The Original OPF Problem	64
5.1.2	Infinite Solutions to the OPF Problem	67
5.1.3	The Modified OPF Problem	68
5.2	The Optimization Dynamics Approach	69
5.2.1	The Associated Optimization Dynamics	69
5.2.2	A Distributed OPF Structure	70
5.3	A Sufficient Characterization for Global Optimality	73
5.4	Comparisons with the SDP Dual Relaxation Approach	75
5.4.1	The SDP Dual Relaxation Approach	75
5.4.2	Comparisons with the SDP Dual Relaxation	77
5.4.3	Two Three-Bus OPF Examples	78
5.5	Convergence Analysis	82
5.6	Simulation Results	84
5.7	Summary	85
CHAPTER 6. SOLVERS FOR THE OPTIMIZATION DYNAMICS		86
6.1	Explicit ODE Solvers	88
6.2	Simulations for Phase Recovery Problems	89
6.3	The Backward Euler ODE Solver	90
6.3.1	The Backward Euler's Method	90
6.3.2	Centralized Computing	93
6.3.3	Distributed Computing	94
6.4	Simulations for OPF Problems	95
6.5	Summary	100

CHAPTER 7. OPF PROBLEMS REVISITED: A CONSENSUS-BASED DECOMPOSED SDP RELAXATION APPROACH	101
7.1 Review of the SDP Relaxation	102
7.2 The Decomposed OPF Problem	103
7.3 The Decomposed SDP Relaxation Approach	106
7.4 Discussions on the Decomposed SDP Relaxation	108
7.4.1 The Problem Size	108
7.4.2 A Distributed Structure	109
7.4.3 Rank-One Solutions	109
7.5 Simulations	110
7.6 Summary	111
CHAPTER 8. CONCLUSIONS	113
APPENDIX PROOF OF THEOREM 24	115
BIBLIOGRAPHY	119

LIST OF TABLES

Table 5.1	Parameters of the three-bus power network	80
Table 5.2	Power demands of the three-bus OPF	80
Table 5.3	Generation costs of the three-bus OPF	80
Table 5.4	A global solution to the three-bus OPF with a line-flow limit 60 MVA	80
Table 5.5	A global solution to the three-bus OPF with a line-flow limit 52 MVA	80
Table 6.1	Power demands of the IEEE 14-bus OPF	98
Table 6.2	Generation costs and constraints of the IEEE 14-bus OPF	98
Table 6.3	A global solution to the IEEE 14-bus OPF	98
Table 6.4	Performance Comparisons on the IEEE 14-bus OPF	98
Table 7.1	Performance of the OPF solver proposed by Molzahn et al. (2013) . . .	110
Table 7.2	Performance of the OPF solver proposed by Madani et al. (2015) . . .	110
Table 7.3	Solving IEEE benchmark OPF tests via decomposed SDP relaxations .	112

LIST OF FIGURES

Figure 1.1	The block diagram of an optimization dynamical system	4
Figure 4.1	A five-node weighted graph	50
Figure 4.2	Convergence of the five-node MAXCUT example	50
Figure 4.3	A block diagram of the optimization dynamics associated with phase recovery	55
Figure 4.4	Convergence of a phase recovery example with $n = 256$ and $m = 2048$	56
Figure 4.5	Trajectories of the primal variables: in the left subfigure we show the convergence of optimization dynamics (4.40a) – (4.40d) associated with Example 3, whereas in the right one we show the convergence of optimization dynamics (4.41a) – (4.41c)	62
Figure 5.1	The equivalent Π model of a transmission line (k, l)	65
Figure 5.2	A four-bus power network	72
Figure 5.3	The Simulink implementation of the four-bus OPF	73
Figure 5.4	A three-bus power network	79
Figure 5.5	Convergence of the three-bus OPF with a line-flow limit 60 MVA	79
Figure 5.6	Convergence of the three-bus OPF with a line-flow limit 52 MVA	79
Figure 5.7	Convergence of the IEEE 57-bus OPF test case	85
Figure 6.1	A performance comparison between our explicit Euler method and the fast phase retrieval approach proposed by Netrapalli et al. (2015)	90
Figure 6.2	The IEEE 14-bus OPF solved by MATLAB ODE solver <code>ode15s</code>	99
Figure 6.3	The IEEE 14-bus OPF solved by our ODE solver with step size $T = 2s$	99

ACKNOWLEDGEMENTS

This research has been supported by NSF grant CNS-1239319.

I would like to express my sincere gratitude here to my advisor, Prof. Nicola Elia, for his continuous support for my Ph.D. study and research. His guidance and encouragement helped me all the time during my Ph.D. research. His immense knowledge and research style will also influence me profoundly on my future career.

Besides my advisor, I would like to thank the rest of my POS Committee: Prof. Wolfgang Kliemann, Prof. Umesh Vaidya, Prof. Venkataramana Ajjarapu, and Prof. Degang Chen, for their insightful comments which have widened my research from various perspectives.

Special thanks also go to my friends Chong Li, Matt Rich, Sambarta Dasgupta, Subhrajit Sinha, Sai Pushpak, Heng Wang, Zhao Song, Guangyuan Zhang, Shiyang Li, and Songtao Lu. I have spent a great time with all of you at Iowa State University.

Last but not least, I am so grateful to my parents for spiritually supporting me throughout my Ph.D. study. You both have sacrificed a lot during the years when I was away from home.

ABSTRACT

This dissertation studies *non-convex* optimizations under the strong duality condition. In general, non-convex problems are non-deterministic polynomial-time (NP) hard and hence are difficult to solve. However, when strong duality holds, one can recover primal optimal solutions by efficiently solving their convex, associated Lagrange dual relaxations instead.

For certain non-convex optimizations, such as optimal power flow (OPF), phase recovery, and etc., it has been shown that strong duality holds under most circumstances. Consequently, their associated Lagrange dual problems, usually expressed in semi-definite programming (SDP) forms, have attracted the attention of researchers. However, we notice that these SDP Lagrange duals are in general not amenable to be solved in a distributed manner. To address this issue, we propose two distributed approaches in this dissertation to study those non-convex optimizations under the condition of strong duality.

Our first approach is called the continuous-time optimization dynamics approach. Rather than considering the Lagrange dual alone, this approach studies the primal and dual problems together at the same time. By viewing primal and dual variables of an optimization problem as opponents playing a min-max game, the evolution of the optimization dynamical system can be interpreted as a competition between two players. This competition will not stop until those players achieve a balance, which turns out to be an equilibrium to the optimization dynamics and is mathematically characterized as a Karush-Kuhn-Tucker (KKT) point.

A convergence analysis is then developed in this dissertation, showing that under certain conditions a KKT equilibrium of the associated optimization dynamics is locally asymptotically stable. However, after the optimization dynamics converges to a KKT equilibrium, we have to further check whether or not the obtained KKT point is globally optimal, since KKT conditions are only necessary for the local optimality of non-convex problems. It motivates us to investigate under what conditions a KKT point can be guaranteed as a global optimum.

Then in the dissertation we derive a global optimality condition for general quadratically constrained quadratic programmings (QCQPs). If an isolated KKT point of a general QCQP satisfies our condition, then it is locally asymptotically stable with respect to the optimization dynamics. We next apply the optimization dynamics approach to a special class of non-convex QCQPs, namely, the OPF problems. We discover that their associated optimization dynamical systems possess an intrinsic distributed structure. Simulations are also provided to show the effectiveness of our continuous-time optimization dynamics approach.

Alternatively, we also propose a consensus-based, decomposed SDP relaxation approach to solve OPF problems. Here we continue to exploit the distributed structure of power networks, which finally enables us to decompose the standard SDP relaxation into a bunch of smaller size SDPs. Then each bus in the power network should locally solve its own decomposed SDP relaxation and meanwhile a global OPF solution can be achieved by running a consensus over the whole power network. Hence this approach can be implemented in a distributed manner. We show that the size of our decomposed SDP relaxation scales linearly as the power network expands, so it can greatly fasten the OPF computation speed.

CHAPTER 1. OVERVIEW

1.1 Introduction

In this dissertation we study *non-convex* optimizations under the condition of strong duality. Generally speaking, non-convex problems are non-deterministic polynomial-time (NP) hard and hence are difficult to solve. However, when strong duality holds, one can recover primal optimal solutions by efficiently solving their convex, associated Lagrange dual relaxations instead.

The existing works, e.g., [Candès et al. \(2011\)](#) and [Lavaei and Low \(2012\)](#), have respectively shown that strong duality condition holds for the non-convex phase recovery and optimal power flow (OPF) problems under most circumstances. Therefore, optimal solutions to these problems can be efficiently recovered from their associated Lagrange duals.

The Lagrange duals associated with above problems are usually expressed in semi-definite programming (SDP) forms. However, we notice that those SDPs are in general not amenable to be solved in a distributed manner, because the evaluation of the positive semi-definite cone requires centralized computing. When the problem size is large, such a centralized computation of an SDP may be cumbersome. To meet this challenge, this dissertation focuses on solving the non-convex optimizations with strong duality via distributed approaches.

One main topic of this dissertation is to utilize the so-called continuous-time optimization dynamics approach to solve non-convex optimizations under the strong duality condition. The optimization dynamics approach, rather than solving the Lagrange dual itself, considers both primal and dual problems together at the same time. Most importantly, we discover that if the original non-convex optimization has sparse coefficient matrices (see the OPF problem as an example), then the associated optimization dynamical system possesses a naturally distributed structure, i.e., each primal or dual variable uses a local information to make update decisions.

Besides the optimization dynamics, in this dissertation we also directly investigate the SDP duals associated with OPF problems and propose a distributed, decomposed SDP relaxation approach. By exploiting the same distributed structure of the OPF problem, we decompose its original large-size SDP Lagrange dual into a bunch of smaller SDPs, each of which can be solved locally and a global solution can be achieved via a consensus coordination. Consequently, this approach can be implemented in a distributed manner. A great advantage of this decomposed SDP relaxation is that its problem size scales nicely as the power network expands, and hence it can greatly fasten the OPF computation speed.

1.1.1 The Continuous-Time Optimization Dynamics

The optimization dynamics, also known as the primal-dual dynamics, was first proposed as a continuous-time primal-dual optimization algorithm by seminal works [Arrow and Hurwicz \(1958\)](#) and [Uzawa \(1958\)](#) for solving strictly convex problems.

Under mild constraint qualification assumptions, the global optimality of a convex problem can be equivalently characterized by Karush-Kuhn-Tucker (KKT) conditions. In other words, every KKT point is also a saddle-point (a pair of primal and dual optima) for the Lagrangian associated with the convex problem under study, and vice versa.

In these circumstances the optimization dynamics approach can be motivated for searching the KKT points, which turn out to be the equilibria of the associated optimization dynamical system. After the optimization dynamics has converged to some KKT point, we can recover a global solution for the convex problem under study from the obtained KKT point, due to its equivalence with the saddle-point for the associated Lagrangian.

By viewing the primal and dual variables as two players in a convex-concave game, the idea behind the optimization dynamics is quite natural: The primal player attempts to minimize the associated Lagrangian by moving against the gradient with respect to itself, while the dual player follows its own gradient direction hoping to maximize the associated Lagrangian. Such a competition stops when a balance between the two players is reached. This balance, which is mathematically characterized by KKT conditions, will be globally optimal for both players if the problem under study is convex.

In both works [Arrow and Hurwicz \(1958\)](#) and [Uzawa \(1958\)](#), it has been shown that the optimization dynamics approach can be successfully applied to solve strictly convex problems. As for those non-strictly convex problems, say, linear programmings (LPs) for instance, we can give counterexamples showing that the associated optimization dynamics may oscillate and does not converge to any equilibrium at all. In these cases, one can still find global solutions by applying the optimization dynamics that is derived instead from the augmented Lagrangian.

Let us present an example illustrating how to define the optimization dynamical system. Consider an equality constrained, strictly convex problem

$$\underset{x \in \mathbb{R}^n}{\text{minimize}} \quad f(x) \quad (1.1a)$$

$$\text{subject to} \quad Ax = b \quad (1.1b)$$

where $A \in \mathbb{R}^{m \times n}$ with $m \leq n$, and $b \in \mathbb{R}^m$. We assume that $f : \mathbb{R}^n \rightarrow \mathbb{R}$ is a strictly convex and continuously differentiable function, that matrix A has a full row rank, and that problem (1.1a) – (1.1b) is strictly feasible and has a finite optimal solution. Let $\lambda \in \mathbb{R}^m$ be the Lagrange multiplier associated with constraint (1.1b), then the Lagrangian can be formulated as

$$L(x, \lambda) = f(x) + \lambda^T (Ax - b). \quad (1.2)$$

By the classical Lagrange duality theory, the Lagrange dual relaxation to the primal problem (1.1a) – (1.1b) is given by

$$\underset{\lambda \in \mathbb{R}^m}{\text{maximize}} \quad \underset{x \in \mathbb{R}^n}{\text{minimize}} \quad L(x, \lambda). \quad (1.3)$$

Under current assumptions, we conclude that the Lagrangian (1.2) is strictly convex in x and concave in λ , and strong duality holds between problems (1.1a) – (1.1b) and (1.3).

Then the optimization dynamical system associated with problem (1.1a) – (1.1b) can be defined as follows

$$\dot{x} := -\nabla_x L(x, \lambda) = -\nabla_x f(x) - A^T \lambda \quad (1.4a)$$

$$\dot{\lambda} := \nabla_\lambda L(x, \lambda) = Ax - b \quad (1.4b)$$

where ∇_x and ∇_λ represent the gradients with respect to x and λ , respectively.

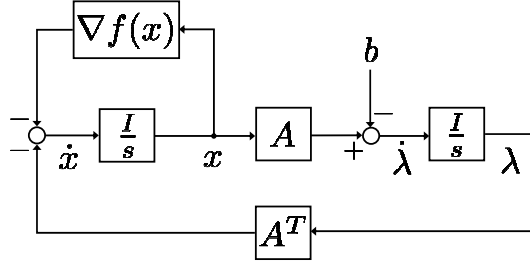


Figure 1.1 The block diagram of an optimization dynamical system

1.1.2 A Control Perspective for the Optimization Dynamical System

Wang and Elia (2011) has studied the optimization dynamical system (1.4a) – (1.4b) from a control perspective. Figure 1.1 shows the block diagram of dynamics (1.4a) – (1.4b). Since the block diagram is interconnected with closed loops, we know that dynamics (1.4a) – (1.4b) must be subject to the fundamental limitations of feedback.

Moreover, the vector b in constraint (1.1b) can be interpreted as an input command to the dynamical system. When b changes over time, the dynamical system will correspondingly track the new command and adapt itself to a new equilibrium point, leading to the possibility of a real-time adaptive optimization.

1.1.3 Motivations for the Continuous-Time Optimization Dynamics

Since those seminal works from 1958, the continuous-time optimization dynamics approach has been almost forgotten until several new applications for the rate control in communication networks Kelly et al. (1998), resource allocation Feijer and Paganini (2010), general distributed convex optimizations Wang and Elia (2011), as well as optimizations over power networks, e.g., Ma and Elia (2013), Dörfler et al. (2014), Zhao et al. (2014), and Mallada et al. (2014).

In this work, we employ the continuous-time optimization dynamics to investigate general *non-convex* optimization problems. If strong duality holds for a given non-convex problem, it may be still possible for us to apply the optimization dynamical system, seeking saddle-points for the associated Lagrangian. Moreover, we have the following reasons that motivate our study on the continuous-time optimization dynamics.

Firstly, when compared with those discrete-time primal-dual optimization algorithms, we find that the continuous-time optimization dynamics approach can be more easily applied to non-convex problems.

We notice that in literature there are many discretized algorithms that are developed based on the primal-dual optimization idea. Some popular ones, for example, include the sub-gradient optimization method by [Nedić and Ozdaglar \(2009\)](#) and the alternating direction method of multipliers (ADMM) by [Boyd et al. \(2011\)](#).

However, those algorithms are mainly conceived for solving convex problems, and hence are difficult to be applied to non-convex optimizations. When a problem under study is non-convex, one major obstacle that hinders the application of those algorithms lies in how to update the primal variable. At each step, for example, the sub-gradient method computes the projection of primal gradient to the primal feasible set as an update direction; while the ADMM yields its update direction by minimizing the associated Lagrangian with respect to the primal variable. If the primal feasible set is a non-convex set and the associated Lagrangian is also non-convex in the primal variable, then neither algorithms can work properly. In contrast, we do not need to worry about these issues for the continuous-time optimization dynamics approach.

Secondly, the optimization dynamical system may help us find certain hidden saddle-point for the Lagrangian associated with a non-convex problem.

In general, it is not easy to derive an explicit Lagrange dual for a non-convex optimization. Sometimes, the Lagrange dual could be developed only after some equivalent transformations have been done to the original non-convex problem. In our research, however, we discover the fact that an equivalent transformation between two non-convex problems may not guarantee the equivalence between their associated Lagrange duals. We find that the Lagrange dual to the original non-convex problem, although we do not know how it looks like, can be stronger than the explicit Lagrange dual which is derived from the equivalent transformation.

For example, an SDP Lagrange dual can be developed for the non-convex OPF problem after the lifting technique has been applied to the original problem. This technique equivalently changes the variables of an OPF problem from an n -dimensional vector space into an $n \times n$ dimensional symmetric matrix space.

We can prove that whenever the SDP dual provides strong duality for the equivalent OPF formulation, the optimization dynamics associated with the original OPF problem must have a saddle-point as equilibrium. On the other hand, we also have counterexamples showing that the original optimization dynamical system may still converge to a saddle-point even though the SDP dual fails to maintain strong duality. Due to the loss of strong duality, of course this saddle-point cannot be found by the SDP dual. However, such a saddle-point really exists for the Lagrangian associated with the original OPF problem, implying that the implicit Lagrange dual to the original OPF must be stronger than the corresponding SDP dual.

Thirdly, when the optimization dynamics is applied to solve certain networked optimization problems, we discover that the associated optimization dynamical systems possess an intrinsic distributed computation structure. To be specific, each individual node in the network only uses the local information from neighboring nodes to compute the gradients for its own primal variables and Lagrange multipliers. Moreover, if any two nodes are not directly connected with each other, then there is no communication between them. In this work we present MAXCUT and OPF problems as examples to illustrate the distributed computation structure. Moreover, such a distributed structure only belongs to the continuous-time optimization dynamics, for it will be destroyed somehow by discretized implementations.

Last but not least, we need to point out that for many real-time optimization problems, the continuous-time optimization dynamics may possess certain physical meanings. Recent works [Mallada et al. \(2014\)](#) and [Zhao et al. \(2014\)](#) have both shown that, for the optimal load control and optimal frequency regulation over power networks, the physical swing dynamics, along with the power flow dynamics, serves as a continuous-time primal-dual optimization algorithm. In these cases, we are able to merge the associated optimization dynamical systems into the real physics. As a result, a real-time optimization can be naturally achieved by physical computing.

1.1.4 The Optimal Power Flow Problem

A main part of this dissertation (see Chapter 5) is to study the non-convex OPF problem via the optimization dynamics approach. The OPF problem is an important economic dispatch problem that has a long research history.

In power systems, an OPF problem seeks an optimal solution of bus voltage magnitudes and phase angles that minimizes a given generation cost, subject to the power balance at each bus and other operating constraints. The power balance is characterized by power flow equations, and the operational constraints include voltage magnitude limits, line flow limits, etc.

The OPF problem was first studied by [Carpentier \(1962\)](#). Since power flow equations are quadratic, OPF problems can be in general formulated as quadratically constrained quadratic programmings (QCQPs). It has been recognized that OPF problems are inherently non-convex and hence they are difficult to solve.

The OPF problem has been widely studied over the past fifty years, and numerous solution methods have been developed. Some classical methods include gradient method, e.g., [Tinney and Hart \(1967\)](#) and [Dommel and Tinney \(1968\)](#), Newton's method [Sun et al. \(1984\)](#), linear programming [Alsac et al. \(1990\)](#), and interior-point method, e.g., [Wu et al. \(1994\)](#) and [Wei et al. \(1998\)](#). However, none of these conventional techniques can guarantee global optimality.

To overcome the weak searching capabilities, several heuristic, random search algorithms have also been attempted for OPF problems, e.g., [Hartati and El-Hawary \(2001\)](#), [Abido \(2002\)](#), [Han and Lu \(2008\)](#), and [Mahdad et al. \(2010\)](#). Nevertheless, all these methods typically lack computation efficiency for large scale OPF problems. Readers may refer to [Frank et al. \(2012a\)](#) and [Frank et al. \(2012b\)](#) for comprehensive surveys about the existing OPF solutions.

Recent work [Lavaei and Low \(2012\)](#) has theoretically shown that under certain conditions there is no optimal duality gap between the primal non-convex OPF problem and its SDP dual relaxation. When strong duality holds, one is able to recover a global OPF solution from its associated SDP dual, which can be solved efficiently by using convex optimization softwares. This result has pointed out a promising approach of studying non-convex OPF problems via convex SDP or second-order cone programming (SOCP) relaxations.

Tutorials [Low \(2014a\)](#) and [Low \(2014b\)](#) have summarized the convex relaxation results for OPF problems developed in the past few years. The conclusion is that power network topology plays a key role in determining whether the relaxation is exact or not. Specifically, both SDP and SOCP relaxations are equally exact for radial (tree) networks, but for mesh networks the SDP relaxation is strictly tighter than the corresponding SOCP relaxation.

Although counterexamples exist in [Lesieutre et al. \(2011\)](#), numerical experience suggests that the SDP relaxation tends to be exact for many OPF cases. As for those counterexamples, [Josz et al. \(2015\)](#) has proposed another numerical SDP method, known as the moment-SOS (sum-of-squares), to search global solutions, but at the expense of a higher computation time.

However, we note that all of above OPF algorithms require centralized computing, which is not suitable for the distributed physical structure of future power systems. Indeed, the future cyber-enabled electric power grids, also known as smart grids, can be envisioned to operate based on distributed transactions and energy management. Future smart grids also desire to embed computation into physical processes, see [Li et al. \(2010\)](#) and [Rajkumar et al. \(2010\)](#).

To address these challenges, we apply the continuous-time optimization dynamics to seek global OPF solutions. The optimization dynamics treats each bus in the power network as an intelligent computing agent, which only requires the local information to update the decision variables. Therefore, it topologically suits the physical structure of the power network.

Most existing distributed OPF algorithms, e.g., [Baldick et al. \(1999\)](#), [Nogales et al. \(2003\)](#), [Hug-Glanzmann and Andersson \(2009\)](#), [Lam et al. \(2012\)](#), [Dall'Anese et al. \(2013\)](#), and [Erseghe \(2014\)](#), are developed based on a regional optimization intuition. To be specific, they first divide the power network into several regions, each region solves its own sub-OPF and then coordinates with others to yield the final solution. In contrast, our approach exploits the distributed OPF structure deeply into the bus level.

Also treating each individual bus as an intelligent computing unit, [Bolognani and Zampieri \(2013\)](#) and [Cavraro et al. \(2014\)](#) have designed gossip-like distributed algorithms for the optimal reactive power compensation and optimal power generation problems, based on a linearized approximation of injected power. This work, however, studies the non-linear power flow without approximations.

1.2 Organization of This Dissertation

This dissertation is organized as follows. In Chapter 2, we briefly review some mathematical preliminaries that are necessary for the presentation of this work, including basic concepts and results in graph theory, optimization theory, and non-linear dynamical systems.

Chapter 3 presents our main approach, i.e., the continuous-time optimization dynamics, for studying general non-convex problems. A convergence analysis for the optimization dynamical system is also developed in this chapter. Specifically, if there is a strictly complementary KKT point at which the evaluated Hessian of the associated Lagrangian with respect to the primal variable is positive definite, then the optimization dynamics locally has a unique solution which converges asymptotically to this KKT point.

Once the optimization dynamical system associated with a non-convex problem converges to a KKT equilibrium, then one would like to further check whether this KKT point is globally optimal or not, since KKT conditions are only necessary for the local optimality of non-convex problems. So, in Chapter 4, we focus on a special class of non-convex optimizations, namely, the non-convex QCQPs, and develop an easily checkable necessary and sufficient global optimality condition for the KKT equilibrium points. We apply the convergence analysis result that has been derived in Chapter 3 to the optimization dynamics associated with non-convex QCQPs. We also present a MAXCUT example to demonstrate that, for certain networked non-convex QCQPs, our optimization dynamics exhibits a naturally distributed computation structure. Moreover, we show by simulations that our optimization dynamics approach can be successfully applied to solve the non-convex phase recovery problems as well as convex SOCPs.

In Chapter 5, we investigate the so-called OPF problem, which can be in general formulated as a networked non-convex QCQP. Our optimization dynamics approach could be applied here because it has been theoretically proved that strong duality holds for many OPF cases. First, we show that the optimization dynamical system associated with OPF problems possesses an intrinsic distributed structure, which makes our OPF algorithm naturally suit the topology of power networks. Then we compare our approach with the SDP dual relaxation approach, and we discover that there exist counterexamples whose associated optimization dynamical systems can still converge to saddle-points but the corresponding SDP dual relaxations fail to provide strong duality. Such a discovery implies the existence of a stronger implicit Lagrange dual to the OPF problem, and a more general applicability of our OPF algorithm. Finally, by applying the convergence analysis in Chapter 3 again, we prove the locally asymptotic stability for the saddle-points associated with OPF problems.

Our next chapter deals with digital implementations of the continuous-time optimization dynamical systems. Specifically, we develop distributed numerical solvers for the optimization dynamics, based on the backward Euler's method and iterative matrix inversion algorithms. The backward Euler's method guarantees the solvers' robustness to large simulation step sizes, and meanwhile the iterative matrix inversion maintains the distributed computation structure. Nevertheless, in each iteration, we notice that these distributed solvers need to use the network topology several times in order to compute an update, which implies that the discretization of our optimization dynamics approach may somehow destroy the intrinsic distributed structure.

In Chapter 7, we revisit OPF problems. Different from what we have studied in Chapter 5, we consider the SDP relaxation approach there. We notice that the size of the SDP relaxation does not scale nicely when the power network expands. To meet this challenge, we exploit the sparsity of power network further and decompose the standard SDP relaxation into a bunch of smaller SDP relaxations. Now each bus in the network needs to locally solve a decomposed SDP relaxation that is associated with itself, and finally a global OPF solution can be achieved by running a consensus over the whole network. We show that our decomposed SDP relaxation scales linearly as the power network expands, so it greatly fastens the OPF computation speed.

In the last chapter, we present concluding remarks of this dissertation and several possible directions for future research.

1.3 The Main Contributions

This dissertation has five main contributions, which are listed below.

Firstly, we present a convergence analysis for the continuous-time optimization dynamics with a correct proof that resolves some gaps in [Arrow and Hurwicz \(1958\)](#).

In Chapter 3, we present a similar convergence result (Theorem 10) as [Arrow and Hurwicz \(1958\)](#). However, [Arrow and Hurwicz \(1958\)](#) did not choose a valid Lyapunov function in its proof. To be specific, [Arrow and Hurwicz \(1958\)](#) used the square distance from the trajectory to the equilibrium as a Lyapunov candidate. It also claimed that the derivative of this Lyapunov candidate with respect to time would be negative definite. But this is not correct. We can give counterexamples showing that the corresponding derivative may be only negative semi-definite.

In order to further prove the asymptotic convergence, one has to invoke LaSalle's invariance principle, which, we believe, had not been invented by the time when [Arrow and Hurwicz \(1958\)](#) was first published. Therefore, the Lyapunov candidate invented by [Arrow and Hurwicz \(1958\)](#) becomes questionable. In our correct proof, we alternatively construct a quadratic Lyapunov candidate by solving the associated Lyapunov equation. We can show that its derivative with respect to time is always negative definite, and hence we need not to invoke LaSalle's invariance principle anymore.

Secondly, we derive a necessary and sufficient condition that characterizes global optimality for general non-convex QCQPs.

Under mild constraint qualification assumptions, it is well known that KKT conditions are necessary and sufficient for the global optimality of convex problems. As for those non-convex optimizations, KKT conditions become only necessary for local optimality. It is also a known fact from [Boyd and Vandenberghe \(2004\)](#) that if a non-convex QCQP has only one quadratic inequality constraint, then strong duality holds. That is to say, KKT points and saddle-points are still equivalent to each other in this case.

This work generalizes the strong duality condition for a non-convex QCQP with any finite number of equality or inequality constraints. Our result states the fact that any KKT point of a non-convex QCQP is globally optimal if and only if it satisfies an extra linear matrix inequality (LMI) condition. If one QCQP is convex or degrades to an LP, then that extra LMI condition will be automatically satisfied. Therefore, under these circumstances, KKT conditions become again necessary and sufficient for global optimality.

Thirdly, to the best of our knowledge, this work is the first that applies the continuous-time optimization dynamics approach to search saddle-points for non-convex QCQPs. We discover that, for certain networked QCQPs, the associated optimization dynamics exhibits an intrinsic distributed computation structure.

Given a networked optimization problem, we treat each node in the network as an individual computing agent. We also assign each node with a group of primal and Lagrange dual variables. The associated optimization dynamics is said to be distributed provided that each computing agent only uses the local information from neighboring nodes to compute its own gradients.

In Chapter 5, we give a detailed discussion about the distributed computation structure of the optimization dynamics associated with OPF problems. This property also makes our OPF algorithm naturally suitable for the topology of power networks. Compared with those existing distributed OPF algorithms that are developed based on regional decomposition intuitions, our continuous-time optimization dynamics approach exploits the distributed OPF structure deeply into the bus level. The fact that OPF problems can be solved in a completely distributed manner, as far as we know, has long been missed in literature.

We note that the distributed computation structure is a special property only possessed by the continuous-time optimization dynamics. Due to the limitations of discretization methods, such a distributed computation structure would be destroyed somehow when implemented in a discrete-time fashion.

Fourthly, by applying the optimization dynamics, we discover the existence of a stronger Lagrange dual relaxation to the non-convex OPF problem.

[Lavai and Low \(2012\)](#) has theoretically proved that for many cases strong duality holds between the primal non-convex OPF and its SDP dual relaxation. In this work we show that whenever the SDP dual maintains strong duality, the associated optimization dynamics must have a saddle-point as equilibrium. On the other hand, we provide counterexamples showing that the optimization dynamical system may still converges to a saddle-point even though the SDP dual loses strong duality. Combining these implies the existence of a stronger Lagrange dual relaxation to the OPF problem. By the same reason, we conclude that our optimization dynamics can find global OPF solutions under more general conditions than the existing SDP dual relaxation approach.

Lastly, by fully exploiting the natural sparsity of power networks, we further decompose the standard SDP relaxation of OPF into a bunch of smaller SDPs. Then each bus in the power network can locally solve its own decomposed SDP and meanwhile a global OPF solution could be achieved by operating a consensus over the whole power network. Besides, the size of our decomposed SDP relaxation scales linearly as the power network expands and hence it may greatly fasten the OPF computation speed. When compared with [Molzahn et al. \(2013\)](#) and [Madani et al. \(2015\)](#), our approach is the fastest for large-scale OPF examples.

CHAPTER 2. PRELIMINARIES

This chapter provides notations and mathematical preliminaries that are necessary for the future development of our work. Some basic concepts and results in graph theory, optimization theory, and dynamical systems will be briefly reviewed here.

2.1 Notations

The following notations will be used throughout this dissertation. The symbol \mathbb{R} denotes the one-dimensional real line. Besides, \mathbb{R}^n and \mathbb{R}_+^n , respectively, denote the real, n -dimensional vector space and its non-negative orthant. Each $x \in \mathbb{R}^n$ is assumed to be a column vector and we use x^T to denote its transpose.

The set of complex numbers is denoted by \mathbb{C} . For a complex number $z = a + ib$, where $a, b \in \mathbb{R}$, we use i to denote the imaginary unit and z^* to denote its conjugate. Besides, $\text{Re}\{z\}$ and $\text{Im}\{z\}$, respectively, return the real and imaginary parts of z .

The set of all $m \times n$ real matrices is denoted by $\mathbb{R}^{m \times n}$. The set of all $n \times n$ real, symmetric matrices is denoted by \mathbb{S}^n . Given $A \in \mathbb{R}^{m \times n}$, $A(k, l)$ denotes the (k, l) entry of A and $A(k, :)$ denotes the k -th row of A . When A is square, $\text{Tr}\{A\}$ returns the trace of A and $\lambda_i(A)$ stands for the i -th eigenvalue of A . Moreover, if $A \in \mathbb{S}^n$, then the notation $A \succ 0$ ($A \succeq 0$) means that A is positive definite (positive semi-definite).

2.2 Basics Concepts in Graph Theory

In this work, we model networks as undirected graphs.

Let $\mathcal{G} = (\mathcal{V}, \mathcal{E})$ denote a graph with the set of nodes \mathcal{V} and the set of edges $\mathcal{E} \subseteq \mathcal{V} \times \mathcal{V}$. We assume that $|\mathcal{E}| = m$ and $|\mathcal{V}| = n$, where $|\cdot|$ returns the cardinality of a countable set.

For each edge $e \in \mathcal{E}$ that connects nodes i and j , we denote it as an unordered pair (i, j) . Moreover, for each node $v \in \mathcal{V}$, we denote $\mathcal{N}(v) := \{u \mid \forall (u, v) \in \mathcal{E}\}$ as the set that contains all the neighbors of v .

An edge $e = (i, j)$ is called a self-loop if $i = j$. Two edges $e_1 = (i_1, j_1)$ and $e_2 = (i_2, j_2)$ are said to be parallel if $i_1 = i_2$ and $j_1 = j_2$. Throughout this work we assume that graph \mathcal{G} has no self-loops or parallel edges.

Definition 1. Let $e = (p, q)$ with $p < q$ be the i -th edge in \mathcal{E} and let v be the j -th node in \mathcal{V} . The **edge incidence matrix** $E \in \mathbb{R}^{m \times n}$ is defined by

$$E(i, j) := \begin{cases} 1 & \text{if } v = p \\ -1 & \text{if } v = q \\ 0 & \text{otherwise.} \end{cases} \quad (2.1)$$

Thus each row of E has exactly one 1 and one -1 element. Using the edge incidence matrix, we can further define the Laplacian and weighted Laplacian matrices associated with graph \mathcal{G} .

Definition 2. The **Laplacian matrix** $L \in \mathbb{S}^n$ associated with graph \mathcal{G} is defined as

$$L := E^T E. \quad (2.2)$$

Definition 3. Let $\Sigma = \text{Diag}(\sigma_1, \dots, \sigma_m)$ be a given weight matrix, whose each diagonal entry $\sigma_i > 0$ represents the weight assigned to edge e_i , for $1 \leq i \leq m$. The **weighted Laplacian matrix** $W \in \mathbb{S}^n$ associated with graph \mathcal{G} is defined as

$$W := E^T \Sigma E. \quad (2.3)$$

Then it easily follows from (2.2) that $L \succeq 0$, i.e., all the eigenvalues of L are non-negative. Suppose that the n eigenvalues of L can be arranged as $\lambda_n(L) \geq \dots \geq \lambda_2(L) \geq \lambda_1(L)$. We know that $\lambda_1(L)$ must be zero because $L\mathbb{1} = 0$, where $\mathbb{1} \in \mathbb{R}^n$ denotes the vector with all 1 entries. Besides, the second least eigenvalue $\lambda_2(L)$ reflects the connectivity of graph \mathcal{G} .

Theorem 1. [Newman (2010)] Let $\mathcal{G} = (\mathcal{V}, \mathcal{E})$ be a graph and also let $\lambda_n(L) \geq \dots \geq \lambda_2(L) \geq \lambda_1(L) = 0$ be the n eigenvalues of the associated Laplacian matrix. Then \mathcal{G} is connected if and only if $\lambda_2(L) > 0$.

Assumption 1. All graphs studied in this work are assumed to be connected.

2.3 Constrained Optimizations

Consider a general optimization problem with both equality and inequality constraints

$$\underset{x \in \mathbb{R}^n}{\text{minimize}} \quad f(x) \quad (2.4a)$$

$$\text{subject to} \quad g_i(x) \leq 0, \quad i = 1, \dots, p \quad (2.4b)$$

$$h_j(x) = 0, \quad j = 1, \dots, q \quad (2.4c)$$

where $f : \mathbb{R}^n \rightarrow \mathbb{R}$, $g_i : \mathbb{R}^n \rightarrow \mathbb{R}$, and $h_j : \mathbb{R}^n \rightarrow \mathbb{R}$, for $i = 1, \dots, p$ and $j = 1, \dots, q$, are all continuously differentiable functions. In this dissertation, we may not assume that optimization (2.4a) – (2.4c) is convex.

Let $\bar{x} \in \mathbb{R}^n$ be a feasible point for optimization (2.4a) – (2.4c). Define \mathcal{I} as the set that contains all indices corresponding to the active inequality constraints when evaluated at \bar{x} , i.e.,

$$\mathcal{I} := \{i \mid g_i(\bar{x}) = 0, i = 1, \dots, p\}.$$

Definition 4. Given a feasible point $\bar{x} \in \mathbb{R}^n$ for optimization (2.4a) – (2.4c), let $\nabla g_i(\bar{x}) \in \mathbb{R}^n$ and $\nabla h_j(\bar{x}) \in \mathbb{R}^n$, respectively, denote the gradients of $g_i(x)$ and $h_j(x)$ evaluated at \bar{x} . We say that \bar{x} is **regular** if all the gradients $\nabla g_r(\bar{x})$ and $\nabla h_j(\bar{x})$, for $r \in \mathcal{I}$ and $j = 1, \dots, q$, are linearly independent.

Remark 1. The concept of regularity is adopted from Bertsekas (1982) and it can be interpreted as a constraint qualification condition, see Lasserre (2010).

Assumption 2. All optimizations studied in this work are assumed to have regular solutions.

Definition 5. The **Lagrangian** $L : \mathbb{R}^n \times \mathbb{R}_+^p \times \mathbb{R}^q \rightarrow \mathbb{R}$ associated with problem (2.4a) – (2.4c) is defined by

$$L(x, \lambda, \nu) := f(x) + \sum_{i=1}^p \lambda_i g_i(x) + \sum_{j=1}^q \nu_j h_j(x) \quad (2.5)$$

where λ_i and ν_j , for $i = 1, \dots, p$ and $j = 1, \dots, q$, respectively, are the **Lagrange multipliers** associated with constraints $g_i(x) \leq 0$ and $h_j(x) = 0$.

Remark 2. Because λ_i , for $i = 1, \dots, p$, are the Lagrange multipliers associated with inequality constraints $g_i(x) \leq 0$, we require that $\lambda_i \geq 0$ for all indices i .

Theorem 2. [KKT optimality conditions, *Lasserre (2010)*] Let $\bar{x} \in \mathbb{R}^n$ be a local minimizer for problem (2.4a) – (2.4c). If \bar{x} is regular, then there exist $\bar{\lambda} \in \mathbb{R}_+^p$ and $\bar{\nu} \in \mathbb{R}^q$ such that

$$\nabla_x L(\bar{x}, \bar{\lambda}, \bar{\nu}) = 0 \quad (2.6a)$$

$$g_i(\bar{x}) \leq 0, \quad \forall i = 1, \dots, p \quad (2.6b)$$

$$h_j(\bar{x}) = 0, \quad \forall j = 1, \dots, q \quad (2.6c)$$

$$\bar{\lambda}_i \geq 0, \quad \forall i = 1, \dots, p \quad (2.6d)$$

$$\bar{\lambda}_i g_i(\bar{x}) = 0, \quad \forall i = 1, \dots, p. \quad (2.6e)$$

Remark 3. The last KKT condition (2.6e) is also known as the complementary slackness.

Definition 6. A vector $(\bar{x}, \bar{\lambda}, \bar{\nu}) \in \mathbb{R}^n \times \mathbb{R}_+^p \times \mathbb{R}^q$ is said to be a **Karush-Kuhn-Tucker (KKT) point** of optimization (2.4a) – (2.4c) if it satisfies conditions (2.6a) – (2.6e).

Definition 7. A KKT point $(\bar{x}, \bar{\lambda}, \bar{\nu})$ is said to be **strictly complementary** if

$$g_i(\bar{x}) < 0, \quad \bar{\lambda}_i = 0 \quad \text{or} \quad g_i(\bar{x}) = 0, \quad \bar{\lambda}_i > 0 \quad \forall i = 1, \dots, p. \quad (2.7)$$

When optimization (2.4a) – (2.4c) is convex, KKT conditions (2.6a) – (2.6e) become also sufficient for characterizing its local optimum. Furthermore, because any local minimizer will be a global solution to a convex optimization, KKT conditions (2.6a) – (2.6e) turn out to be necessary and sufficient optimality conditions for optimization (2.4a) – (2.4c) if it is convex.

Definition 8. A vector (x^*, λ^*, ν^*) is said to be a **saddle-point** for the Lagrangian $L(x, \lambda, \nu)$ if for all $x \in \mathbb{R}^n$, $\lambda \in \mathbb{R}_+^p$, and $\nu \in \mathbb{R}^q$

$$L(x^*, \lambda, \nu) \leq L(x^*, \lambda^*, \nu^*) \leq L(x, \lambda^*, \nu^*). \quad (2.8)$$

Theorem 3. [Boyd and Vandenberghe (2004)] A vector (x^*, λ^*, ν^*) is a saddle-point for the Lagrangian $L(x, \lambda, \nu)$ if and only if x^* is a primal optimum to optimization (2.4a) – (2.4c), (λ^*, ν^*) is a dual optimum, and the optimal duality gap is zero.

Under mild constraint qualification conditions (Slater's condition or regularity condition), strong duality holds for convex problems. In this case, therefore, KKT points and saddle-points are equivalent to each other. However, as for general optimization problems, a KKT point may not necessarily be a saddle-point.

2.4 Sum of Squares Relaxations

Definition 9. A multivariate polynomial $p(x) := p(x_1, \dots, x_n)$ is said to be a **sum of squares (SOS)** if there exists a series of polynomials $\{f_i(x)\}_{i=1}^m$ such that

$$p(x) = \sum_{i=1}^m f_i^2(x). \quad (2.9)$$

It is clear that if a polynomial $p(x)$ is an SOS then $p(x) \geq 0$ for all $x \in \mathbb{R}^n$. However, the converse statement may not be true.

Theorem 4. [*Papachristodoulou et al. (2013)*] In the following cases, the sum of squares condition and non-negativity are equivalent:

- Univariate polynomials, in any even degree;
- Quadratic polynomials, in any number of variables;
- Quartic polynomials in two variables.

Consider the unconstrained polynomial optimization

$$\underset{x \in \mathbb{R}^n}{\text{minimize}} \quad p(x) \quad (2.10)$$

where $p(x)$ with $x \in \mathbb{R}^n$ is a multivariate polynomial of degree $2d$. As is well known, problem (2.10) is NP-hard when $d \geq 2$. However, a lower bound can always be efficiently computed using the following SOS relaxation

$$\text{maximize} \quad \gamma \quad (2.11)$$

$$\text{subject to} \quad p(x) - \gamma \succeq_{\text{SOS}} 0 \quad (2.12)$$

where the inequality notation $g \succeq_{\text{SOS}} 0$ means that polynomial g is an SOS.

The SOS relaxation (2.11) – (2.12) was first proposed by Shor (1987). It is equivalent to an semi-definite programming (SDP) and hence is convex. If the SOS relaxation (2.11) – (2.12) is tight, then we can recover a global solution to problem (2.10). Practical experience indicates that in many cases the above SOS relaxation approach leads to exact optimal solutions.

2.5 Continuous-Time Dynamical Systems

This work models a **dynamical system** using a first-order ordinary differential equation

$$\dot{x}(t) = f(t, x(t)), \quad \forall t \geq 0 \text{ and } x(t_0) = x_0 \quad (2.13)$$

where t denotes time; $x(t) \in \mathbb{R}^n$ denotes an n -dimensional vector at time t ; and the function $f : \mathbb{R}_+ \times \mathbb{R}^n \rightarrow \mathbb{R}^n$ associates, with each value of t and $x(t)$, a corresponding n -dimensional vector. The quantity $x(t)$ is generally referred to as the **state** of the system at time t . It is clear that (2.13) represents a continuous-time system.

The system (2.13) is said to be **autonomous** if the function f does not explicitly depend on time t ; that is, $\dot{x} = f(x)$. For an autonomous system, the **equilibrium points** are the real roots of the equation $f(x) = 0$.

We present below several fundamental properties regarding the solution to the dynamical system (2.13). All of these results are cited from Khalil (2002).

Theorem 5. *[Local Existence and Uniqueness] Let $f(t, x)$ be piecewise continuous in time t and satisfy the Lipschitz condition*

$$\|f(t, x) - f(t, y)\| \leq L\|x - y\|$$

for all $x, y \in B_r = \{x \in \mathbb{R}^n \mid \|x - x_0\| \leq r\}$ and all $t \in [t_0, t_1]$. Then, there exists some $\delta > 0$ such that system (2.13) has a unique solution over $[t_0, t_0 + \delta]$.

Theorem 5 is a local result because it guarantees existence and uniqueness of the solution only over an interval $[t_0, t_0 + \delta]$, where δ may be very small. Since we have no control on δ , we cannot ensure existence and uniqueness of the solution over a given time interval $[t_0, t_1]$. One may try to extend the interval of existence by repeated applications of the local theorem. However, in general, the interval of existence cannot be extended indefinitely. The conditions of Theorem 5 will cease to hold when the system's state escapes to infinity at a finite time. Therefore, we require additional conditions to establish the existence of a unique solution over the time interval $[t_0, t_1]$.

Theorem 6. *[Global Existence and Uniqueness] Suppose that $f(t, x)$ is piecewise continuous in time t and satisfies*

$$\|f(t, x) - f(t, y)\| \leq L\|x - y\|$$

for all $x, y \in \mathbb{R}^n$ and all $t \in [t_0, t_1]$. Then system (2.13) has a unique solution over $[t_0, t_1]$.

In view of the conservative nature of the global Lipschitz condition, it would be useful to have a global existence and uniqueness theorem that requires the function f to be only locally Lipschitz. The next theorem achieves that at the expense of having to know more about the solution of the system.

Theorem 7. *Let $f(t, x)$ be piecewise continuous in t and locally Lipschitz in x for all $t \geq t_0$ and all x in a domain $D \subset \mathbb{R}^n$. Let W be a compact subset of D , $x_0 \in W$, and suppose that every solution of $\dot{x} = f(t, x)$ with $x(t_0) = x_0$ lies entirely in W . Then system (2.13) has a unique solution for all $t \geq t_0$.*

The trick in applying Theorem 7 is in checking the assumption that every solution lies in a compact set without actually solving the differential equation. In this regard, the Lyapunov's method for studying stability will be very valuable.

Definition 10. *Let $x = 0$ be an equilibrium point of the autonomous system $\dot{x} = f(x)$, where $f : D \rightarrow \mathbb{R}^n$ is a locally Lipschitz map from a domain D into \mathbb{R}^n . The equilibrium $x = 0$ is*

- **stable** if, for each $\varepsilon > 0$, there is some $\delta > 0$ such that $\|x(0)\| < \delta \Rightarrow \|x(t)\| < \varepsilon, \forall t \geq 0$;
- **asymptotically stable** if it is stable and $\|x(0)\| < \delta \Rightarrow \lim_{t \rightarrow \infty} x(t) = 0$.

Theorem 8. *[Lyapunov's Stability Theorem] Let $x = 0$ be an equilibrium of the autonomous system $\dot{x} = f(x)$ and $D \subset \mathbb{R}^n$ be a domain containing $x = 0$. Let $V : D \rightarrow \mathbb{R}$ be a continuously differentiable function such that*

$$V(0) = 0, \quad V(x) > 0 \text{ in } D \setminus \{0\}, \quad \dot{V}(x) \leq 0 \text{ in } D \quad (2.14)$$

then the equilibrium $x = 0$ is stable. Moreover, if

$$\dot{V}(x) < 0 \text{ in } D \setminus \{0\} \quad (2.15)$$

then the equilibrium $x = 0$ is asymptotically stable.

A continuously differentiable function $V(x)$ satisfying (2.14) is called a **Lyapunov function**. Moreover, the surface $V(x) = c$, for some $c > 0$, is called a **Lyapunov surface**. The condition $\dot{V} \leq 0$ implies that when a trajectory crosses a Lyapunov surface $V(x) = c$, it moves inside the compact set $\Omega_c = \{x \in \mathbb{R}^n \mid V(x) \leq c\}$ and can never leave it again.

Finally, let us present how to construct a Lyapunov function for a linear, time-invariant system $\dot{x} = Ax$, where $A \in \mathbb{R}^{n \times n}$. This system has an equilibrium at the origin. When all eigenvalues of A satisfy $\text{Re}\{\lambda_i(A)\} < 0$, A is called a **Hurwitz matrix**. It can be shown that the origin is asymptotically stable if and only if A is Hurwitz.

Theorem 9. *A matrix A is Hurwitz if and only if for any given positive definite symmetric matrix Q there is a positive definite symmetric matrix P that satisfies the Lyapunov equation $PA + A^T P = -Q$. Moreover, if A is Hurwitz, then P is the unique solution.*

By Theorem 9, we can always construct a Lyapunov function $V(x) = x^T P x$ with $P \succ 0$ for the linear system $\dot{x} = Ax$ if A is Hurwitz. When a $Q \succ 0$ is given, the corresponding P matrix can be solved from the Lyapunov equation. Then the derivative of V along the trajectories of the linear system is given by $\dot{V}(x) = x^T P \dot{x} + \dot{x}^T P x = x^T (PA + A^T P)x = -x^T Q x$, which satisfies condition (2.15).

CHAPTER 3. THE CONTINUOUS-TIME OPTIMIZATION DYNAMICS

This chapter presents the main approach of our work. Specifically, we would like to study optimization (2.4a) – (2.4c) via the continuous-time optimization dynamics.

The continuous-time optimization dynamics, also known as the primal-dual dynamics, was first studied by [Arrow and Hurwicz \(1958\)](#) and [Uzawa \(1958\)](#) for strictly convex programmings. The former investigated locally strictly convex problems and proved local convergence of the associated optimization dynamics. The latter obtained a global convergence result for a stronger setup, requiring an assumption of globally strict convexity. Recently, modern proofs for this global convergence result have been given by [Wang and Elia \(2011\)](#) and [Cherukuri et al. \(2016\)](#).

Since the seminal work of Arrow, however, the optimization dynamics approach seems to be mostly forgotten until its new applications for resource allocation [Feijer and Paganini \(2010\)](#), and power optimizations [Ma and Elia \(2013\)](#), [Mallada et al. \(2014\)](#), and [Zhao et al. \(2014\)](#).

In this work, by applying the continuous-time optimization dynamics, we will show that certain *non-convex* networked optimizations can be solved in a completely distributed manner when strong duality holds and the network is sparsely connected.

This chapter is organized as follows. In Section 3.1, we define the optimization dynamics for problem (2.4a) – (2.4c). We note that any equilibrium of the optimization dynamical system is in fact a KKT point. Then we present a local convergence result in Section 3.2, which answers under what conditions there exists a unique, asymptotically stable solution with respect to the proposed optimization dynamics. Finally, we give our convergence proof in Section 3.3.

We need to point out here that the optimization dynamics is a hybrid automation, which, fortunately, can be equivalently modeled by a sequence of dynamical systems, called the R-S-T systems. Thus, our convergence proof is developed based on showing that each R-S-T system has a unique solution which shrinks towards the desired equilibrium.

3.1 Definition of the Optimization Dynamics

Let us consider the general optimization problem (2.4a) – (2.4c). One possible approach for solving (2.4a) – (2.4c) is to search a saddle-point, if it exists, for the associated Lagrangian (2.5). We may employ the following continuous-time dynamical system to achieve this goal

$$\dot{x} := -\frac{\partial L(x, \lambda, \nu)}{\partial x} = -\nabla_x L(x, \lambda, \nu) \quad (3.1a)$$

$$\dot{\lambda}_i := \left[\frac{\partial L(x, \lambda, \nu)}{\partial \lambda_i} \right]_{\lambda_i}^+ = [g_i(x)]_{\lambda_i}^+ \quad \text{for } i = 1, \dots, p \quad (3.1b)$$

$$\dot{\nu}_j := \frac{\partial L(x, \lambda, \nu)}{\partial \nu_j} = h_j(x) \quad \text{for } j = 1, \dots, q \quad (3.1c)$$

where the positive projection is defined as

$$[g_i(x)]_{\lambda_i}^+ := \begin{cases} g_i(x) & \text{if } \lambda_i > 0 \text{ or } g_i(x) > 0 \\ 0 & \text{otherwise.} \end{cases}$$

The above definition of positive projection is adopted from [Feijer and Paganini \(2010\)](#). We can show that it is equivalent to the dynamics approach studied in [Arrow and Hurwicz \(1958\)](#) and [Uzawa \(1958\)](#). When started from an initial point $\lambda^0 \in \mathbb{R}_+^p$, dynamics (3.1b) guarantees that the trajectory of λ will never escape from \mathbb{R}_+^p .

By viewing the primal variable x and the dual variables λ and ν as two players participating in a min-max game, dynamics (3.1a) – (3.1c) can be interpreted as follows: The primal player tries to minimize the Lagrangian (2.5) by moving against the gradient with respect to itself, while the dual variables follow their own gradient directions in order to maximize the Lagrangian (2.5). This evolution stops at an equilibrium of dynamics (3.1a) – (3.1c). Such an equilibrium must be a KKT point since it satisfies (2.6a) – (2.6e). If we further assume that optimization (2.4a) – (2.4c) is convex, this KKT point is exactly a saddle-point for the Lagrangian (2.5).

The continuous-time dynamics (3.1a) – (3.1c) has multiple names in literature. For example, it was referred to as a *Arrow-Hurwicz system* in [Uzawa \(1958\)](#) and as a *primal-dual gradient dynamics* in [Feijer and Paganini \(2010\)](#). In this work, we follow the terminology used in [Wang and Elia \(2011\)](#) and call dynamics (3.1a) – (3.1c) as an *optimization dynamical system* or an *optimization dynamics*.

3.2 A Local Convergence Result

In this section, we study the convergence behavior of dynamics (3.1a) – (3.1c). Specifically, one may pose the following questions: 1) Does dynamics (3.1a) – (3.1c) have a unique solution? 2) If yes, then under what conditions will an equilibrium be asymptotically stable with respect to dynamics (3.1a) – (3.1c)? These questions can be answered by the next theorem, which is also the main result of this chapter.

Theorem 10. *Suppose that problem (2.4a) – (2.4c) has a strictly complementary KKT point (x^*, λ^*, ν^*) . Also suppose that x^* is regular. If the Hessian of the Lagrangian (2.5) with respect to x is positive definite when evaluated at (x^*, λ^*, ν^*) , then there is a small neighborhood around (x^*, λ^*, ν^*) such that*

- *Optimization dynamics (3.1a) – (3.1c) has a unique solution within this neighborhood;*
- *Any trajectory starting inside this neighborhood converges to (x^*, λ^*, ν^*) asymptotically.*

3.3 The Convergence Proof

We note that dynamics (3.1a) – (3.1c) is a hybrid automaton due to the positive projections. For more details about hybrid automata, the reader may refer to Lygeros et al. (2003). Nevertheless, the conditions proposed in Lygeros et al. (2003) are not very convenient to be applied here to show existence and uniqueness of the solution. Moreover, those conditions only guarantee that the solution to a hybrid automaton is non-blocking, which cannot rule out the possibilities of Zeno solutions. Therefore, in this work, we follow the approach proposed by Arrow and Hurwicz (1958) and also resolve some technical gaps in it.

The basic idea of the convergence proof is to open the brackets of positive projections in (3.1b) and to equivalently model dynamics (3.1a) – (3.1c) by a sequence of R-S-T systems. We would like to show that each R-S-T system has a unique solution that is shrinking towards the desired equilibrium. Then we can piece together the solutions of the R-S-T systems following the correct time sequence, and finally obtain a unique and asymptotically stable solution for dynamics (3.1a) – (3.1c).

When showing asymptotic stability of the R-S-T systems, [Arrow and Hurwicz \(1958\)](#) chose the square distance between the trajectory and the desired equilibrium as a Lyapunov function candidate. But this Lyapunov function candidate was not valid, since its derivative along the trajectories was only negative semi-definite. To further prove asymptotic stability, one must invoke LaSalle's invariance principle, which, however, had not been invented before [Arrow and Hurwicz \(1958\)](#) was published.

We present a counterexample below to illustrate in details the technical gaps that exist in Arrow and Hurwicz's proof.

Example 1. *Consider a strictly convex optimization problem*

$$\text{minimize } (x_1 - 1)^2 + (x_2 - 3)^2 \quad (3.2a)$$

$$\text{subject to } x_1 + x_2 - 2 = 0. \quad (3.2b)$$

The Lagrangian associated with problem (3.2a) – (3.2b) is given by $L(x_1, x_2, \lambda) := (x_1 - 1)^2 + (x_2 - 3)^2 + \lambda(x_1 + x_2 - 2)$ and hence the associated optimization dynamics can be written as

$$\dot{x}_1 := -2(x_1 - 1) - \lambda \quad (3.3a)$$

$$\dot{x}_2 := -2(x_2 - 3) - \lambda \quad (3.3b)$$

$$\dot{\lambda} := x_1 + x_2 - 2. \quad (3.3c)$$

There exists a unique saddle-point $(x_1^*, x_2^*, \lambda^*) = (0, 2, 2)$ for the Lagrangian L . We can verify that the Hessian of the Lagrangian L with respect to the primal variable x is positive definite when evaluated at the saddle-point $(0, 2, 2)$. Moreover, regularity and strict complementarity conditions are both satisfied by this saddle-point.

Then, following the convergence proof in [Arrow and Hurwicz \(1958\)](#), we choose the square distance of the dynamics' trajectory from the saddle-point $V := x_1^2 + (x_2 - 2)^2 + (\lambda - 2)^2$ as the Lyapunov candidate. Taking the derivative of V with respect to time along the trajectories of dynamics (3.3a) – (3.3c) yields

$$\begin{aligned} \dot{V} &= -2x_1(2x_1 - 2 + \lambda) - 2(x_2 - 2)(2x_2 - 6 + \lambda) + 2(\lambda - 2)(x_1 + x_2 - 2) \\ &= -4x_1^2 - 4(x_2 - 2)^2 \end{aligned} \quad (3.4)$$

where all terms involving the dual variable λ have been canceled out. Then \dot{V} is only negative semi-definite, because we have $\dot{V} = 0$ along the whole vector space $(0, 2, \lambda)$ with any $\lambda \in \mathbb{R}^+$. To further prove the asymptotic convergence of the saddle-point $(0, 2, 2)$, one must invoke LaSalle's invariance principle. Now we can clearly see that such a square distance cannot be used as a valid Lyapunov function without the help of LaSalle's invariance principle.

To bridge these technical gaps, in this work we alternatively choose a quadratic Lyapunov function by solving the associated Lyapunov equation. We can prove that the derivative of our Lyapunov function is negative definite along the system's trajectories, and thus we do not need to invoke LaSalle's invariance principle anymore.

Now we are ready to present the proof of Theorem 10.

3.3.1 Initialization

Suppose that (x^*, λ^*, ν^*) is a strictly complementary KKT point of problem (2.4a) – (2.4c).

Define $\mathcal{P} := \{(x, \lambda, \nu) \mid \lambda \geq 0\}$ and $B_\delta := \{(x, \lambda, \nu) \mid \|(x, \lambda, \nu) - (x^*, \lambda^*, \nu^*)\| \leq \delta\}$ as a closed ball centered at (x^*, λ^*, ν^*) with radius δ . A neighborhood of (x^*, λ^*, ν^*) in \mathcal{P} is defined of the form $B_\delta \cap \mathcal{P}$. Choose a small $\delta_0 > 0$ such that for any point $(x, \lambda, \nu) \in B_{\delta_0} \cap \mathcal{P}$, we have

$$(i) \ \lambda_i > 0 \text{ if } i \in \mathcal{I} \quad \text{and} \quad (ii) \ g_i(x) < 0 \text{ if } i \notin \mathcal{I}.$$

Recall that \mathcal{I} is defined in Section 2.3 as the set containing indices associated with the active inequality constraints that are evaluated at (x^*, λ^*, ν^*) . Both parts of this initialization are achievable, since $\lambda_i^* > 0$ for all $i \in \mathcal{I}$ (by the strict complementarity), and the functions $g_i(x)$ are continuous and $g_i(x^*) < 0$ for all $i \notin \mathcal{I}$.

3.3.2 The R-S-T Systems

Let $0 < \delta^* \leq \delta_0$ be another small positive number, and the value of δ^* will be determined later (see the proof of Lemma 2). Let (x^0, λ^0, ν^0) be an arbitrary initial point that belongs to the neighborhood $B_{\delta^*} \cap \mathcal{P}$. Elements of the initial multiplier λ^0 can be divided into three classes based on their values and their indices: (i) $\lambda_r^0 > 0$ where $r \in \mathcal{I}$; (ii) $\lambda_s^0 > 0$ where $s \notin \mathcal{I}$; and (iii) $\lambda_t^0 = 0$ where $t \notin \mathcal{I}$.

According to the above classification, we define the following (R_0, S_0, T_0) system

$$\dot{x} := -\nabla_x L(x, \lambda, \nu) \quad (3.5a)$$

$$\dot{\nu}_j := h_j(x) \quad \text{for } j = 1, \dots, q \quad (3.5b)$$

$$\dot{\lambda}_r := g_r(x) \quad \text{if } r \in \mathcal{I} \quad (3.5c)$$

$$\dot{\lambda}_s := g_s(x) \quad \text{if } s \notin \mathcal{I} \text{ and } \lambda_s^0 > 0 \quad (3.5d)$$

$$\dot{\lambda}_t := 0 \quad \text{if } t \notin \mathcal{I} \text{ and } \lambda_t^0 = 0. \quad (3.5e)$$

Note that the (R_0, S_0, T_0) system (3.5a) – (3.5e) is locally Lipschitz everywhere in x , λ , and ν , since functions $f(x)$, $g_i(x)$, and $h_j(x)$, for all $i = 1, \dots, p$ and $j = 1, \dots, q$, are continuously differentiable. We would like to show that the (R_0, S_0, T_0) system has a unique solution inside the neighborhood $B_{\delta^*} \cap \mathcal{P}$.

Define the errors $\tilde{x} := x - x^*$, $\tilde{\lambda} := \lambda - \lambda^*$, and $\tilde{\nu} := \nu - \nu^*$. Then the (R_0, S_0, T_0) system can be equivalently transformed into the following error dynamics. Here, we apply the Taylor expansion at (x^*, λ^*, ν^*) .

$$\dot{\tilde{x}} = -H(x^*, \lambda^*, \nu^*)\tilde{x} - \sum_j \nabla h_j(x^*)\tilde{\nu}_j - \sum_r \nabla g_r(x^*)\tilde{\lambda}_r - \sum_s \nabla g_s(x^*)\tilde{\lambda}_s + \mathcal{O}(\tilde{x}) \quad (3.6a)$$

$$\dot{\tilde{\nu}}_j = \nabla h_j(x^*)^T \tilde{x} + \mathcal{O}_j(\tilde{x}) \quad (3.6b)$$

$$\dot{\tilde{\lambda}}_r = \nabla g_r(x^*)^T \tilde{x} + \mathcal{O}_r(\tilde{x}) \quad (3.6c)$$

$$\dot{\tilde{\lambda}}_s = g_s(x^*) + \nabla g_s(x^*)^T \tilde{x} + \mathcal{O}_s(\tilde{x}) \quad (3.6d)$$

$$\dot{\tilde{\lambda}}_t = 0 \quad (3.6e)$$

where $H(x^*, \lambda^*, \nu^*)$ denotes the Hessian of the Lagrangian (2.5) with respect to x evaluated at (x^*, λ^*, ν^*) . We have also applied the KKT condition (2.6a) in dynamics (3.6a), $h_j(x^*) = 0$ in dynamics (3.6b), $g_r(x^*) = 0$ in dynamics (3.6c), and $\tilde{\lambda}_t \equiv 0$ in dynamics (3.6e), respectively. Moreover, $\mathcal{O}(\tilde{x})$, $\mathcal{O}_j(\tilde{x})$, $\mathcal{O}_r(\tilde{x})$, and $\mathcal{O}_s(\tilde{x})$ are all higher order terms in \tilde{x} .

Lemma 1. *Suppose that all the conditions in Theorem 10 hold. Let all indices $r \in \mathcal{I}$ be labeled as $r_1, \dots, r_{|\mathcal{I}|}$, where $|\mathcal{I}|$ denotes the cardinality of \mathcal{I} . Define $D(x^*)$ as the matrix that stacks*

all the gradient vectors

$$D(x^*) := \begin{bmatrix} \nabla h_1(x^*) & \cdots & \nabla h_q(x^*) & \nabla g_{r_1}(x^*) & \cdots & \nabla g_{r_{|I|}}(x^*) \end{bmatrix} \in \mathbb{R}^{n \times (q+|I|)}.$$

Then the Jacobian

$$J := \begin{bmatrix} -H(x^*, \lambda^*, \nu^*) & -D(x^*) \\ D(x^*)^T & \mathbf{0} \end{bmatrix} \in \mathbb{R}^{(n+q+|I|) \times (n+q+|I|)}$$

is Hurwitz, i.e., all eigenvalues of J have negative real parts.

Proof of Lemma 1. Because the two diagonal blocks of the Jacobian J are respectively given by $-H(x^*, \lambda^*, \nu^*) \prec 0$ and $\mathbf{0}$, according to the Bendixson's Theorem in [Marshall and Olkin \(1979\)](#), all eigenvalues of J must have non-positive real parts. To further prove J is Hurwitz, we need to show that J has no zero or purely imaginary eigenvalues.

Let us first suppose, for the sake of contradiction, that J has a zero eigenvalue with an associated eigenvector $z = [z_1^T \ z_2^T]^T \neq 0$. That is, we have

$$-H(x^*, \lambda^*, \nu^*)z_1 - D(x^*)z_2 = 0 \quad (3.7)$$

$$D(x^*)^T z_1 = 0. \quad (3.8)$$

Left-multiplying (3.7) with z_1^T yields

$$-z_1^T H(x^*, \lambda^*, \nu^*) z_1 - z_1^T D(x^*) z_2 = -z_1^T H(x^*, \lambda^*, \nu^*) z_1 = 0 \quad (3.9)$$

where we have applied (3.8) in the second step. Since $H(x^*, \lambda^*, \nu^*) \succ 0$, (3.9) implies $z_1 = 0$. Substituting $z_1 = 0$ back into (3.7) we get $D(x^*)z_2 = 0$. Also, by the regularity Assumption 2, $D(x^*)$ has a full column rank, which implies z_2 is also zero. This contradicts our assumption that $z \neq 0$. Hence, J does not have any zero eigenvalues.

Next, for the sake of contradiction, let us suppose that J has a pair of purely imaginary eigenvalues $\pm i\mu$, where $\mu \in \mathbb{R}$ and $\mu > 0$. Let $a + ib \neq 0$ be an eigenvector associated with the eigenvalue $i\mu$, where $a = [a_1^T \ a_2^T]^T$ and $b = [b_1^T \ b_2^T]^T$ are real vectors. So we have

$$J(a + jb) = i\mu(a + ib) = -\mu b + i\mu a. \quad (3.10)$$

which implies that $Ja = -\mu b$ and $Jb = \mu a$. Now left-multiplying these two identities with a^T and $-b^T$, respectively, we obtain

$$a^T Ja = -\mu a^T b = -\mu b^T a = -b^T Jb. \quad (3.11)$$

However, we also notice that

$$a^T Ja = -a_1^T H(x^*, \lambda^*, \nu^*) a_1 \leq 0 \quad \text{and} \quad b^T Jb = -b_1^T H(x^*, \lambda^*, \nu^*) b_1 \leq 0. \quad (3.12)$$

Hence, we must have $a_1^T H(x^*, \lambda^*, \nu^*) a_1 = b_1^T H(x^*, \lambda^*, \nu^*) b_1 = 0$, which implies $a_1 = b_1 = 0$ since $H(x^*, \lambda^*, \nu^*) \succ 0$. Thus $Ja = -\mu b$ and $Jb = \mu a$ can be simplified as $D(x^*)a_2 = -\mu b_1 = 0$ and $D(x^*)b_2 = \mu a_1 = 0$. Again, applying the regularity Assumption 2 that $D(x^*)$ has a full column rank, we must have $a_2 = b_2 = 0$, which contradicts our assumption that $a + ib \neq 0$. Therefore, J does not have any purely imaginary eigenvalues, either. \square

Lemma 1 can help us construct a Lyapunov function for the error dynamics (3.6a) – (3.6e).

Lemma 2. *Suppose that all the conditions in Theorem 10 hold. There is a Lyapunov function V and a small positive number δ^* such that the derivative \dot{V} along the trajectories of the error dynamics (3.6a) – (3.6e) is strictly less than zero inside the closed neighborhood $B_{\delta^*} \cap \mathcal{P}$.*

Proof of Lemma 2. As we have shown in Lemma 1, the Jacobian J is a Hurwitz matrix under the conditions of Theorem 10. Hence, by Theorem 9, we know that for any given symmetric $Q \succ 0$ there is a unique symmetric $P \succ 0$ satisfying $PJ + J^T P = -Q$. Now suppose that

$$P = \begin{bmatrix} P_{11} & P_{12} \\ P_{12}^T & P_{22} \end{bmatrix} \succ 0$$

is the corresponding solution to the Lyapunov equation, with blocks P_{11} , P_{12} , and P_{22} having appropriate dimensions. Also define $\tilde{u} := [\tilde{\nu}_1 \cdots \tilde{\nu}_q \tilde{\lambda}_{r_1} \cdots \tilde{\lambda}_{r_{|Z|}}]^T \in \mathbb{R}^{q+|Z|}$, $\tilde{v} := [\tilde{x}^T \tilde{u}^T]^T \in \mathbb{R}^{n+q+|Z|}$, and $\tilde{w} := [\mathcal{O}(\tilde{x})^T \mathcal{O}_{j_1}(\tilde{x}) \cdots \mathcal{O}_{j_q}(\tilde{x}) \mathcal{O}_{r_1}(\tilde{x}) \cdots \mathcal{O}_{r_{|Z|}}(\tilde{x})]^T \in \mathbb{R}^{n+q+|Z|}$. Then we may choose the following Lyapunov candidate

$$V(\tilde{x}, \tilde{\lambda}, \tilde{\nu}) = \tilde{v}^T P \tilde{v} + \sum_s \tilde{\lambda}_s^2 + \sum_t \tilde{\lambda}_t^2 \quad (3.13)$$

for the error dynamics (3.6a) – (3.6e).

The derivative of (3.13) along the trajectories of the error dynamics (3.6a) – (3.6e) is

$$\dot{V} = -\tilde{v}^T Q \tilde{v} + 2\tilde{v}^T P \tilde{w} + 2 \left\{ \sum_s \tilde{\lambda}_s \left[g_s(x^*) + \nabla g_s(x^*)^T (\tilde{x} - P_{11}\tilde{x} - P_{12}\tilde{u}) + \mathcal{O}_s(\tilde{x}) \right] \right\}. \quad (3.14)$$

Let us look at the first two terms $-\tilde{v}^T Q \tilde{v} + 2\tilde{v}^T P \tilde{w}$ in (3.14). Since \tilde{w} is a higher order term in \tilde{x} , we have $\|\tilde{w}\|/\|\tilde{v}\| \rightarrow 0$ as $\|\tilde{v}\| \rightarrow 0$. Hence, for any $\varepsilon > 0$, there exists a small $\delta > 0$ such that $\|\tilde{w}\| < \varepsilon\|\tilde{v}\|$ for all $\|\tilde{v}\| < \delta$. Therefore, we have $\tilde{v}^T P \tilde{w} < \varepsilon\|P\|\|\tilde{v}\|^2$ for all $\|\tilde{v}\| < \delta$. Let $\mu_{\min} > 0$ denote the minimum eigenvalue of Q . We can choose a δ_1 such that $\varepsilon < \frac{1}{2}\mu_{\min}/\|P\|$. Then we have $-\tilde{v}^T Q \tilde{v} + 2\tilde{v}^T P \tilde{w} < (2\varepsilon\|P\| - \mu_{\min})\|\tilde{v}\|^2 < 0$ for all $\|\tilde{v}\| < \delta_1$ and $\tilde{v} \neq 0$.

We next consider the remaining terms in (3.14). Recall that for all indices $s \notin \mathcal{I}$, we have $\lambda_s^* = 0$ and $g_s(x^*) < 0$ by the strict complementarity condition. When the trajectories of λ_s remain strictly inside the non-negative orthant, we have $\tilde{\lambda}_s = \lambda_s - \lambda_s^* = \lambda_s > 0$. Moreover, since the term $\nabla g_s(x^*)^T (\tilde{x} - P_{11}\tilde{x} - P_{12}\tilde{u}) + \mathcal{O}_s(\tilde{x})$ is a function of \tilde{x} , $\tilde{\lambda}_r$, and $\tilde{\nu}$, we can always find a small neighborhood of (x^*, λ^*, ν^*) in \mathcal{P} with a radius δ_2 such that the negative $g_s(x^*)$ terms dominate for all indices $s \notin \mathcal{I}$, i.e.,

$$g_s(x^*) + \nabla g_s(x^*)^T (\tilde{x} - P_{11}\tilde{x} - P_{12}\tilde{u}) + \mathcal{O}_s(\tilde{x}) < 0, \quad \forall s \notin \mathcal{I}. \quad (3.15)$$

Then we choose $\delta^* = \min\{\delta_0, \delta_1, \delta_2\}$ and the Lyapunov derivative along the trajectories of the error dynamics (3.6a) – (3.6e) is negative definite over $B_{\delta^*} \cap \mathcal{P}$. \square

The result of Lemma 2 implies the following facts:

- If started from an initial point $(x^0, \lambda^0, \nu^0) \in B_{\delta^*} \cap \mathcal{P}$ and when the λ_s states remain inside the positive orthant, the trajectories of x , λ_r , and ν are shrinking towards x^* , λ_r^* , and ν^* with respect to dynamics (3.5a) – (3.5c).
- Since the trajectories of x , λ_r , and ν cannot escape from $B_{\delta^*} \cap \mathcal{P}$, the λ_s states will keep decreasing towards zero with respect to dynamics (3.5d).
- According to dynamics (3.5e), the λ_t states remain zero all the time.
- Due to the locally Lipschitz continuity as well as the Lyapunov stability, by Theorem 7 the (R_0, S_0, T_0) system (3.5a) – (3.5e) has a unique solution.

3.3.3 Existence and Uniqueness of the Solution

In this subsection, we present the proof for the first statement of Theorem 10.

Proof of Theorem 10, Statement 1. By the definition of positive projections, the optimization dynamics (3.1a) – (3.1c) is the same as the (R_0, S_0, T_0) system (3.5a) – (3.5e) when started from any initial condition $(x^0, \lambda^0, \nu^0) \in B_{\delta^*} \cap \mathcal{P}$. Hence, dynamics (3.1a) – (3.1c) has the same solution as the (R_0, S_0, T_0) system until some λ_s state in the (R_0, S_0, T_0) system reaches zero. Suppose the states at this time instant is given by (x^1, λ^1, ν^1) . We know that (x^1, λ^1, ν^1) still belongs to $B_{\delta^*} \cap \mathcal{P}$. We can redefine the (R_1, S_1, T_1) system based on the new initial condition.

The new dynamics of x , λ_r , and ν in the (R_1, S_1, T_1) system are the same as those in the (R_0, S_0, T_0) system. The only difference between the (R_1, S_1, T_1) and the (R_0, S_0, T_0) systems is that the (R_1, S_1, T_1) system has less λ_s states and more λ_t states, because some λ_s state in the (R_0, S_0, T_0) system has changed into a λ_t state in the (R_1, S_1, T_1) system. It is not difficult to show that the same Lyapunov function (3.13) still works for the (R_1, S_1, T_1) system. Same as before, by both the locally Lipschitz continuity and the Lyapunov stability, the (R_1, S_1, T_1) system also has a unique solution.

Repeating the above procedure, there must be a finite K (the number of λ_s states is finite) such that the (R_K, S_K, T_K) system starting from the initial condition $(x^K, \lambda^K, \nu^K) \in B_{\delta^*} \cap \mathcal{P}$ does not have any λ_s states. Moreover, the (R_K, S_K, T_K) system has a unique solution for all the time due to the disappearance of λ_s states. We can piece together all the unique solutions of the $K + 1$ dynamical systems $(R_0, S_0, T_0), \dots, (R_K, S_K, T_K)$ by following the correct time sequence, and obtain a unique solution for dynamics (3.1a) – (3.1c). This proves existence and uniqueness of the solution for the optimization dynamical system. \square

3.3.4 Locally Asymptotic Stability

In this subsection, we present the proof for the second statement of Theorem 10.

Proof of Theorem 10, Statement 2. As discussed above, there must finally exist a (R_K, S_K, T_K) system such that it has no λ_s states. In other words, the (S_K, R_K, T_K) system has only λ_t states and $\lambda_t \equiv \lambda_t^* = 0$ for all $t \notin \mathcal{I}$.

Moreover, because the derivative of the Lyapunov function (3.13) along the trajectories of the (R_K, S_K, T_K) system is negative definite over $B_{\delta^*} \cap \mathcal{P}$, we conclude that the trajectories of x, λ_r, ν are locally asymptotically stable, i.e., $\lim_{t \rightarrow \infty} (x, \lambda_r, \nu) = (x^*, \lambda_r^*, \nu^*)$. \square

3.4 Summary

This chapter has introduced the continuous-time optimization dynamics for solving general optimization problems. The basic idea of this approach is to seek a KKT point as the dynamical system evolves. It has been shown that, if there exists a strictly complementary KKT point at which the evaluated Hessian of the associated Lagrangian with respect to the primal variable is positive definite, then the optimization dynamics locally has a unique solution which converges asymptotically to the desired KKT point.

The continuous-time optimization dynamics approach has been successfully applied to solve convex problems, because the KKT conditions are both necessary and sufficient for optimality there. As for general optimization problems, however, this may not be true. Therefore, when a KKT point of a general optimization problem is found, we should also check whether or not it is a global optimum. In the next chapter, we will discuss this topic in details for a specific class of optimizations, the non-convex quadratically constrained quadratic programmings.

CHAPTER 4. THE NON-CONVEX QCQP PROBLEMS

In Chapter 3, we have introduced a continuous-time optimization dynamics approach to study the general optimization problem (2.4a) – (2.4c) by searching the KKT points. Due to the possible non-convexity of (2.4a) – (2.4c), however, the KKT conditions are only necessary for local optimality. Then, once a KKT point is found by our optimization dynamical system, one would ask whether or not it is a global optimum.

In this chapter, we answer the above question for a specific class of optimizations, namely, the non-convex quadratically constrained quadratic programmings (QCQPs). The non-convex QCQPs have widely applications, e.g., Boolean least squares, minimum cardinality problems, two way partitioning, and polynomial minimizations. Certain problems are classic in networked optimizations, e.g., the MAXCUT and OPF problems, see [d’Aspremont and Boyd \(2003\)](#) and [Lavaei and Low \(2012\)](#). However, these problems are NP-hard and difficult to solve. Popular approaches for solving those non-convex QCQPs are mainly based on convex relaxations.

This chapter, different from all those approaches above, studies the non-convex QCQPs via the continuous-time optimization dynamics without any convex relaxations. We can show the fact that, in addition to the KKT necessary conditions, one would only require a linear matrix inequality (LMI) to equivalently characterize the global optimality for non-convex QCQPs. Our result says, specifically, that a positive semi-definite Hessian of the associated Lagrangian, with respect to the primal variable and evaluated at a KKT point, implies the global optimality of a non-convex QCQP, and vice versa. In other words, under these circumstances KKT points and saddle-points are equivalent to each other. Moreover, if we assume the saddle-point is isolated, then we guarantee the asymptotic convergence of optimization dynamics to that saddle-point.

This chapter is organized as follows. In Section 4.1, we present a general formulation for the non-convex QCQPs and also derive their necessary and sufficient global optimality conditions.

In Section 4.2, we briefly review two convex relaxations, namely, the Lagrange dual relaxation and the semi-definite programming (SDP) relaxation, and then we build a connection between these relaxations. In Section 4.3, we argue that traditional primal-dual optimization methods such as sub-gradient and ADMM algorithms fail to solve non-convex QCQPs. Then we apply the optimization dynamics to the non-convex QCQPs in Section 4.4 and present a convergence analysis. In Section 4.5, we employ a MAXCUT problem example to show that its associated optimization dynamics is completely distributable. Finally, some more applications including the phase recovery problem and convex SOCPs are discussed in Sections 4.6 and 4.7.

4.1 Global Optimality Conditions

Consider a non-convex QCQP that is formulated as

$$\underset{x \in \mathbb{R}^n}{\text{minimize}} \quad x^T A_0 x + b_0^T x + c_0 \quad (4.1a)$$

$$\text{subject to} \quad x^T A_i x + b_i^T x + c_i \leq 0, \quad \forall i = 1, \dots, k \quad (4.1b)$$

$$x^T P_j x + q_j^T x + r_j = 0, \quad \forall j = 1, \dots, l \quad (4.1c)$$

where the parameters are $A_0, A_1, \dots, A_k, P_1, \dots, P_l \in \mathbb{S}^n$, $b_0, b_1, \dots, b_k, q_1, \dots, q_l \in \mathbb{R}^n$, and $c_0, c_1, \dots, c_k, r_1, \dots, r_l \in \mathbb{R}$. Here, we do not assume that matrices $A_0, A_1, \dots, A_k, P_1, \dots, P_l$ are positive semi-definite.

Assumption 3. *Problem (4.1a) – (4.1c) is strictly feasible and has a finite optimal solution.*

Let $\lambda = [\lambda_1 \ \dots \ \lambda_k]^T \in \mathbb{R}_+^k$ and $\nu = [\nu_1 \ \dots \ \nu_l]^T \in \mathbb{R}^l$, respectively, be the Lagrange multipliers associated with constraints (4.1b) and (4.1c). By Definition 5 the Lagrangian associated with QCQP (4.1a) – (4.1c) is given by

$$\begin{aligned} L(x, \lambda, \nu) &= x^T A_0 x + b_0^T x + c_0 + \sum_{i=1}^k \lambda_i (x^T A_i x + b_i^T x + c_i) + \sum_{j=1}^l \nu_j (x^T P_j x + q_j^T x + r_j) \\ &= x^T \left(A_0 + \sum_{i=1}^k \lambda_i A_i + \sum_{j=1}^l \nu_j P_j \right) x + \left(b_0^T + \sum_{i=1}^k \lambda_i b_i^T + \sum_{j=1}^l \nu_j q_j^T \right) x \\ &\quad + \left(c_0 + \sum_{i=1}^k \lambda_i c_i + \sum_{j=1}^l \nu_j r_j \right). \end{aligned} \quad (4.2)$$

From the Lagrangian (4.2), we can derive the KKT conditions for QCQP (4.1a) – (4.1c).

Let (x^*, λ^*, ν^*) be a KKT point of QCQP (4.1a) – (4.1c). Applying (2.6a) – (2.6e) we obtain

$$2 \left(A_0 + \sum_{i=1}^k \lambda_i^* A_i + \sum_{j=1}^l \nu_j^* P_j \right) x^* + b_0 + \sum_{i=1}^k \lambda_i^* b_i + \sum_{j=1}^l \nu_j^* q_j = 0 \quad (4.3a)$$

$$x^{*T} A_i x^* + b_i^T x^* + c_i \leq 0, \quad \forall i = 1, \dots, k \quad (4.3b)$$

$$x^{*T} P_j x^* + q_j^T x^* + r_j = 0, \quad \forall j = 1, \dots, l \quad (4.3c)$$

$$\lambda_i^* \geq 0, \quad \forall i = 1, \dots, k \quad (4.3d)$$

$$\lambda_i^* \left(x^{*T} A_i x^* + b_i^T x^* + c_i \right) = 0, \quad \forall i = 1, \dots, k. \quad (4.3e)$$

Because QCQP (4.1a) – (4.1c) may not be a convex optimization, by Theorem 2 we know that KKT conditions (4.3a) – (4.3e) are only necessary for local optimality.

The main result of this chapter is presented below. It reveals the fact that, due to certain structures of QCQP (4.1a) – (4.1c), the associated KKT points are equivalent to saddle-points (and hence globally optimal) provided that an additional linear matrix inequality (LMI) holds.

Theorem 11. *Suppose that the vector $(x^*, \lambda^*, \nu^*) \in \mathbb{R}^n \times \mathbb{R}_+^k \times \mathbb{R}^l$ is a KKT point of QCQP (4.1a) – (4.1c). Then (x^*, λ^*, ν^*) is also a saddle-point for the Lagrangian (4.2) if and only if*

$$A_0 + \sum_{i=1}^k \lambda_i^* A_i + \sum_{j=1}^l \nu_j^* P_j \succeq 0. \quad (4.4)$$

Proof of Theorem 11. We will prove this result by applying Definition 8. In other words, we would like to show that both inequalities in (2.8) hold for the Lagrangian (4.2).

Showing the left inequality in (2.8) is quite straight forward, because

$$\begin{aligned} & L(x^*, \lambda^*, \nu^*) - L(x^*, \lambda, \nu) \\ &= \sum_{i=1}^k (\lambda_i^* - \lambda_i) \left(x^{*T} A_i x^* + b_i^T x^* + c_i \right) + \sum_{j=1}^l (\nu_j^* - \nu_j) \left(x^{*T} P_j x^* + q_j^T x^* + r_j \right) \\ &= \sum_{i=1}^k -\lambda_i \left(x^{*T} A_i x^* + b_i^T x^* + c_i \right) \\ &\geq 0 \end{aligned} \quad (4.5)$$

where we have applied KKT conditions (4.3c) and (4.3e) at the second step. Then, inequality (4.5) easily follows from another KKT condition (4.3b) and $\lambda_i \geq 0$, for all $i = 1, \dots, k$.

Next we prove the right inequality in (2.8). We have

$$\begin{aligned}
& L(x, \lambda^*, \nu^*) - L(x^*, \lambda^*, \nu^*) \\
&= x^T \left(A_0 + \sum_{i=1}^k \lambda_i^* A_i + \sum_{j=1}^l \nu_j^* P_j \right) x \\
&\quad - x^{*T} \left(A_0 + \sum_{i=1}^k \lambda_i^* A_i + \sum_{j=1}^l \nu_j^* P_j \right) x^* + \left(b_0^T + \sum_{i=1}^k \lambda_i^* b_i^T + \sum_{j=1}^l \nu_j^* q_j^T \right) (x - x^*) \\
&= \left[(x - x^*) + x^* \right]^T \left(A_0 + \sum_{i=1}^k \lambda_i^* A_i + \sum_{j=1}^l \nu_j^* P_j \right) \left[(x - x^*) + x^* \right] \\
&\quad - x^{*T} \left(A_0 + \sum_{i=1}^k \lambda_i^* A_i + \sum_{j=1}^l \nu_j^* P_j \right) x^* + (x - x^*)^T \left(b_0 + \sum_{i=1}^k \lambda_i^* b_i + \sum_{j=1}^l \nu_j^* q_j \right) \\
&= (x - x^*)^T \left(A_0 + \sum_{i=1}^k \lambda_i^* A_i + \sum_{j=1}^l \nu_j^* P_j \right) (x - x^*) \\
&\quad + 2(x - x^*)^T \left(A_0 + \sum_{i=1}^k \lambda_i^* A_i + \sum_{j=1}^l \nu_j^* P_j \right) x^* + (x - x^*)^T \left(b_0 + \sum_{i=1}^k \lambda_i^* b_i + \sum_{j=1}^l \nu_j^* q_j \right) \\
&= (x - x^*)^T \left(A_0 + \sum_{i=1}^k \lambda_i^* A_i + \sum_{j=1}^l \nu_j^* P_j \right) (x - x^*) \\
&\quad + (x - x^*)^T \left[2 \left(A_0 + \sum_{i=1}^k \lambda_i^* A_i + \sum_{j=1}^l \nu_j^* P_j \right) x^* + b_0 + \sum_{i=1}^k \lambda_i^* b_i + \sum_{j=1}^l \nu_j^* q_j \right] \\
&= (x - x^*)^T \left(A_0 + \sum_{i=1}^k \lambda_i^* A_i + \sum_{j=1}^l \nu_j^* P_j \right) (x - x^*) \\
&\geq 0
\end{aligned} \tag{4.6}$$

where at the last step we have used KKT condition (4.3a) and LMI (4.4) to obtain inequality (4.6). From inequality (4.6) we also notice that $L(x, \lambda^*, \nu^*) - L(x^*, \lambda^*, \nu^*)$ can be expressed as a sum-of-squares (SOS) in terms of x .

It is a well-known result (Theorem 4) that any quadratic, multi-variate polynomial is non-negative if and only if it can be written in an SOS form. Turning back to our case, because $L(x, \lambda^*, \nu^*) - L(x^*, \lambda^*, \nu^*)$ is indeed a quadratic polynomial in vector $x \in \mathbb{R}^n$, we conclude that inequality (4.6) holds if and only if LMI (4.4) is satisfied. Now, combining both inequalities (4.5) and (4.6) completes the proof. \square

Remark 4. *KKT conditions (4.3a) – (4.3e) and LMI (4.4) have together characterized the global optimality for QCQP (4.1a) – (4.1c). If QCQP (4.1a) – (4.1c) is convex or degrades to a linear programming (LP), then LMI (4.4) will always be satisfied. Under these circumstances, KKT conditions (4.3a) – (4.3e) themselves become the necessary and sufficient global optimality conditions.*

4.2 Relations to the Convex Relaxations

This section briefly reviews two convex relaxation approaches that have been developed for studying the non-convex QCQPs. These relaxations are the Lagrange dual relaxation and the SDP relaxation, respectively. We also build relations between these relaxations and our global optimality conditions derived in the previous section.

4.2.1 The Lagrange Dual Relaxation

Let us first discuss about the QCQP's global optimality conditions (4.3a) – (4.3e) and (4.4) from the Lagrange dual point of view. The Lagrange dual of QCQP (4.1a) – (4.1c) is given by

$$\underset{\xi, \eta, \gamma}{\text{maximize}} \quad \gamma \quad (4.7a)$$

$$\text{subject to} \quad \xi \geq 0 \quad (4.7b)$$

$$\begin{bmatrix} A_0 + \sum_{i=1}^k \xi_i A_i + \sum_{j=1}^l \eta_j P_j & \frac{1}{2} \left(b_0 + \sum_{i=1}^k \xi_i b_i + \sum_{j=1}^l \eta_j q_j \right) \\ \frac{1}{2} \left(b_0 + \sum_{i=1}^k \xi_i b_i + \sum_{j=1}^l \eta_j q_j \right)^T & c_0 + \sum_{i=1}^k \xi_i c_i + \sum_{j=1}^l \eta_j r_j - \gamma \end{bmatrix} \succeq 0 \quad (4.7c)$$

whose optimum $(\xi^*, \eta^*, \gamma^*)$ directly satisfies conditions (4.3d) and (4.4), according to the dual constraints (4.7b) and (4.7c). Also suppose that x^* is an optimal solution to the primal QCQP (4.1a) – (4.1c), then x^* must be primal feasible. Thus, conditions (4.3b) and (4.3c) are satisfied.

One fact we should notice is that during the derivation of the Lagrange dual (4.7a) – (4.7c), we have already applied condition (4.3a) to minimize the Lagrangian (4.2) with respect to the primal variable x . Therefore, condition (4.3a) is satisfied at (x^*, ξ^*, η^*) , too.

Now the only condition left is the complementary slackness (4.3e). We have already known that if there exists a zero duality gap between QCQP (4.1a) – (4.1c) and its Lagrange dual (4.7a) – (4.7c), then the complementary slackness (4.3d) holds, see Boyd and Vandenberghe (2004). Conversely, if the complementary slackness (4.3d) is satisfied, by Theorems 11 and 3, we conclude that strong duality holds between problems (4.1a) – (4.1c) and (4.7a) – (4.7c). In other words, the complementary slackness (4.3e) becomes a necessary and sufficient condition that characterizes strong duality between problems (4.1a) – (4.1c) and (4.7a) – (4.7c).

4.2.2 The SDP Relaxation

Alternatively, we can also formulate an SDP relaxation for the non-convex QCQP problem (4.1a) – (4.1c). Let us introduce a new matrix variable $W := xx^T$, then QCQP (4.1a) – (4.1c) can be equivalently written as

$$\underset{x \text{ and } W}{\text{minimize}} \quad \text{Tr}\{A_0W\} + b_0^T x + c_0 \quad (4.8a)$$

$$\text{subject to} \quad \text{Tr}\{A_iW\} + b_i^T x + c_i \leq 0, \quad \forall i = 1, \dots, k \quad (4.8b)$$

$$\text{Tr}\{P_jW\} + q_j^T x + r_j = 0, \quad \forall j = 1, \dots, l \quad (4.8c)$$

$$W = xx^T \quad (4.8d)$$

where all the objective function and constraints (4.8a) – (4.8c) are linear in x and W , while the only non-convex constraint comes from (4.8d). Then we can replace (4.8d) with a convex SDP constraint $W - xx^T \succeq 0$ and obtain

$$\underset{x \text{ and } W}{\text{minimize}} \quad \text{Tr}\{A_0W\} + b_0^T x + c_0 \quad (4.9a)$$

$$\text{subject to} \quad \text{Tr}\{A_iW\} + b_i^T x + c_i \leq 0, \quad \forall i = 1, \dots, k \quad (4.9b)$$

$$\text{Tr}\{P_jW\} + q_j^T x + r_j = 0, \quad \forall j = 1, \dots, l \quad (4.9c)$$

$$\begin{bmatrix} W & x \\ x^T & 1 \end{bmatrix} \succeq 0. \quad (4.9d)$$

Note that the last constraint (4.9d) has equivalently expressed $W - xx^T \succeq 0$ using the Schur complement. Now problem (4.9a) – (4.9d) becomes as a convex SDP, which is also called an SDP relaxation for QCQP (4.1a) – (4.1c).

Theorem 12. *Suppose that the SDP relaxation (4.9a) – (4.9d) has an optimal solution (x^*, W^*) . Then the SDP relaxation provides the same optimal cost as QCQP (4.1a) – (4.1c) if and only if the optimum W^* is rank-one with $W^* = (x^*)(x^*)^T$.*

Proof of Theorem 12. Necessity (\Rightarrow): Suppose that x^* is an optimal solution to the non-convex QCQP (4.1a) – (4.1c). Then, by definition, we may construct (x^*, W^*) with $W^* = (x^*)(x^*)^T$ as a solution to the SDP relaxation (4.9a) – (4.9d). Since the relaxation between (4.1a) – (4.1c) and (4.9a) – (4.9d) is tight, we know that (x^*, W^*) must be optimal to (4.9a) – (4.9d).

Sufficiency (\Leftarrow): Conversely, since (x^*, W^*) with $W^* = (x^*)(x^*)^T$ is an optimal solution to the SDP relaxation (4.9a) – (4.9d), we know that x^* must be a solution to the non-convex QCQP (4.1a) – (4.1c), which implies that the optimal cost of (4.1a) – (4.1c) is no more than that of (4.9a) – (4.9d). On the other hand, because (4.9a) – (4.9d) is a relaxation for problem (4.1a) – (4.1c), the optimal cost of (4.9a) – (4.9d) is no more than that of (4.1a) – (4.1c), either. Therefore, we conclude that the SDP relaxation (4.9a) – (4.9d) is tight. \square

4.2.3 Relations to the Global Optimality Conditions

Because both optimizations (4.7a) – (4.7c) and (4.9a) – (4.9d) are convex relaxations for the non-convex QCQP (4.1a) – (4.1c), an interesting question that one would ask is: what is the relationship between these two relaxations? Reference d’Aspremont and Boyd (2003) has shown that the Lagrange dual relaxation (4.7a) – (4.7c) and the SDP relaxation (4.9a) – (4.9d) are dual problems to each other. Since both relaxations are convex problems, under general assumptions for constraint qualification (e.g., Slater’s conditions), strong duality holds between them. In other words, both relaxations (4.7a) – (4.7c) and (4.9a) – (4.9d) provide a same lower bound for QCQP (4.1a) – (4.1c).

We next summarize the relation between the tightness of the SDP relaxation (4.9a) – (4.9d) and global optimality conditions (4.3a) – (4.3e) and (4.4).

Theorem 13. *Suppose that Slater’s conditions hold for the SDP relaxation (4.9a) – (4.9d). Then the SDP relaxation has a rank-one optimal solution with the same optimal cost as QCQP (4.1a) – (4.1c) if and only if global optimality conditions (4.3a) – (4.3e) and (4.4) are satisfied.*

Proof of Theorem 13. Necessity (\Rightarrow): If the SDP relaxation (4.9a) – (4.9d) is tight, by strong duality between relaxations (4.9a) – (4.9d) and (4.7a) – (4.7c), we conclude that there is a zero optimal duality gap between problems (4.1a) – (4.1c) and (4.7a) – (4.7c). By Theorem 3, it implies the existence of a saddle-point for the Lagrangian (4.2). Then Theorem 11 says that this saddle-point must satisfy global optimality conditions (4.3a) – (4.3e) and (4.4).

Sufficiency (\Leftarrow): If global optimality conditions (4.3a) – (4.3e) and (4.4) are satisfied, by Theorem 11 we know that there is a saddle-point for the Lagrangian (4.2). Moreover, Theorem 3 tells us that strong duality must hold between QCQP (4.1a) – (4.1c) and its Lagrange dual (4.7a) – (4.7c). Therefore, we conclude that the SDP relaxation (4.9a) – (4.9d) is tight, because strong duality also holds between the two relaxations (4.7a) – (4.7c) and (4.9a) – (4.9d). \square

Remark 5. *In the following sections we will show that the optimization dynamics associated with QCQP (4.1a) – (4.1c) may exhibit an intrinsic computation structure. In contrast, both convex relaxations (4.7a) – (4.7c) and (4.9a) – (4.9d) are not directly amenable to be solved by distributed optimization methods.*

4.3 Issues in the Application of Traditional Primal-Dual Algorithms

We note that in literature there are many discretized algorithms that are developed based on the primal-dual optimization idea, for example, the sub-gradient optimization method by Nedić and Ozdaglar (2009) and the alternating direction method of multipliers (ADMM) by Boyd et al. (2011). However, those algorithms are primarily conceived for solving convex problems, and hence are difficult or even problematic to be applied to non-convex optimizations. In this section, we point out several technical issues that appear in the application of these algorithms for solving non-convex QCQPs.

To simplify our presentation, we consider the following non-convex QCQP

$$\underset{x \in \mathbb{R}^n}{\text{minimize}} \quad x^T A_0 x \tag{4.10a}$$

$$\text{subject to} \quad x^T A_1 x + c_1 = 0 \tag{4.10b}$$

where $c_1 \neq 0$ and A_0 and A_1 may not be positive semi-definite matrices.

The Lagrangian associated with QCQP (4.10a) – (4.10b) is given by

$$L(x, \lambda) := x^T A_0 x + \lambda(x^T A_1 x + c_1) = x^T (A_0 + \lambda A_1) x + \lambda c_1 \quad (4.11)$$

and next we try to seek a saddle-point for the Lagrangian (4.11) via two traditional primal-dual optimization methods, namely, the sub-gradient and the ADMM algorithms.

4.3.1 The Sub-Gradient Method

Let us first focus on the sub-gradient method proposed by Nedić and Ozdaglar (2009). In that work the authors have studied the following *convex-concave* saddle-point problem

$$\min_{x \in X} \max_{\mu \in M} \mathcal{L}(x, \mu) \quad (4.12)$$

where X is a closed convex set in \mathbb{R}^n , M is a closed convex set in \mathbb{R}^m , and \mathcal{L} is a convex-concave function defined over $X \times M$. In particular, $\mathcal{L}(\cdot, \mu) : X \rightarrow \mathbb{R}$ is convex for every $\mu \in M$, and $\mathcal{L}(x, \cdot) : M \rightarrow \mathbb{R}$ is concave for every $x \in X$. This function $\mathcal{L}(x, \mu)$, in fact, can be viewed as a generalization of the Lagrangian associated with a convex optimization.

To solve problem (4.12), A. Nedić and A. Ozdaglar proposed a sub-gradient algorithm

$$x_{k+1} = \mathcal{P}_X[x_k - \alpha \mathcal{L}_x(x_k, \mu_k)] \quad \text{for } k = 0, 1, 2, \dots \quad (4.13a)$$

$$\mu_{k+1} = \mathcal{P}_M[\mu_k + \alpha \mathcal{L}_\mu(x_k, \mu_k)] \quad \text{for } k = 0, 1, 2, \dots \quad (4.13b)$$

where \mathcal{L}_x and \mathcal{L}_μ denote the gradient of \mathcal{L} with respect to x and μ , and \mathcal{P}_X and \mathcal{P}_M denote the projections on sets X and M , respectively.

If we would like to apply the sub-gradient method (4.13a) – (4.13b) to solve the non-convex QCQP (4.10a) – (4.10b), we will encounter some difficulties in the primal update (4.13a).

The reason is the following. We note that the feasible set X associated with the non-convex QCQP (4.10a) – (4.10b) is $X := \{x \in \mathbb{R}^n \mid x^T A_1 x + c_1 = 0\}$, which is a non-convex set. Consequently, computing the projection operation \mathcal{P}_X onto the feasible set X is generally very hard due to the non-convexity of set X . Therefore, we conclude that applying the sub-gradient method to solve non-convex QCQPs is problematic.

4.3.2 The ADMM Algorithm

Now let us turn to study the ADMM algorithm. Applying the ADMM algorithm in [Boyd et al. \(2011\)](#) to the Lagrangian (4.11) associated with non-convex QCQP (4.10a) – (4.10b), we obtain the following update law

$$x^{k+1} := \operatorname{argmin}_x L(x, \lambda^k) = \operatorname{argmin}_x x^T (A_0 + \lambda^k A_1) x \quad (4.14a)$$

$$\lambda^{k+1} := \lambda^k + \rho \left[(x^{k+1})^T A_1 x^{k+1} + c_1 \right] \quad (4.14b)$$

where ρ is some positive scaling for the dual update. Here we would like to argue that, because of the non-convexity of the Lagrangian (4.11) in terms of x , the primal update law (4.14a) in the ADMM algorithm may fail due to certain critical issues.

Suppose that after the $(k-1)$ -th iteration, we have already obtained a pair of primal and dual variables (x^k, λ^k) , and we next want to figure out the values of (x^{k+1}, λ^{k+1}) . Due to the non-positive semi-definiteness of matrices A_0 and A_1 , the matrix $(A_0 + \lambda^k A_1)$ can be either positive semi-definite or not positive semi-definite.

If $(A_0 + \lambda^k A_1)$ is not positive semi-definite, there must exist a normalized eigenvector v such that $(A_0 + \lambda^k A_1)v = -\alpha v$ with $-\alpha < 0$ being the corresponding negative eigenvalue of $(A_0 + \lambda^k A_1)$. In this case, we choose $x = tv$ with $t > 0$ and hence $x^T (A_0 + \lambda^k A_1) x = -\alpha t^2$. To minimize $x^T (A_0 + \lambda^k A_1) x$ we let $t \rightarrow \infty$, and therefore $x^T (A_0 + \lambda^k A_1) x = -\alpha t^2 \rightarrow -\infty$. Under this circumstance, the ADMM algorithm fails because $x^{k+1} = tv \rightarrow \infty$.

If $(A_0 + \lambda^k A_1)$ is positive semi-definite, then $x = 0$ is always a minimizer for the quadratic term $x^T (A_0 + \lambda^k A_1) x$. Suppose we choose $x^{k+1} = 0$, then by the dual update law (4.14b) we have $\lambda^{k+1} = \lambda^k + \rho c_1$. Although it seems that we have finished the update for (x^{k+1}, λ^{k+1}) , in fact we have fallen into another trap. On the one hand, if in the subsequent iterations the dual variable $\lambda^{k+1}, \lambda^{k+2}, \dots$ maintains the positive semi-definiteness of matrix $(A_0 + \lambda A_1)$, then the primal variable x^{k+1}, x^{k+2}, \dots will remain at the origin. As a result, after n iterations with n large enough, the dual variable $\lambda^{k+n} = \lambda^k + n\rho c_1$ will become unbounded. On the other hand, if at some l -th step we have $(A_0 + \lambda^{k+l} A_1) \not\geq 0$, then by our previous argument, the ADMM algorithm will fail again since the primal variable becomes unbounded.

4.4 The Associated Optimization Dynamics

After pointing out the technical issues related to the application of traditional primal-dual optimization algorithms, in this section we apply the continuous-time optimization dynamics to solve non-convex QCQPs. We show that our continuous-time optimization dynamics approach is more easily applicable than the existing sub-gradient and ADMM algorithms. Moreover, our optimization dynamics approach guarantees a local convergence to the saddle-points associated with non-convex QCQPs provided they exist.

From definitions (3.1a) – (3.1c), the optimization dynamical system associated with problem (4.1a) – (4.1c) can be formulated as

$$\dot{x} = -2 \left(A_0 + \sum_{i=1}^k \lambda_i A_i + \sum_{j=1}^l \nu_j P_j \right) x - b_0 - \sum_{i=1}^k \lambda_i b_i - \sum_{j=1}^l \nu_j q_j \quad (4.15a)$$

$$\dot{\lambda}_i = \left[x^T A_i x + b_i^T x + c_i \right]_{\lambda_i}^+ \quad \forall i = 1, \dots, k \quad (4.15b)$$

$$\dot{\nu}_j = x^T P_j x + q_j^T x + r_j \quad \forall j = 1, \dots, l. \quad (4.15c)$$

4.4.1 Convergence Analysis

We notice that any equilibrium to optimization dynamics (4.15a) – (4.15c) satisfies KKT conditions (4.3a) – (4.3e). By Theorem 11, we know that if the LMI condition (4.4) is satisfied then this equilibrium must be a saddle-point for the Lagrangian (4.2), and vice versa.

Luckily, the matrix that appears in (4.4) is indeed the Hessian of the Lagrangian (4.2) with respect to the primal variable and evaluated at the given equilibrium. It turns out that we can apply Theorem 10 here to describe the saddle-point's locally asymptotic stability with respect to optimization dynamics (4.15a) – (4.15c).

Theorem 14. *Suppose that QCQP (4.1a) – (4.1c) has a strictly complementary KKT point (x^*, λ^*, ν^*) . Also suppose that x^* is regular. If $A_0 + \sum_{i=1}^k \lambda_i^* A_i + \sum_{j=1}^l \nu_j^* P_j \succ 0$, then there is a small neighborhood around (x^*, λ^*, ν^*) such that*

- *Optimization dynamics (4.15a) – (4.15c) has a unique solution within this neighborhood;*
- *Any trajectory starting inside this neighborhood converges to (x^*, λ^*, ν^*) asymptotically.*

Proof of Theorem 14. This is a direct result derived from Theorem 10. \square

Compared with Theorem 11, the convergence analysis given in Theorem 14 is conservative. We require the LMI condition (4.4) to be positive definite, not positive semi-definite. Moreover, we need to assume both regularity and strict complementarity. All of these conditions ensure that the saddle-point under study is an isolated point. Specifically, the positive definiteness of the Hessian of the Lagrangian guarantees the local uniqueness of the primal optimum, while regularity and strict complementarity guarantee the local uniqueness of the dual optimum.

We will leave the extension of positive semi-definite cases to future research. Here let us just consider an extreme case. If we have $A_0 = A_1 = \dots = A_k = P_1 = \dots = P_l = 0$, then the non-convex QCQP (4.1a) – (4.1c) degrades to an LP. In this case, the LMI condition (4.4) is still satisfied because it is always zero. However, we know from Arrow and Hurwicz (1958) that the optimization dynamics associated with an LP may oscillate and hence does not converge to any equilibrium. One direction we can explore to handle these cases is to add appropriate quadratic augmentation terms in the Lagrangian. It has been shown in Wang and Elia (2016) that this approach works for convex problems.

Corollary 1. *Suppose that dynamics (4.15a) – (4.15c) converges to an equilibrium (x^*, λ^*, ν^*) . Then (x^*, λ^*, ν^*) is a saddle-point for the Lagrangian (4.2) if it satisfies LMI condition (4.4).*

Proof of Corollary 1. This is a direct result by applying Theorem 11. \square

Another point we need to point out is that, for certain networked non-convex QCQPs, their coefficient matrices $A_0, A_1, \dots, A_k, P_1, \dots, P_l$ can be viewed as parts of the weighted Laplacian matrix, and hence they reflect some topological information about network's connection. Under these circumstances, the associated optimization dynamics (4.15a) – (4.15c) will exhibit a nice, distributed computation structure. In the Section 4.5, we will present a two-way partitioning example to illustrate this property.

4.4.2 Global Convergence Analysis for Equality-Constrained QCQPs

In the previous subsection, we have proved a local convergence result for the optimization dynamics associated with non-convex QCQPs. A natural question that one would ask is: Can

we talk about the behavior of dynamics (4.15a) – (4.15c) in a global sense? Generally speaking, it is difficult to develop a global convergence analysis for the optimization dynamical system (4.15a) – (4.15c), due to the non-linearity and positive projections. Nevertheless, we can present more discussions about the optimization dynamics if the original QCQP problem only contains quadratic equality constraints.

Let us consider an equality constrained non-convex QCQP

$$\underset{x \in \mathbb{R}^n}{\text{minimize}} \quad x^T A_0 x + b_0^T x + c_0 \quad (4.16a)$$

$$\text{subject to} \quad x^T A_i x + b_i^T x + c_i = 0, \quad \forall i = 1, \dots, m \quad (4.16b)$$

where $A_0, A_1, \dots, A_m \in \mathbb{S}^n$, $b_0, b_1, \dots, b_m \in \mathbb{R}^n$, and $c_0, c_1, \dots, c_m \in \mathbb{R}$, with $m \leq n$. Same as before, we assume that QCQP (4.16a) – (4.16b) is feasible and has a finite optimal solution. Due to the non-convexity of QCQP (4.16a) – (4.16b), it may have multiple local minimizers.

Let $\lambda \in \mathbb{R}^m$ be the Lagrange multiplier associated with constraint (4.16b). Following from definitions (3.1a) – (3.1c), the optimization dynamics associated with (4.16a) – (4.16b) is

$$\dot{x} = -2 \left(A_0 + \sum_{i=1}^m \lambda_i A_i \right) x - \left(b_0 + \sum_{i=1}^m \lambda_i b_i \right) \quad (4.17a)$$

$$\dot{\lambda}_i = x^T A_i x + b_i^T x + c_i, \quad \forall i = 1, \dots, m \quad (4.17b)$$

where we do not need positive projections since the problem is only equality constrained.

Because of the possible existence of multiple KKT points of QCQP (4.16a) – (4.16b), we know that the associated optimization dynamics (4.17a) – (4.17b) may have multiple equilibria. In fact, the equilibrium points of (4.17a) – (4.17b) can be divided into two disjoint sets

$$\mathcal{Q}_1 := \left\{ (x^*, \lambda^*) \text{ is KKT} \mid A_0 + \sum_{i=1}^m \lambda_i^* A_i \succeq 0 \right\}$$

$$\mathcal{Q}_2 := \left\{ (\bar{x}, \bar{\lambda}) \text{ is KKT} \mid A_0 + \sum_{i=1}^m \bar{\lambda}_i A_i \not\succeq 0 \right\}.$$

According to Theorem 11, \mathcal{Q}_1 contains all the saddle-points, whereas \mathcal{Q}_2 contains other KKT points that are not saddle-points. Of course, we would like the optimization dynamical system converges to \mathcal{Q}_1 but diverges from \mathcal{Q}_2 . To achieve this goal, we may modify the optimization

dynamics (4.17a) – (4.17b) as

$$\dot{z} = -2\alpha^2 \left(A_0 + \sum_{i=1}^m \xi_i A_i \right) z - \alpha \left(b_0 + \sum_{i=1}^m \xi_i b_i \right) \quad (4.18a)$$

$$\dot{\xi}_i = \alpha^2 z^T A_i z + \alpha b_i^T z + c_i, \quad \forall i = 1, \dots, m \quad (4.18b)$$

where $\alpha > 0$ is some constant parameter that scales the primal variable x . It is easy to check that if $(\bar{x}, \bar{\lambda})$ is an equilibrium of dynamics (4.17a) – (4.17b), then $(\bar{x}/\alpha, \bar{\lambda})$ is an equilibrium of dynamics (4.18a) – (4.18b), and vice versa.

Now we can analyze the stability of dynamics (4.18a) – (4.18b) by studying its linearized systems. We define $B(z) = [A_1 z \ \dots \ A_m z] \in \mathbb{R}^{n \times m}$ and $C = [\frac{1}{2} b_1 \ \dots \ \frac{1}{2} b_m] \in \mathbb{R}^{n \times m}$, then the Jacobian matrix associated with dynamics (4.18a) – (4.18b) is given by

$$J(z, \xi) = 2 \begin{bmatrix} -\alpha^2 \left(A_0 + \sum_{i=1}^m \xi_i A_i \right) & -\alpha^2 B(z) - \alpha C \\ \alpha^2 B(z)^T + \alpha C^T & \mathbf{0} \end{bmatrix} \in \mathbb{R}^{(n+m) \times (n+m)}. \quad (4.19)$$

Then based on the Jacobian (4.19) we can derive the following convergence analysis results.

Theorem 15. *Suppose that QCQP (4.16a) – (4.16b) has a KKT point (x^*, λ^*) that belongs to set \mathcal{Q}_1 . If x^* is regular and λ^* satisfies $A_0 + \sum_{i=1}^m \lambda_i^* A_i \succ 0$, then the equilibrium $(x^*/\alpha, \lambda^*)$ is locally asymptotically stable with respect to dynamics (4.18a) – (4.18b) for any $\alpha > 0$.*

Proof of Theorem 15. By a same argument of Lemma 1 in Chapter 3, we can prove that under the conditions above, the Jacobian (4.19) evaluated at equilibrium $(x^*/\alpha, \lambda^*)$ is Hurwitz for any positive constant α . Therefore, according to the stability of the linearized system, we conclude that dynamics (4.18a) – (4.18b) is locally asymptotically stable at $(x^*/\alpha, \lambda^*)$. \square

Before analyzing the stability for those KKT points in \mathcal{Q}_2 , we introduce an analytical result on matrix perturbations.

Theorem 16. *[Stewart and Sun (1990)] Let A be an $n \times n$ Hermitian matrix with real eigenvalues ordered as $\mu_1 \geq \dots \geq \mu_n$. Let $\tilde{A} = A + E$ be a non-Hermitian perturbation of matrix A . The eigenvalues of \tilde{A} are denoted as $\tilde{\mu}_1, \dots, \tilde{\mu}_n$ with $\text{Re}\{\tilde{\mu}_1\} \geq \dots \geq \text{Re}\{\tilde{\mu}_n\}$. Then we have*

$$\sum_{i=1}^n |\mu_i - \tilde{\mu}_i|^2 \leq 2\|E\|_F^2 \quad (4.20)$$

where $\|\cdot\|_F$ denotes the Frobenius norm of a matrix.

Theorem 17. *Suppose that QCQP (4.16a) – (4.16b) has a KKT point $(\bar{x}, \bar{\lambda})$ that belongs to set \mathcal{Q}_2 . Then there always exists some α_0 such that for any $\alpha > \alpha_0$, the equilibrium $(\bar{x}/\alpha, \bar{\lambda})$ is unstable with respect to dynamics (4.18a) – (4.18b).*

Proof of Theorem 17. Note the Jacobian (4.19) evaluated at equilibrium $(\bar{x}/\alpha, \bar{\lambda})$ is given by

$$\tilde{J} := 2\alpha^2 \begin{bmatrix} -A_0 - \sum_{i=1}^m \bar{\lambda}_i A_i & -\frac{B(\bar{x})+C}{\alpha} \\ \frac{B(\bar{x})^T+C^T}{\alpha} & \mathbf{0} \end{bmatrix} = 2\alpha^2(J + E)$$

where we define

$$J := \begin{bmatrix} -A_0 - \sum_{i=1}^m \bar{\lambda}_i A_i & \mathbf{0} \\ \mathbf{0} & \mathbf{0} \end{bmatrix} \quad \text{and} \quad E := \begin{bmatrix} \mathbf{0} & -\frac{B(\bar{x})+C}{\alpha} \\ \frac{B(\bar{x})^T+C^T}{\alpha} & \mathbf{0} \end{bmatrix}.$$

Because the KKT point $(\bar{x}, \bar{\lambda}) \in \mathcal{Q}_2$, by definition we know that $A_0 + \sum_{i=1}^m \bar{\lambda}_i A_i \not\equiv 0$. Suppose the eigenvalues of J are denoted as $\mu_1 \geq \dots \geq \mu_{n+m} = 0$, then we must have $\mu_1 > 0$. Also suppose that the eigenvalues of the Jacobian \tilde{J} can be ordered as $\text{Re}\{\tilde{\mu}_1\} \geq \dots \geq \text{Re}\{\tilde{\mu}_{n+m}\}$. Thus, according to Theorem 16, we can choose a constant α

$$\alpha > \alpha_0 := \sqrt{\frac{4}{\mu_1^2} \text{Tr}\{[B(\bar{x}) + C][B(\bar{x}) + C]^T\}}$$

such that the following inequality holds

$$\sum_{i=1}^{n+m} |\mu_i - \tilde{\mu}_i|^2 \leq 2\|E\|_F^2 = \frac{4}{\alpha^2} \text{Tr}\{[B(\bar{x}) + C][B(\bar{x}) + C]^T\} < \mu_1^2$$

which further implies $|\mu_1 - \tilde{\mu}_1| < \mu_1 \Rightarrow \text{Re}\{\tilde{\mu}_1\} > 0$. Then the instability result follows. \square

Corollary 2. *Suppose that optimization dynamics (4.18a) – (4.18b) has an α large enough. If it can converge to an equilibrium $(x^*/\alpha, \lambda^*)$ as time goes to infinity, then (x^*, λ^*) must be a saddle-point for the Lagrangian associated with QCQP (4.16a) – (4.16b).*

Proof of Corollary 2. Because we have assumed that α is large enough, by Theorem 17 we know that none of the KKT points in \mathcal{Q}_2 is stable with respect to dynamics (4.18a) – (4.18b).

Consequently, this equilibrium must belong to \mathcal{Q}_1 . This completes the proof. \square

4.5 Partitioning and MAXCUT Problems

This section gives a MAXCUT example, which is casted as a networked non-convex QCQP, to demonstrate the distributed structure of our optimization dynamics approach.

4.5.1 The Two-Way Partitioning Problem

Consider the two-way partitioning problem formulated by [Boyd and Vandenberghe \(2004\)](#)

$$\underset{x \in \mathbb{R}^n}{\text{minimize}} \quad x^T W x \quad (4.21a)$$

$$\text{subject to} \quad x_i^2 = 1, \quad \forall i = 1, 2, \dots, n \quad (4.21b)$$

where $W \in \mathbb{S}^n$. The constraints restrict the values of x_i to 1 or -1 , so the problem is equivalent to finding the vector with components ± 1 that minimizes $x^T W x$.

The feasible set here is finite (it contains 2^n points), so this problem can in principle be solved by simply checking the objective value of each feasible point. Since the number of feasible points grows exponentially, however, this is possible only for small problems. In general, the two-way partitioning problem (4.21a) – (4.21b) is very difficult to solve.

A feasible x to the two-way partitioning problem corresponds to the partition

$$\{1, \dots, n\} = \{i \mid x_i = -1\} \cup \{i \mid x_i = 1\}$$

and the matrix coefficient $W(i, j)$ can be interpreted as the cost of having the elements i and j in the same partition, and $-W(i, j)$ is the cost of having i and j in different partitions. The objective in (4.21a) is the total cost, over all pairs of elements, and problem (4.21a) – (4.21b) seeks to find a partition with the least total cost.

4.5.2 The MAXCUT Problem

A MAXCUT problem can be formulated as a particular two-way partitioning problem that is defined over a network. On a given graph \mathcal{G} that consists of n nodes, we assign a non-negative weight w_{ij} with each edge (i, j) , where $w_{ij} = 0$ if there is no edge that connects node i and node j . Then the MAXCUT problem seeks to find a cut of the graph with the largest possible

weight, i.e., a partition of the set of nodes in two parts \mathcal{G}_1 and \mathcal{G}_2 such that the total weight of all edges linking these parts is maximized. The MAXCUT problem is a classic problem in networked optimization.

The weight of a particular cut x_i is computed as

$$\frac{1}{2} \sum_{\{i | x_i x_j = -1\}} w_{ij}$$

which is also equal to

$$\frac{1}{4} \sum_{i,j=1}^n w_{ij} (1 - x_i x_j).$$

Hence, we would like to define $W \in \mathbb{S}^n$ as $W(i, j) := -w_{ij}$ if $i \neq j$ and $W(i, i) := \sum_{j \neq i} w_{ij}$. Note that the W matrix here is exactly the weighted Laplacian defined in Definition 3, and, therefore, we have $W \succeq 0$.

Utilizing the W matrix, we can formulate the MAXCUT problem as

$$\underset{x \in \mathbb{R}^n}{\text{minimize}} \quad -x^T W x \quad (4.22a)$$

$$\text{subject to} \quad x_i^2 = 1, \quad \forall i = 1, 2, \dots, n \quad (4.22b)$$

where we have changed the objective from maximizing $x^T W x$ into minimizing $-x^T W x$. Thus, we can see that the MAXCUT problem is a special case of the two-way partitioning problem. Moreover, both its objective (4.22a) and constraint (4.22b) are non-convex.

4.5.3 A MAXCUT Example

We now use a MAXCUT example to illustrate the distributedness and effectiveness of our continuous-time optimization dynamics approach.

Example 2. Consider the five-node graph in Fig. 4.1. Its weighted Laplacian is given by

$$W = \begin{bmatrix} 1.6 & -0.4 & -1 & 0 & -0.2 \\ -0.4 & 2.2 & 0 & -0.6 & -1.2 \\ -1 & 0 & 2.2 & -0.8 & -0.4 \\ 0 & -0.6 & -0.8 & 1.8 & -0.4 \\ -0.2 & -1.2 & -0.4 & -0.4 & 2.2 \end{bmatrix}.$$

In order to ensure that the MAXCUT problem has an isolated saddle-point, we select node 1 as the reference node, i.e., we require that the optimal value of x_1 should be 1. To achieve this goal, we add an extra cost $(x_1 - 1)^2$ to (4.22a) and form an equivalent problem

$$\underset{x \in \mathbb{R}^n}{\text{minimize}} \quad -x^T W x + (x_1 - 1)^2 \quad (4.23a)$$

$$\text{subject to} \quad x_i^2 = 1, \quad \forall i = 1, 2, \dots, 5. \quad (4.23b)$$

Let ν_i , for $i = 1, \dots, 5$, be the Lagrange multipliers associated with constraint $x_i^2 = 1$. Let us also assign both primal and dual variables (x_i and ν_i) to each node i .

We say that an optimization algorithm is *distributed* if, during the optimization process, each node only shares its individual variables with its directly connected neighbors.

Applying optimization dynamics (4.15a) – (4.15c) to problem (4.23a) – (4.23b), we obtain the following dynamical system

$$\dot{x}_1 = 2(0.6 - \nu_1)x_1 - 0.8x_2 - 2x_3 - 0.4x_5 + 2 \quad (4.24a)$$

$$\dot{x}_2 = 2(2.2 - \nu_2)x_2 - 0.8x_1 - 1.2x_4 - 2.4x_5 \quad (4.24b)$$

$$\dot{x}_3 = 2(2.2 - \nu_3)x_3 - 2x_1 - 1.6x_4 - 0.8x_5 \quad (4.24c)$$

$$\dot{x}_4 = 2(1.8 - \nu_4)x_4 - 1.2x_2 - 1.6x_3 - 0.8x_5 \quad (4.24d)$$

$$\dot{x}_5 = 2(2.2 - \nu_5)x_5 - 0.4x_1 - 2.4x_2 - 0.8x_3 - 0.8x_4 \quad (4.24e)$$

$$\dot{\nu}_i = x_i^2, \quad \forall i = 1, \dots, 5. \quad (4.24f)$$

We can see from dynamics (4.24f) that each Lagrange multiplier ν_i only uses the local primal variable x_i to update itself. As for the primal dynamics (4.24a) – (4.24e), it is clear that node i requires x_i , ν_i , and x_j , for all node j which is directly connected with node i , to compute \dot{x}_i . Let us take node 1 as an example to illustrate this. Since node 1 is not directly connected with node 4, in dynamics (4.24a) all x_1 , ν_1 , x_2 , x_3 , and x_5 are involved except x_4 . Therefore, we conclude that dynamical system (4.24a) – (4.24f) has a distributed structure.

When we feed dynamics (4.24a) – (4.24f) with a random initial point with ℓ_∞ norm less than 1, the dynamical system evolves and converges to a KKT point $x^* = (1, -1, -1, 1, 1)$ and $\nu^* = (2.8, 4.4, 4.4, 2.8, 3.2)$ in less than 50 simulation seconds. Trajectories of the primal and dual variables are, respectively, plotted above in Fig. 4.2.

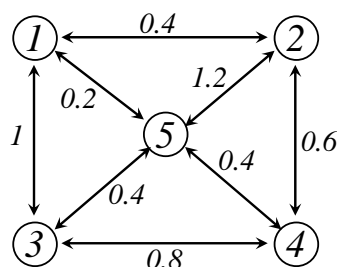


Figure 4.1 A five-node weighted graph

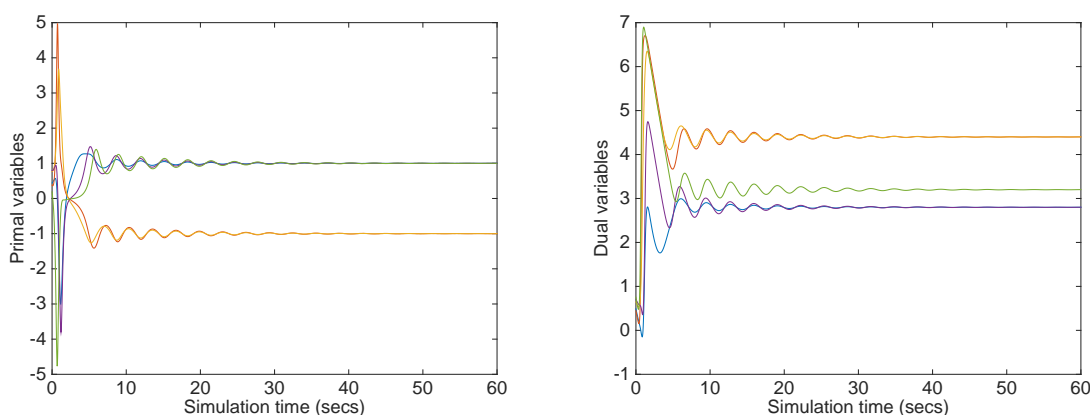


Figure 4.2 Convergence of the five-node MAXCUT example

We next substitute this KKT point (x^*, ν^*) back to check the LMI condition (4.4), we find the eigenvalues of (4.4) are given by 0.1037, 0.4230, 1.6096, 2.6273, and 3.8452. Thus, Theorem 11 is satisfied and we can guarantee that (x^*, ν^*) is exactly a saddle-point. The primal optimum we have obtained partitions these five nodes into two groups $\mathcal{G}_1 = \{1, 4, 5\}$ and $\mathcal{G}_2 = \{2, 3\}$ with the largest total weight $(x^*)^T W x^* / 4 = 4.4$.

Remark 6. We should point out that the LMI condition (4.4) cannot be checked in a distributed manner. Nevertheless, we notice that the MAXCUT problem (4.22a) – (4.22b) has exactly the same form as QCQP (4.16a) – (4.16b), so we can apply the modified optimization dynamics (4.18a) – (4.18b) to seek saddle-points associated with the MAXCUT problem. With a constant α large enough, we can guarantee that whenever the optimization dynamics converges, it must converge to a saddle-point. As a result, we practically may avoid checking LMI (4.4).

4.6 Phase Recovery Problems

The phase recovery problem, namely, the problem of reconstructing a complex phase vector given only the magnitude of linear measurements, appears in a wide range of engineering and physical applications, including audio signal estimation [Griffin and Lim \(1984\)](#), crystallography imaging [Harrison \(1993\)](#) and [Miao et al. \(2008\)](#), and diffraction imaging [Bunk et al. \(2007\)](#).

4.6.1 Problem Formulation

The phase recovery problem seeks to retrieve a signal $x \in \mathbb{C}^n$ from the amplitude $|Ax| = b$ of m linear measurements, where $A \in \mathbb{C}^{m \times n}$ and $b \in \mathbb{R}^m$. Here, we usually assume that $m > n$. Thus, the phase recovery problem can be cast as a complex-valued non-convex QCQP

$$\underset{x \in \mathbb{C}^n}{\text{minimize}} \quad x^* x \quad (4.25a)$$

$$\text{subject to} \quad x^* A_k x = b_k^2, \quad \forall k = 1, \dots, m \quad (4.25b)$$

where x^* denotes the conjugate transpose of vector x and matrix $A_k \in \mathbb{C}^{n \times n}$ is defined as $A_k := A(k, :)^* A(k, :)$. Observing that the phase recovery problem (4.25a) – (4.25b) is in general NP hard, [Candès et al. \(2011\)](#) has relaxed it as a trace minimization problem over an affine slice of the positive semi-definite cone

$$\underset{X \in \mathbb{C}^{n \times n}}{\text{minimize}} \quad \text{Tr}\{X\} \quad (4.26a)$$

$$\text{subject to} \quad \text{Tr}\{A_k X\} = b_k^2, \quad \forall k = 1, \dots, m \quad (4.26b)$$

$$X \succeq 0. \quad (4.26c)$$

If the optimal solution of (4.26a) – (4.26c) has rank one, then we can recover the signal x from factorizing the optimal solution as $X = xx^*$.

This methodology which lifts up the problem of vector recovery from quadratic constraints into that of recovering a rank-one matrix from affine constraints via semi-definite programming is known under the name of *phase lift*, and, of course, problem (4.26a) – (4.26c) is the SDP relaxation for the non-convex QCQP (4.25a) – (4.25b).

It has been shown that the SDP relaxation (4.26a) – (4.26c) recovers the signal x exactly with high probability if the number m of magnitude measurements is on the order of $n \log n$.

Theorem 18. [Candès et al. (2011)] Consider an arbitrary signal x in \mathbb{R}^n or \mathbb{C}^n and suppose that the number of measurements obeys $m \geq c_0 n \log n$, where c_0 is a sufficiently large constant. Then in both the real and complex cases, the solution to the trace minimization program is exact with high probability in the sense that (4.26a) – (4.26c) has a unique solution obeying $X = xx^*$. This holds with probability at least $1 - 3e^{-\gamma \frac{m}{n}}$, where γ is a positive absolute constant.

Theorem 18 establishes a rigorous equivalence between a class of phase recovery problems and a class of convex SDP relaxations. In other words, under the oversampling assumption, strong duality holds for the non-convex QCQP (4.25a) – (4.25b) with high probability. Therefore, our optimization dynamics approach can be applied to the phase recovery problem.

We note that the phase recovery problem (4.25a) – (4.25b) is complex-valued optimization. To apply the optimization dynamics approach, we should reformulate it as an optimization over real numbers. To achieve this, we define

$$u := [\operatorname{Re}\{x_1\} \cdots \operatorname{Re}\{x_n\} \operatorname{Im}\{x_1\} \cdots \operatorname{Im}\{x_n\}]^T \in \mathbb{R}^{2n}$$

$$\mathbf{A}_k := \begin{bmatrix} \operatorname{Re}\{A_k\} & -\operatorname{Im}\{A_k\} \\ \operatorname{Im}\{A_k\} & \operatorname{Re}\{A_k\} \end{bmatrix} \in \mathbb{R}^{2n \times 2n}.$$

Now for each index $k = 1, \dots, m$, the equality $u^T \mathbf{A}_k u = x^* A_k x = b_k^2$ holds. Therefore, the phase recovery problem (4.25a) – (4.25b) can be recast as a real-valued non-convex QCQP

$$\underset{u \in \mathbb{R}^{2n}}{\text{minimize}} \quad u^T u \quad (4.27a)$$

$$\text{subject to} \quad u^T \mathbf{A}_k u = b_k^2, \quad \forall k = 1, \dots, m. \quad (4.27b)$$

Then our optimization dynamics approach can be utilized to solve problem (4.27a) – (4.27b).

4.6.2 The Augmented Lagrangian and Associated Optimization Dynamics

Next we would like to apply our optimization dynamics approach to solve the real-valued phase recovery problem (4.27a) – (4.27b). First of all, the Lagrangian associated with problem (4.27a) – (4.27b) is given by

$$L(u, \lambda) := u^T u + \sum_{k=1}^m \lambda_k (u^T \mathbf{A}_k u - b_k^2). \quad (4.28)$$

To achieve a better convergence to the saddle-point, however, here we are going to derive our optimization dynamics from the augmented Lagrangian

$$\tilde{L}(u, \lambda) := u^T u + \frac{\rho}{2} \sum_{k=1}^m (u^T \mathbf{A}_k u - b_k^2)^2 + \sum_{k=1}^m \lambda_k (u^T \mathbf{A}_k u - b_k^2). \quad (4.29)$$

We call the polynomial (4.29) above as the ‘‘augmented Lagrangian’’ since it has an quartic augmented term $\frac{\rho}{2} \sum_{k=1}^m (u^T \mathbf{A}_k u - b_k^2)^2$ with parameter $\rho > 0$ when compared to the standard Lagrangian (4.28). This augmented term comes from the equality constraint (4.27b) and can be viewed as a penalty cost that is added to the objective function (4.27a). By adding such a quartic penalty cost to the phase recovery problem (4.27a) – (4.27b), it should improve the convergence of our optimization dynamics.

Now we define our optimization dynamics associated with phase recovery (4.27a) – (4.27b) based on the augmented Lagrangian (4.29)

$$\dot{u} := -\frac{\partial \tilde{L}(u, \lambda)}{\partial u} = -2 \left\{ I_{2n} + \sum_{k=1}^m \left[\lambda_k + \rho (u^T \mathbf{A}_k u - b_k^2) \right] \mathbf{A}_k \right\} u \quad (4.30a)$$

$$\dot{\lambda}_k := \frac{\partial \tilde{L}(u, \lambda)}{\partial \lambda_k} = u^T \mathbf{A}_k u - b_k^2, \quad \forall k = 1, \dots, m. \quad (4.30b)$$

Substituting dynamics (4.30b) into (4.30a), we can rewrite dynamics (4.30a) as

$$\dot{u} = -2 \left[I_{2n} + \sum_{k=1}^m (\lambda_k + \rho \dot{\lambda}_k) \mathbf{A}_k \right] u \quad (4.31)$$

where the derivative term of the dual variable $\dot{\lambda}$ in dynamics (4.31) comes exactly from the augmented term $\frac{\rho}{2} \sum_{k=1}^m (u^T \mathbf{A}_k u - b_k^2)^2$.

Before we utilize optimization dynamics (4.30a) – (4.30b) to search saddle-points for the phase recovery problem (4.27a) – (4.27b), one may ask whether the augmented term changes the locations of saddle-points from the standard Lagrangian. The answer is no. The standard and augmented Lagrangians share the same saddle-points.

Theorem 19. *Suppose that (u^*, λ^*) is a KKT point of the phase recovery (4.27a) – (4.27b). Then (u^*, λ^*) is an equilibrium of dynamics (4.30a) – (4.30b) and a saddle-point for the augmented Lagrangian (4.29), provided it is a saddle-point for the Lagrangian (4.28). The converse is also true. If (u^*, λ^*) is an equilibrium of dynamics (4.30a) – (4.30b) and a saddle-point for the augmented Lagrangian (4.29), then it is a saddle-point for the Lagrangian (4.28).*

Proof of Theorem 19. Let us first suppose that (u^*, λ^*) is a KKT point of the phase recovery problem (4.27a) – (4.27b) and is also a saddle-point for the Lagrangian (4.28). Then from the KKT conditions $(I_{2n} + \sum_{k=1}^m \lambda_k^* \mathbf{A}_k) u^* = 0$ and $(u^*)^T \mathbf{A}_k u^* - b_k^2 = 0$, for $k = 1, \dots, m$, it is easy to check that (u^*, λ^*) is an equilibrium of dynamics (4.30a) – (4.30b). Moreover, by the definition of saddle-points, we have $L(u^*, \lambda) \leq L(u^*, \lambda^*) \leq L(u, \lambda^*)$, so we can substitute (u^*, λ^*) into the augmented Lagrangian (4.29) and check whether it satisfies the saddle-point's definition. On the one hand, we have $\tilde{L}(u^*, \lambda^*) - \tilde{L}(u^*, \lambda) = (u^*)^T u^* - (u^*)^T u^* = 0$, because $(u^*)^T \mathbf{A}_k u^* - b_k^2 = 0$ for all $k = 1, \dots, m$. On the other hand, by applying the same KKT condition we obtain

$$\tilde{L}(u, \lambda^*) - \tilde{L}(u^*, \lambda^*) = L(u, \lambda^*) - L(u^*, \lambda^*) + \frac{\rho}{2} \sum_{k=1}^m (u^T \mathbf{A}_k u - b_k^2)^2 \geq 0.$$

Therefore, (u^*, λ^*) is a saddle-point for the augmented Lagrangian (4.29).

Next let us suppose that (u^*, λ^*) is an equilibrium of dynamics (4.30a) – (4.30b). Hence (u^*, λ^*) satisfies $(u^*)^T \mathbf{A}_k u^* - b_k^2 = 0$ for all $k = 1, \dots, m$, and, as a result, substituting (u^*, λ^*) into the Lagrangian (4.28) yields $L(u^*, \lambda^*) - L(u^*, \lambda) = (u^*)^T u^* - (u^*)^T u^* = 0$. On the other hand, since (u^*, λ^*) is a saddle-point for the augmented Lagrangian (4.29), we know that u^* globally minimizes the objective function $u^T u + \frac{\rho}{2} \sum_{k=1}^m (u^T \mathbf{A}_k u - b_k^2)^2$ subject to constraint (4.27b). Noticing that the extra penalty cost $\frac{\rho}{2} \sum_{k=1}^m (u^T \mathbf{A}_k u - b_k^2)^2$ achieves zero at u^* , we conclude that u^* is indeed a global solution to the phase recovery problem (4.27a) – (4.27b). In other words, we must have $L(u, \lambda^*) - L(u^*, \lambda^*) \geq 0$. Then by definition (u^*, λ^*) is a saddle-point for the Lagrangian (4.28). This completes the proof. \square

4.6.3 Simulations

Now we are ready to present our simulation results showing the effectiveness of optimization dynamics (4.30a) – (4.30b). We implement optimization dynamics (4.30a) – (4.30b) via the MATLAB Simulink and the block diagram of dynamics (4.30a) – (4.30b) is shown in Fig. 4.3. The red, dashed box in Fig. 4.3 consists of a summation between the state of the dual variable (output from the integrator) and a proportional term of the dual derivative, and therefore it can be viewed as a PI controller. In simulations we choose the proportional coefficient $\rho = 10$.

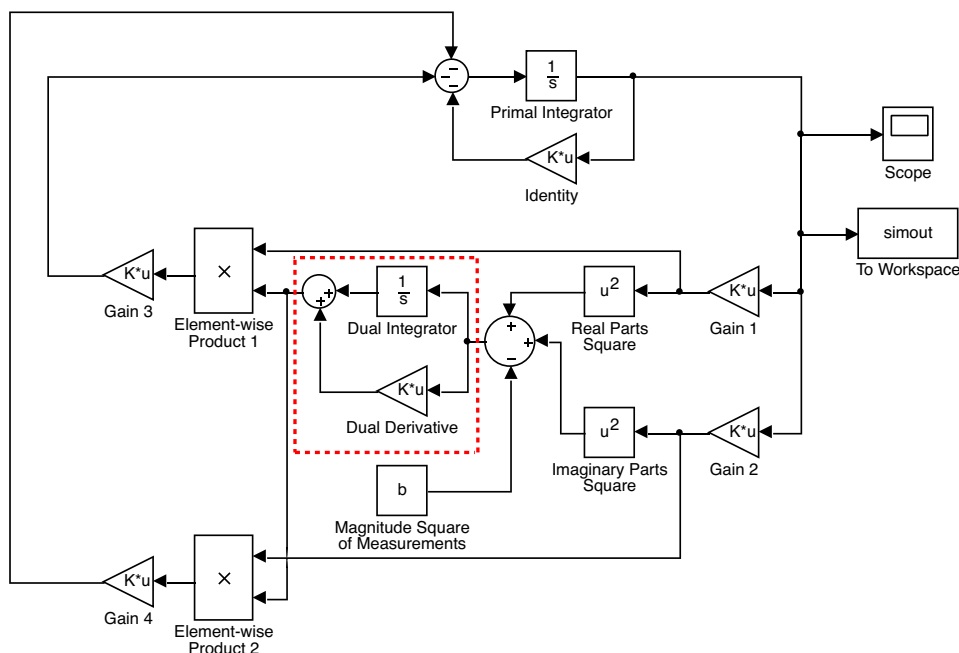


Figure 4.3 A block diagram of the optimization dynamics associated with phase recovery

We next apply our optimization dynamics algorithm to solve phase recovery problems with $n = 256$ and $m = 2048$. The coefficient matrix A is chosen as a random Gaussian matrix with an appropriate size. Optimization dynamics (4.30a) – (4.30b) is simulated by the MATLAB Simulink toolbox (shown in Fig. 4.3) as if it were truly implemented via physical computing.

We first run the simulation without the proportional controller of the dual derivative and we find that the primal dynamics will converge to zero, which is not our desired solution.

Then, in comparison, we enable the proportional controller of the dual derivative and this time our optimization dynamics converges to a phase recovery solution with the relative error about 10^{-6} within 0.001 seconds (in actual time).

The simulations above demonstrate those good effects caused by the PI controller of the dual derivative. Introduced by the augmented Lagrangian (4.29), the additional proportional controller of the dual derivative stabilizes our optimization dynamics (4.30a) – (4.30b) and forces the primal dynamics converge to the correct phase recovery solution. Moreover, we can see that our PI controller of the dual derivative results in a fast convergence with respect to optimization dynamics (4.30a) – (4.30b).

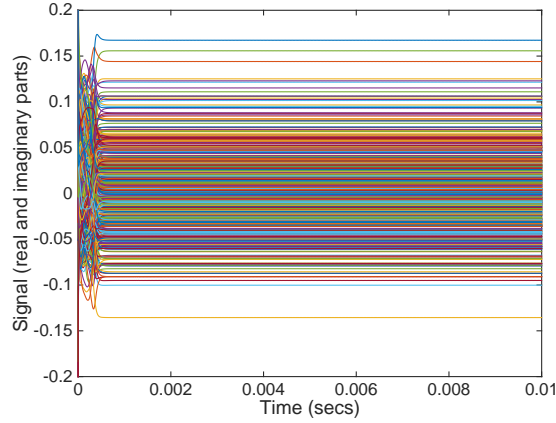


Figure 4.4 Convergence of a phase recovery example with $n = 256$ and $m = 2048$

Remark 7. *In Section 6, we will utilize our optimization dynamics approach to solve phase recovery problems with larger problem sizes. We will also compare our approach with existing phase recovery algorithms, e.g., [Netrapalli et al. \(2015\)](#), showing that our optimization dynamics is even faster when implemented in a discrete-time manner.*

4.7 The Convex SOCPs

We discover that the convex second-order cone programmings (SOCPs) can be equivalently written as general QCQPs. In this section, we show that under mild conditions those equivalent QCQPs have zero optimal duality gaps with their associated Lagrange duals. Hence, we can apply our approach here and we also find that our dynamics exhibits a distributed structure.

4.7.1 Problem Formulation

A convex SOCP can be generally formulated as

$$\underset{x \in \mathbb{R}^n}{\text{minimize}} \quad f^T x \quad (4.32a)$$

$$\text{subject to} \quad \|A_i x + b_i\|_2 \leq c_i^T x + d_i, \quad \forall i = 1, \dots, m \quad (4.32b)$$

$$Fx = g \quad (4.32c)$$

where $A_i \in \mathbb{R}^{n_i \times n}$, $b_i \in \mathbb{R}^{n_i}$, $c_i \in \mathbb{R}^n$, $d_i \in \mathbb{R}$, for $i = 1, \dots, m$, $F \in \mathbb{R}^{p \times n}$, $f \in \mathbb{R}^n$, and $g \in \mathbb{R}^p$.

We note that most convex optimization softwares treat an SOCP as a special SDP. For example, [Boyd and Vandenberghe \(2004\)](#) equivalently transforms SOCP constraint (4.32b) into the following SDP constraint via Schur complement

$$\underset{x \in \mathbb{R}^n}{\text{minimize}} \quad f^T x \quad (4.33a)$$

$$\text{subject to} \quad \begin{bmatrix} (c_i^T x + d_i)I & A_i x + b_i \\ (A_i x + b_i)^T & c_i^T x + d_i \end{bmatrix} \succeq 0, \quad \forall i = 1, \dots, m \quad (4.33b)$$

$$Fx = g \quad (4.33c)$$

and formulation (4.33a) – (4.33c) is not amenable to be solved in a distributed manner.

Next we show that a convex SOCP can be equivalently rewritten as a non-convex QCQP. By squaring both sides of constraint (4.32b) and requiring $c_i^T x + d_i \geq 0$ for $i = 1, \dots, m$, the SOCP (4.32a) – (4.32c) can be equivalently transformed into

$$\underset{x \in \mathbb{R}^n}{\text{minimize}} \quad f^T x \quad (4.34a)$$

$$\text{subject to} \quad \|A_i x + b_i\|_2^2 \leq (c_i^T x + d_i)^2, \quad \forall i = 1, \dots, m \quad (4.34b)$$

$$-c_i^T x - d_i \leq 0, \quad \forall i = 1, \dots, m \quad (4.34c)$$

$$Fx = g. \quad (4.34d)$$

Define $P_i := A_i^T A_i - c_i c_i^T$, $q_i := A_i^T b_i - d_i c_i$, and $r_i := b_i^T b_i - d_i^2$, then problem (4.34a) – (4.34d) can be further simplified as a non-convex QCQP, since P_i may not be positive semi-definite

$$\underset{x \in \mathbb{R}^n}{\text{minimize}} \quad f^T x \quad (4.35a)$$

$$\text{subject to} \quad x^T P_i x + 2q_i^T x + r_i \leq 0, \quad \forall i = 1, \dots, m \quad (4.35b)$$

$$-c_i^T x - d_i \leq 0, \quad \forall i = 1, \dots, m \quad (4.35c)$$

$$Fx = g. \quad (4.35d)$$

We notice that QCQP (4.35a) – (4.35d) is equivalent to the original SOCP (4.32a) – (4.32c). Because (4.32a) – (4.32c) is convex, under mild constraint qualification assumptions, there is a zero optimal duality gap between (4.32a) – (4.32c) and its Lagrange dual relaxation. This further implies that strong duality holds for problem (4.35a) – (4.35d).

4.7.2 Strong Duality

Let x^* be an optimal solution to the SOCP (4.32a) – (4.32c) and $\lambda_1^*, \dots, \lambda_m^*, \nu^*$ be the optimal Lagrange multipliers that are associated with constraints (4.32b) and (4.32c).

Due to the equivalent transformation between (4.32a) – (4.32c) and (4.35b) – (4.35d), we know that x^* is also an optimal solution to problem (4.35b) – (4.35d). Now we let $\xi_1^*, \dots, \xi_m^*, \eta_1^*, \dots, \eta_m^*$, and μ^* be the optimal Lagrange multipliers that are associated with constraints (4.35b) – (4.35d). We have the following result to characterize the relationship between these points (x^*, λ^*, ν^*) and $(x^*, \xi^*, \eta^*, \mu^*)$.

Theorem 20. *Suppose that (x^*, λ^*, ν^*) is a saddle-point for the Lagrangian associated with SOCP (4.32a) – (4.32c). Also suppose that x^* satisfies $A_i x^* + b_i \neq 0$ for all $i = 1, \dots, m$. Then there exists $(x^*, \xi^*, \eta^*, \mu^*)$ with*

$$\xi_i^* := \lambda_i^*/2 \|A_i x^* + b_i\|_2, \quad \eta^* := 0, \quad \text{and} \quad \mu^* := \nu^*$$

being a saddle-point for the Lagrangian associated with problem (4.35a) – (4.35d).

Proof of Theorem 20. Since (x^*, λ^*, ν^*) is a saddle-point, it satisfies KKT conditions

$$f + \sum_{i=1}^m \lambda_i^* \left[\frac{A_i^T (A_i x^* + b_i)}{\|A_i x^* + b_i\|_2} - c_i \right] + F^T \nu^* = 0 \quad (4.36a)$$

$$\|A_i x^* + b_i\|_2 - c_i^T x^* - d_i \leq 0, \quad \forall i = 1, \dots, m \quad (4.36b)$$

$$F x^* = g \quad (4.36c)$$

$$\lambda_i^* \geq 0, \quad \forall i = 1, \dots, m \quad (4.36d)$$

$$\lambda_i^* (\|A_i x^* + b_i\|_2 - c_i^T x^* - d_i) = 0, \quad \forall i = 1, \dots, m \quad (4.36e)$$

where we assume $A_i x^* + b_i \neq 0$ for all $i = 1, \dots, m$ to guarantee that KKT condition (4.36a) is not meaningless.

Moreover, the Lagrangian associated with problem (4.35a) – (4.35d) is given by

$$\begin{aligned} L(x, \xi, \eta, \mu) := & f^T x + \sum_{i=1}^m \xi_i [(A_i x + b_i)^T (A_i x + b_i) - (c_i^T x + d_i)^2] \\ & - \sum_{i=1}^m \eta_i (c_i^T x + d_i) + \mu^T (F x - g) \end{aligned} \quad (4.37)$$

and hence a KKT point of problem (4.35a) – (4.35d) should satisfy the following conditions

$$f + \sum_{i=1}^m 2\xi_i^* [A_i^T(A_i x^* + b_i) - (c_i^T x^* + d_i)c_i] - \sum_{i=1}^m \eta_i^* c_i + F^T \mu^* = 0 \quad (4.38a)$$

$$(A_i x^* + b_i)^T (A_i x^* + b_i) - (c_i^T x^* + d_i)^2 \leq 0, \quad \forall i = 1, \dots, m \quad (4.38b)$$

$$c_i^T x^* + d_i \geq 0, \quad \forall i = 1, \dots, m \quad (4.38c)$$

$$F x^* = g \quad (4.38d)$$

$$\xi_i^* \geq 0, \quad \forall i = 1, \dots, m \quad (4.38e)$$

$$\eta_i^* \geq 0, \quad \forall i = 1, \dots, m \quad (4.38f)$$

$$\xi_i^* [(A_i x^* + b_i)^T (A_i x^* + b_i) - (c_i^T x^* + d_i)^2] = 0, \quad \forall i = 1, \dots, m \quad (4.38g)$$

$$\eta_i^* (c_i^T x^* + d_i) = 0, \quad \forall i = 1, \dots, m. \quad (4.38h)$$

According to conditions (4.36b) – (4.36e) and by our definition $\xi_i^* = \lambda_i^*/2 \|A_i x^* + b_i\|_2$, $\eta^* = 0$, and $\mu^* = \nu^*$, it is not difficult to check that KKT conditions (4.38b) – (4.38h) are satisfied. Here we need to point out that, due to our previous assumption $A_i^* x + b_i \neq 0$, we must have $c_i^T x^* + d_i \geq \|A_i x^* + b_i\|_2 > 0$, for all $i = 1, \dots, m$. This is the reason why we require $\eta^* = 0$.

Next we show that condition (4.38a) is also satisfied. Substituting $\xi_i^* = \lambda_i^*/2 \|A_i x^* + b_i\|_2$, $\eta^* = 0$, and $\mu^* = \nu^*$ into the left-hand-side of (4.38a) we obtain

$$\begin{aligned} & f + \sum_{i=1}^m 2\xi_i^* [A_i^T(A_i x^* + b_i) - (c_i^T x^* + d_i)c_i] - \sum_{i=1}^m \eta_i^* c_i + F^T \mu^* \\ &= f + \sum_{i=1}^m \lambda_i^* \left[\frac{A_i^T(A_i x^* + b_i)}{\|A_i x^* + b_i\|_2} - \frac{(c_i^T x^* + d_i)c_i}{\|A_i x^* + b_i\|_2} \right] + F^T \nu^*. \end{aligned} \quad (4.39)$$

Comparing (4.39) with the left-hand-side of condition (4.36a), we find that they are equal to each other. On the one hand, for any index k with $\|A_k x^* + b_k\|_2 < c_k^T x^* + d_k$ we must have $\lambda_k^* = 0$ by the complementary slackness (4.36e). Hence, for those indices

$$\lambda_k^* \left[\frac{A_k^T(A_k x^* + b_k)}{\|A_k x^* + b_k\|_2} - \frac{(c_k^T x^* + d_k)c_k}{\|A_k x^* + b_k\|_2} \right] = \lambda_k^* \left[\frac{A_k^T(A_k x^* + b_k)}{\|A_k x^* + b_k\|_2} - c_k \right] = 0.$$

On the other hand, for those indices with $\|A_i x^* + b_i\|_2 = c_i^T x^* + d_i$, we have

$$\lambda_i^* \left[\frac{A_i^T(A_i x^* + b_i)}{\|A_i x^* + b_i\|_2} - \frac{(c_i^T x^* + d_i)c_i}{\|A_i x^* + b_i\|_2} \right] = \lambda_i^* \left[\frac{A_i^T(A_i x^* + b_i)}{\|A_i x^* + b_i\|_2} - c_i \right].$$

Therefore, condition (4.38a) is satisfied and we conclude that $(x^*, \xi^*, \eta^*, \mu^*)$ is a KKT point.

Finally, we show that $(x^*, \xi^*, \eta^*, \mu^*)$ is also a saddle-point for the Lagrangian (4.37). By KKT conditions (4.38b) – (4.38h) it is easy to check that $L(x^*, \xi, \eta, \mu) - L(x^*, \xi^*, \eta^*, \mu^*) \leq 0$ for all $\xi \in \mathbb{R}_+^m$ and $\eta \in \mathbb{R}_+^m$. Moreover, because (x^*, λ^*) is a saddle-point for the Lagrangian associated with SOCP (4.32a) – (4.32c), we know that x^* must be a global solution. Due the equivalence between problems (4.32a) – (4.32c) and (4.35a) – (4.35d), x^* is a global optimum for problem (4.35a) – (4.35d), too. In other words, x^* minimizes $L(x, \xi^*, \eta^*, \mu^*)$, i.e., we have $L(x, \xi^*, \eta^*, \mu^*) - L(x^*, \xi^*, \eta^*, \mu^*) \geq 0$ for all $x \in \mathbb{R}^n$. This completes the proof. \square

Due to the satisfaction of strong duality, our optimization dynamics can be applied here to solve QCQP (4.35a) – (4.35d) instead of SOCP (4.32a) – (4.32c).

4.7.3 The Associated Optimization Dynamics

The optimization dynamics associated with problem (4.35a) – (4.35d) can be written as

$$\begin{aligned} \dot{x} &:= -f - \sum_{i=1}^m 2\xi_i [A_i^T(A_i x + b_i) - (c_i^T x + d_i)c_i] + \sum_{i=1}^m \eta_i c_i - F^T \mu \\ &= -f - \sum_{i=1}^m 2\xi_i (P_i x + q_i) + \sum_{i=1}^m \eta_i c_i - F^T \mu \end{aligned} \quad (4.40a)$$

$$\dot{\xi}_i := \left[(A_i x + b_i)^T (A_i x + b_i) - (c_i^T x + d_i)^2 \right]_{\xi_i}^+ = \left[x^T P_i x + 2q_i^T x + r_i \right]_{\xi_i}^+ \quad (4.40b)$$

$$\dot{\eta}_i := \left[-c_i^T x - d_i \right]_{\eta_i}^+ \quad (4.40c)$$

$$\dot{\mu} := Fx - g. \quad (4.40d)$$

We are here interested in applying dynamics (4.40a) – (4.40d) to solve SOCP (4.32a) – (4.32c) because it has a distributed structure, as we have illustrated in Section 4.5.

In comparison, we discover that the optimization dynamics directly associated with SOCP (4.32a) – (4.32c) itself does not have such a distributed structure. To be more specific, SOCP (4.32a) – (4.32c) has the following optimization dynamics

$$\dot{x} := -f - \sum_{i=1}^m \lambda_i \left[\frac{A_i^T(A_i x + b_i)}{\|A_i x + b_i\|_2} - c_i \right] - F^T \nu \quad (4.41a)$$

$$\dot{\lambda}_i := \left[\|A_i x + b_i\|_2 - c_i^T x - d_i \right]_{\lambda_i}^+ \quad (4.41b)$$

$$\dot{\nu} := Fx - g. \quad (4.41c)$$

Now comparing dynamics (4.41a) with (4.40a) we notice that (4.41a) contains 2-norm terms $\|A_i x + b_i\|_2$, for $i = 1, \dots, m$, in its expression. To compute each term $\|A_i x + b_i\|_2$ we need to know every element of $A_i x + b_i$, and, therefore, dynamics (4.41a) is difficult to be computed in a distributed manner. This is the major difference between dynamics (4.41a) and (4.40a).

4.7.4 Simulations

In this subsection, we present an SOCP example and employ both optimization dynamics (4.40a) – (4.40d) and (4.41a) – (4.41c), respectively, to solve this example. We would like to demonstrate the effectiveness of dynamics (4.40a) – (4.40d). Moreover, when compared with (4.41a) – (4.41c), we would also like to show that dynamics (4.40a) – (4.40d) has an even better convergence performance.

Example 3. Consider the SOCP (4.32a) – (4.32c) with following coefficient matrices

$$\begin{aligned} f &= [1 \ 1 \ 1]^T \\ A_1 &= I_3, \quad b_1 = [1 \ 0 \ 1]^T, \quad c_1 = [2 \ 0 \ 0]^T, \quad d_1 = 10 \\ A_2 &= \begin{bmatrix} 2 & 1 & -3 \\ 1 & -2 & 0 \end{bmatrix}, \quad b_2 = [-6 \ -4]^T, \quad c_2 = [0 \ 1 \ 1]^T, \quad d_2 = 10 \\ F &= [1 \ -1 \ 2], \quad g = 5. \end{aligned}$$

Solving Example 3 using the MATLAB-based convex optimization software CVX toolbox, we obtain the global optimal solution $x^* = (2.2408, -3.3532, -0.2970)$.

Next we apply optimization dynamics (4.40a) – (4.40d) and (4.41a) – (4.41c), respectively, to solve this same SOCP example and compare their performances.

We use MATLAB ODE solver `ode45` to compute the solutions of optimization dynamics (4.40a) – (4.40d) and (4.41a) – (4.41c) associated with Example 3. Trajectories of the primal variables are respectively plotted in Fig. 4.5. Starting from the same initial point, we can see that both dynamical systems converge to the correct optimal solution x^* .

If we further compare the performances of dynamics (4.40a) – (4.40d) and (4.41a) – (4.41c), we find that the former system has a faster convergence.

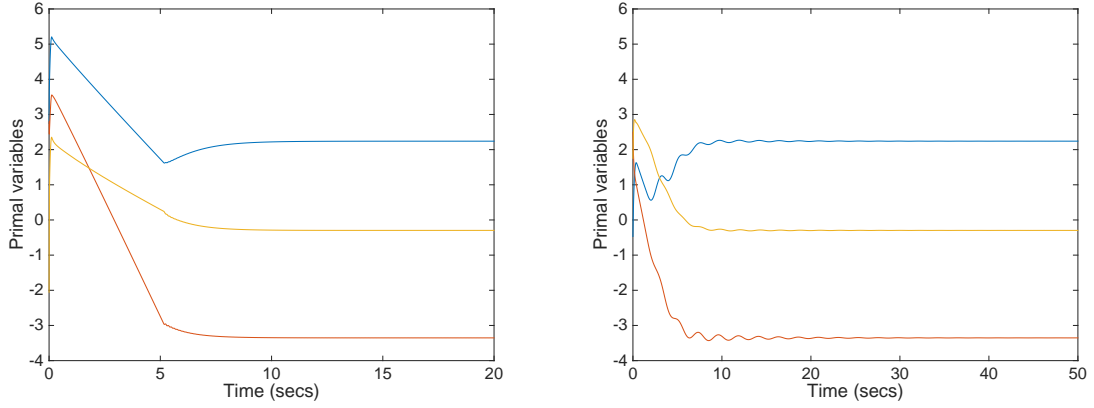


Figure 4.5 Trajectories of the primal variables: in the left subfigure we show the convergence of optimization dynamics (4.40a) – (4.40d) associated with Example 3, whereas in the right one we show the convergence of optimization dynamics (4.41a) – (4.41c)

Specifically, dynamics (4.40a) – (4.40d) converges to the optimal solution within 10 seconds while in comparison dynamics (4.41a) – (4.41c) takes more than 20 seconds to settle down. Besides, the trajectories of dynamics (4.40a) – (4.40d) is smoother and without any oscillations. This suggests that our optimization dynamics (4.40a) – (4.40d) not only possesses a distributed computation structure but also has a better convergence behavior.

4.8 Summary

In this chapter, we have studied the non-convex QCQP problems via the continuous-time optimization dynamics approach. We have developed a necessary and sufficient condition to characterize saddle-points for those non-convex QCQPs. Based on this result, we have further derived a convergence analysis for the associated optimization dynamics. For certain networked non-convex QCQPs, we have also pointed out an intrinsic distributed computation structure of the optimization dynamics approach when the network is sparsely connected. Moreover, we have presented several applications, including MAXCUT, phase recovery, and convex SOCPs, to demonstrate the effectiveness of our approach.

CHAPTER 5. OPTIMAL POWER FLOW PROBLEMS

In power systems, the optimal power flow (OPF) problem seeks an optimal solution of bus voltage magnitudes and phase angles that minimizes a given generation cost, subject to the power balance at each bus as well as other network operating constraints. The power balance is characterized by power flow equations and operational constraints usually include voltage magnitude limits, line flow limits, etc. In general, OPF problems are non-convex quadratically constrained quadratic programmings (QCQPs).

[Lavaci and Low \(2012\)](#) has theoretically proved that under certain conditions there is no optimal duality gap between the primal OPF problem and its semi-definite programming (SDP) dual relaxation. Although counterexamples exist, numerical experience suggests that this SDP dual relaxation approach tends to be exact in many cases.

Note that strong duality implies existence of saddle-points, so we can apply the optimization dynamical system proposed in Chapter 4 to search them. Luckily, due to the sparsity of power networks, our optimization dynamics approach unveils a deep, distributed structure of the OPF problem at the bus level.

Specifically, the optimization dynamics treats each bus in the power network as an intelligent computing agent, which only requires the local information from neighboring buses to update its own voltage variables and Lagrange multipliers. Discovering such a distributed structure of the optimization dynamics is also the main contribution of this chapter.

Moreover, we discover that our optimization dynamics may still converge to a saddle-point even when the SDP dual relaxation fails to maintain a zero optimal duality gap. This fact reveals the existence of a stronger Lagrange dual to the OPF problem. It also suggests that the optimization dynamics approach can find global OPF solutions under more general conditions than the SDP dual relaxation approach.

This chapter is organized as follows. In Section 5.1, we first present the formulation of OPF problems. In Section 5.2, we apply the continuous-time optimization dynamics and unveil a distributed OPF structure. In Section 5.3, we derive a sufficient condition for the global OPF solution. In Section 5.4, we compare our approach with the SDP dual relaxations. Finally, a convergence analysis and simulation results are presented in Sections 5.5 and 5.6, respectively.

5.1 Formulation of the OPF Problem

Consider an n -bus power network with the set of all buses $\mathcal{N} = \{1, 2, \dots, n\}$. We denote the set of generator buses as $\mathcal{G} = \{1, 2, \dots, m\} \subseteq \mathcal{N}$ and the set of all transmission lines as $\mathcal{L} \subseteq \mathcal{N} \times \mathcal{N}$, respectively. In this work, we model the power network as an undirected graph.

5.1.1 The Original OPF Problem

Let V_k and I_k , respectively, denote the complex-valued voltage and current at each bus $k \in \mathcal{N}$. Let $P_k^d + iQ_k^d$ represent the active and reactive power demands for each bus $k \in \mathcal{N}$. Let $P_l^g + iQ_l^g$ represent the active and reactive power generated at each generator bus $l \in \mathcal{G}$. Besides, let S_{kl} represent the apparent power flow on the transmission line $(k, l) \in \mathcal{L}$. We define the cost function $f_l(P_l^g) := c_{l2}(P_l^g)^2 + c_{l1}P_l^g + c_{l0}$ with $c_{l2} > 0$ to account for the quadratic cost of the active power generation at each generator bus $l \in \mathcal{G}$. Thus, the OPF problem can be formulated as

$$\underset{P_l^g, V_k, I_k}{\text{minimize}} \quad \sum_{l \in \mathcal{G}} f_l(P_l^g) \quad (5.1a)$$

subject to

$$P_l^{\min} \leq P_l^g \leq P_l^{\max} \quad \forall l \in \mathcal{G} \quad (5.1b)$$

$$Q_l^{\min} \leq Q_l^g \leq Q_l^{\max} \quad \forall l \in \mathcal{G} \quad (5.1c)$$

$$(V_k^{\min})^2 \leq |V_k|^2 \leq (V_k^{\max})^2 \quad \forall k \in \mathcal{N} \quad (5.1d)$$

$$|S_{kl}| \leq S_{kl}^{\max} \quad \forall (k, l) \in \mathcal{L} \quad (5.1e)$$

$$V_l I_l^* = (P_l^g - P_l^d) + i(Q_l^g - Q_l^d) \quad \forall l \in \mathcal{G} \quad (5.1f)$$

$$V_k I_k^* = -P_k^d - iQ_k^d \quad \forall k \in \mathcal{N} \setminus \mathcal{G} \quad (5.1g)$$

where the optimization variables are $P_l^g \in \mathbb{R}$, $V_k \in \mathbb{C}$, and $I_k \in \mathbb{C}$, for all $l \in \mathcal{G}$ and $k \in \mathcal{N}$. The constants P_l^{\min} , P_l^{\max} , Q_l^{\min} , Q_l^{\max} , V_k^{\min} , V_k^{\max} , and S_{kl}^{\max} are the given operating limits on the power system. Particularly, we require $V_k^{\min} > 0$ for all $k \in \mathcal{N}$ because voltage magnitudes should usually range from 0.9 to 1.1 (PU) for all buses.

Assumption 4. *We assume that OPF problem (5.1a) – (5.1g) is feasible and that at least one generator bus has a nonzero net generation.*

Remark 8. *The second part of Assumption 4 is reasonable since the load buses must absorb some nonzero power from the generators to satisfy their load demands.*

This work prefers using rectangular coordinates to represent OPF problem (5.1a) – (5.1g), so we apply the equivalent Π model for every transmission line $(k, l) \in \mathcal{L}$, as shown in Fig. 5.1. Let $y_{kl} := (R_{kl} + jX_{kl})^{-1}$ be the series admittance, and let b_{kl} denote the total shunt capacitance. If there is no transmission line between bus k and bus l , i.e., $(k, l) \notin \mathcal{L}$, then $y_{kl} := 0$. Define the admittance matrix Y to be an $n \times n$ complex-valued matrix, whose (k, l) entry $Y(k, l) := -y_{kl}$ if $k \neq l$, and $Y(k, l) := \frac{1}{2} \sum_{m \in \mathcal{N}(k)} b_{km} + \sum_{m \in \mathcal{N}(k)} y_{km}$ if $k = l$. Thus, we can rewrite the Kirchhoff's law as $I = YV$, where both V and I are complex-valued column vectors with $V := [V_1 \ V_2 \ \dots \ V_n]^T \in \mathbb{C}^n$ and $I := [I_1 \ I_2 \ \dots \ I_n]^T \in \mathbb{C}^n$.

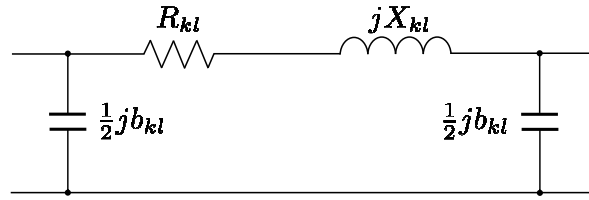


Figure 5.1 The equivalent Π model of a transmission line (k, l)

Next, let us split the real and imaginary parts of the complex voltage variable V and stack them into a $2n$ -dimensional real-valued vector

$$U := [\operatorname{Re}\{V_1\} \ \dots \ \operatorname{Re}\{V_n\} \ \operatorname{Im}\{V_1\} \ \dots \ \operatorname{Im}\{V_n\}]^T \in \mathbb{R}^{2n}.$$

Also let e_1, \dots, e_n denote the n standard basis vectors in \mathbb{R}^n . For all $k \in \mathcal{N}$ and $(k, l) \in \mathcal{L}$, we define $Y_k := e_k e_k^T Y$ and $Y_{kl} := (\bar{y}_{kl} + y_{kl}) e_l e_l^T - (y_{kl}) e_l e_m^T$. Then, we adopt the following

coefficient matrix definitions from [Lavaei and Low \(2012\)](#):

$$\begin{aligned} \mathbf{Y}_k &:= \frac{1}{2} \begin{bmatrix} \operatorname{Re}\{Y_k + Y_k^T\} & \operatorname{Im}\{Y_k^T - Y_k\} \\ \operatorname{Im}\{Y_k - Y_k^T\} & \operatorname{Re}\{Y_k + Y_k^T\} \end{bmatrix} \in \mathbb{R}^{2n \times 2n} \\ \mathbf{Y}_{kl} &:= \frac{1}{2} \begin{bmatrix} \operatorname{Re}\{Y_{kl} + Y_{kl}^T\} & \operatorname{Im}\{Y_{kl}^T - Y_{kl}\} \\ \operatorname{Im}\{Y_{kl} - Y_{kl}^T\} & \operatorname{Re}\{Y_{kl} + Y_{kl}^T\} \end{bmatrix} \in \mathbb{R}^{2n \times 2n} \\ \bar{\mathbf{Y}}_k &:= -\frac{1}{2} \begin{bmatrix} \operatorname{Im}\{Y_k + Y_k^T\} & \operatorname{Re}\{Y_k - Y_k^T\} \\ \operatorname{Re}\{Y_k^T - Y_k\} & \operatorname{Im}\{Y_k + Y_k^T\} \end{bmatrix} \in \mathbb{R}^{2n \times 2n} \\ \bar{\mathbf{Y}}_{kl} &:= -\frac{1}{2} \begin{bmatrix} \operatorname{Im}\{Y_{kl} + Y_{kl}^T\} & \operatorname{Re}\{Y_{kl} - Y_{kl}^T\} \\ \operatorname{Re}\{Y_{kl}^T - Y_{kl}\} & \operatorname{Im}\{Y_{kl} + Y_{kl}^T\} \end{bmatrix} \in \mathbb{R}^{2n \times 2n} \\ \mathbf{M}_k &:= \begin{bmatrix} e_k e_k^T & \mathbf{0} \\ \mathbf{0} & e_k e_k^T \end{bmatrix} \in \mathbb{R}^{2n \times 2n}. \end{aligned}$$

By the coefficient matrices defined above, we have $\operatorname{Re}\{V_k I_k^*\} = U^T \mathbf{Y}_k U$, $\operatorname{Im}\{V_k I_k^*\} = U^T \bar{\mathbf{Y}}_k U$, $|V_k|^2 = U^T \mathbf{M}_k U$, and $|S_{kl}|^2 = (U^T \mathbf{Y}_{kl} U)^2 + (U^T \bar{\mathbf{Y}}_{kl} U)^2$. Thus OPF problem (5.1a) – (5.1g) can be rewritten as

$$\underset{U \in \mathbb{R}^{2n}}{\text{minimize}} \quad \sum_{l \in \mathcal{G}} f_l(U^T \mathbf{Y}_l U + P_l^d) \quad (5.2a)$$

subject to

$$P_k^{\min} - P_k^d \leq U^T \mathbf{Y}_k U \leq P_k^{\max} - P_k^d \quad \forall k \in \mathcal{N} \quad (5.2b)$$

$$Q_k^{\min} - Q_k^d \leq U^T \bar{\mathbf{Y}}_k U \leq Q_k^{\max} - Q_k^d \quad \forall k \in \mathcal{N} \quad (5.2c)$$

$$(V_k^{\min})^2 \leq U^T \mathbf{M}_k U \leq (V_k^{\max})^2 \quad \forall k \in \mathcal{N} \quad (5.2d)$$

$$(U^T \mathbf{Y}_{kl} U)^2 + (U^T \bar{\mathbf{Y}}_{kl} U)^2 \leq (S_{kl}^{\max})^2 \quad \forall (k, l) \in \mathcal{L} \quad (5.2e)$$

where we define $P_k^{\min} = P_k^{\max} = Q_k^{\min} = Q_k^{\max} := 0$ for all load buses $k \in \mathcal{N} \setminus \mathcal{G}$. Note that in OPF problem (5.2a) – (5.2e) the only optimization variable is the $2n$ -dimensional real vector $U \in \mathbb{R}^{2n}$. Moreover, all coefficient matrices \mathbf{Y}_k , $\bar{\mathbf{Y}}_k$, \mathbf{M}_k , \mathbf{Y}_{kl} , and $\bar{\mathbf{Y}}_{kl}$ are derived from the admittance matrix Y and hence are sparse. We will use this sparsity property later to unveil a distributed OPF structure via the associated optimization dynamics.

5.1.2 Infinite Solutions to the OPF Problem

Here, we would also like to point out some structural properties of the coefficient matrices \mathbf{Y}_k , $\bar{\mathbf{Y}}_k$, \mathbf{M}_k , \mathbf{Y}_{kl} , and $\bar{\mathbf{Y}}_{kl}$. These matrices are in fact of the same structure

$$\mathbf{Y} = \begin{bmatrix} Y_1 & Y_2 \\ Y_2^T & Y_1 \end{bmatrix} = \begin{bmatrix} Y_1 & Y_2 \\ -Y_2 & Y_1 \end{bmatrix}$$

where Y_1 is symmetric and Y_2 is anti-symmetric.

Lemma 3. *The \mathbf{Y} matrix has the following structural properties:*

- \mathbf{Y} is symmetric and hence all its eigenvalues are real.
- Let λ be an eigenvalue of \mathbf{Y} with associated eigenvector $x = [x_1^T \ x_2^T]^T$; that is, $\mathbf{Y}x = \lambda x$. Then there exists another eigenvector $\bar{x} = [-x_2^T \ x_1^T]^T$ such that \bar{x} is perpendicular to x and $\mathbf{Y}\bar{x} = \lambda\bar{x}$. In other words, each eigenvalue of \mathbf{Y} has a geometric multiplicity of at least two.
- Given $x = [x_1^T \ x_2^T]^T$ and $\bar{x} = [-x_2^T \ x_1^T]^T$, we can always have (i) $\bar{x}^T \mathbf{Y}x = 0$ and (ii) $x^T \mathbf{Y}x = \bar{x}^T \mathbf{Y}\bar{x} = \hat{x}^T \mathbf{Y}\hat{x}$, where $\hat{x} = \cos(\theta)x + \sin(\theta)\bar{x}$, for all $0 \leq \theta < 2\pi$.

Proof of Lemma 3. These results can be derived via basic linear algebra. \square

Such structural properties of the coefficient matrices \mathbf{Y}_k , $\bar{\mathbf{Y}}_k$, \mathbf{M}_k , \mathbf{Y}_{kl} , and $\bar{\mathbf{Y}}_{kl}$ result in an infinite number of solutions to OPF problem (5.2a) – (5.2e).

Corollary 3. *Suppose that OPF problem (5.2a) – (5.2e) has an optimal solution, which is given by $U^* = [(U_1^*)^T \ (U_2^*)^T]^T$, then there is another orthonormal solution $\bar{U}^* = [(-U_2^*)^T \ (U_1^*)^T]^T$ such that all optimal solutions to OPF problem (5.2a) – (5.2e) can be expressed as*

$$\mathcal{U} := \left\{ \hat{U} \mid \hat{U} = \cos(\theta)U^* + \sin(\theta)\bar{U}^*, \ 0 \leq \theta < 2\pi \right\}.$$

Proof of Corollary 3. Applying Lemma 3 to (5.2a) – (5.2e) yields the result easily. \square

Remark 9. *Each $\hat{U} \in \mathcal{U}$, in fact, represents the same OPF solution but seen from a different phase angle reference. If we select one bus in the network as the reference (zero phase angle), then there exists a unique representative for the equivalent optimal solution set \mathcal{U} .*

5.1.3 The Modified OPF Problem

To avoid the technical challenges caused by the uncountably infinite number of equivalent OPF solutions, we propose the following modified OPF problem

$$\underset{U \in \mathbb{R}^{2n}}{\text{minimize}} \quad \sum_{l \in \mathcal{G}} f_l(U^T \mathbf{Y}_l U + P_l^d) + (e_{n+1}^T U)^2 \quad (5.3a)$$

subject to

$$P_k^{\min} - P_k^d \leq U^T \mathbf{Y}_k U \leq P_k^{\max} - P_k^d \quad \forall k \in \mathcal{N} \quad (5.3b)$$

$$Q_k^{\min} - Q_k^d \leq U^T \bar{\mathbf{Y}}_k U \leq Q_k^{\max} - Q_k^d \quad \forall k \in \mathcal{N} \quad (5.3c)$$

$$(V_k^{\min})^2 \leq U^T \mathbf{M}_k U \leq (V_k^{\max})^2 \quad \forall k \in \mathcal{N} \quad (5.3d)$$

$$(U^T \mathbf{Y}_{kl} U)^2 + (U^T \bar{\mathbf{Y}}_{kl} U)^2 \leq (S_{kl}^{\max})^2 \quad \forall (k, l) \in \mathcal{L}. \quad (5.3e)$$

The only difference between OPF problems (5.2a) – (5.2e) and (5.3a) – (5.3e) is that (5.3a) has an extra term $(e_{n+1}^T U)^2$ at the cost function. This fixes bus 1 as the slack bus by setting $\text{Im}\{V_1\} = 0$. Recall that e_{n+1} denotes the $(n+1)$ -th elementary vector in \mathbb{R}^{2n} and therefore we have $e_{n+1}^T U = \text{Im}\{V_1\}$. Note that the optimal cost in (5.3a) will force $\text{Im}\{V_1\}$ to zero.

Compared with the solution set of OPF (5.2a) – (5.2e), problem (5.3a) – (5.3e) now locally has two isolated optima, i.e., the 0-degree ($\text{Re}\{V_1\} > 0$) and 180-degree ($\text{Re}\{V_1\} < 0$) solutions with respect to the slack bus.

Lemma 4. *OPF formulations (5.2a) – (5.2e) and (5.3a) – (5.3e) are equivalent to each other, in the sense that given an optimum to one problem, we can recover a corresponding optimum to the other problem with a same optimal cost.*

Proof of Lemma 4. Suppose that U^* minimizes problem (5.2a) – (5.2e). Then in its solution set there must be one \hat{U} for some θ such that $\hat{U}^T \mathbf{Y}_l \hat{U} = U^{*T} \mathbf{Y}_l U^*$ for all $l \in \mathcal{G}$ and $e_{n+1}^T \hat{U} = 0$. Thus, \hat{U} minimizes problem (5.3a) – (5.3e) and yields a same optimal cost as (5.2a) – (5.2e).

Conversely, let U^* be an optimum to problem (5.3a) – (5.3e). Then both terms in the cost function $\sum_{l \in \mathcal{G}} f_l(U^T \mathbf{Y}_l U + P_l^d)$ and $(e_{n+1}^T U)^2$ should be minimized. Since $(e_{n+1}^T U)^2 \geq 0$, we must have $e_{n+1}^T U^* = 0$. Therefore, U^* minimizes problem (5.2a) – (5.2e), too. \square

5.2 The Optimization Dynamics Approach

In this section, we employ the optimization dynamical system (3.1a) – (3.1c) defined in Chapter 3 to solve the non-convex, modified OPF problem (5.3a) – (5.3e).

5.2.1 The Associated Optimization Dynamics

Let $\underline{\lambda}_k, \bar{\lambda}_k, \underline{\gamma}_k, \bar{\gamma}_k, \underline{\mu}_k, \bar{\mu}_k$, and ν_{kl} be the Lagrange multipliers associated with constraints (5.3b) – (5.3e), respectively. Also define the bold Greek variables

$$\boldsymbol{\lambda}_k := \bar{\lambda}_k - \underline{\lambda}_k, \quad \boldsymbol{\gamma}_k := \bar{\gamma}_k - \underline{\gamma}_k, \quad \boldsymbol{\mu}_k := \bar{\mu}_k - \underline{\mu}_k, \quad \forall k \in \mathcal{N}.$$

Then the Lagrangian associated with OPF problem (5.3a) – (5.3e) is given by

$$L(U, \lambda, \gamma, \mu, \nu) := L_1(U) + L_2(U, \lambda, \gamma, \mu) + L_3(U, \nu) + (e_{n+1}^T U)^2 \quad (5.4)$$

where

$$\begin{aligned} L_1(U) &:= \sum_{l \in \mathcal{G}} \left[c_{l2} (U^T \mathbf{Y}_l U + P_l^d)^2 + c_{l1} (U^T \mathbf{Y}_l U + P_l^d) + c_{l0} \right] \\ L_2(U, \lambda, \gamma, \mu) &:= \sum_{k \in \mathcal{N}} \left[\boldsymbol{\lambda}_k (U^T \mathbf{Y}_k U + P_k^d) + \boldsymbol{\gamma}_k (U^T \bar{\mathbf{Y}}_k U + Q_k^d) + \boldsymbol{\mu}_k U^T \mathbf{M}_k U \right. \\ &\quad \left. + \underline{\lambda}_k P_k^{\min} - \bar{\lambda}_k P_k^{\max} + \underline{\gamma}_k Q_k^{\min} - \bar{\gamma}_k Q_k^{\max} + \underline{\mu}_k (V_k^{\min})^2 - \bar{\mu}_k (V_k^{\max})^2 \right] \\ L_3(U, \nu) &:= \sum_{(k,l) \in \mathcal{L}} \nu_{kl} \left[(U^T \mathbf{Y}_{kl} U)^2 + (U^T \bar{\mathbf{Y}}_{kl} U)^2 - (S_{kl}^{\max})^2 \right]. \end{aligned}$$

We need to point out that the Lagrangian (5.4) is a quartic polynomial function of the primal variable U , and, at present, we do not know either how to globally minimize (5.4) over $U \in \mathbb{R}^{2n}$ or how to derive an explicit Lagrange dual for OPF problem (5.3a) – (5.3e).

Now we can use the Lagrange (5.4) to derive an optimization dynamics for OPF problem (5.3a) – (5.3e). Let $\mathbf{B}(U, \lambda, \gamma, \mu, \nu)$ be the $2n \times 2n$ symmetric matrix

$$\begin{aligned} \mathbf{B}(U, \lambda, \gamma, \mu, \nu) &:= \sum_{l \in \mathcal{G}} \left[2c_{l2} (U^T \mathbf{Y}_l U + P_l^d) \mathbf{Y}_l + c_{l1} \mathbf{Y}_l \right] + \sum_{k \in \mathcal{N}} \left(\boldsymbol{\lambda}_k \mathbf{Y}_k + \boldsymbol{\gamma}_k \bar{\mathbf{Y}}_k + \boldsymbol{\mu}_k \mathbf{M}_k \right) \\ &\quad + \sum_{(k,l) \in \mathcal{L}} 2\nu_{kl} \left[(U^T \mathbf{Y}_{kl} U) \mathbf{Y}_{kl} + (U^T \bar{\mathbf{Y}}_{kl} U) \bar{\mathbf{Y}}_{kl} \right]. \end{aligned} \quad (5.5)$$

Then following definitions (3.1a) – (3.1c), we formulate the optimization dynamics associated with OPF problem (5.3a) – (5.3e) as

$$\dot{U} := -2\alpha \left[\mathbf{B}(U, \lambda, \gamma, \mu, \nu) + (e_{n+1} e_{n+1}^T) \right] U \quad (5.6a)$$

$$\dot{\underline{\lambda}}_k := \alpha \left[P_k^{\min} - P_k^d - U^T \mathbf{Y}_k U \right]_{\underline{\lambda}_k}^+ \quad (5.6b)$$

$$\dot{\bar{\lambda}}_k := \alpha \left[U^T \mathbf{Y}_k U - P_k^{\max} + P_k^d \right]_{\bar{\lambda}_k}^+ \quad (5.6c)$$

$$\dot{\underline{\gamma}}_k := \alpha \left[Q_k^{\min} - Q_k^d - U^T \bar{\mathbf{Y}}_k U \right]_{\underline{\gamma}_k}^+ \quad (5.6d)$$

$$\dot{\bar{\gamma}}_k := \alpha \left[U^T \bar{\mathbf{Y}}_k U - Q_k^{\max} + Q_k^d \right]_{\bar{\gamma}_k}^+ \quad (5.6e)$$

$$\dot{\underline{\mu}}_k := \alpha \left[(V_k^{\min})^2 - U^T \mathbf{M}_k U \right]_{\underline{\mu}_k}^+ \quad (5.6f)$$

$$\dot{\bar{\mu}}_k := \alpha \left[U^T \mathbf{M}_k U - (V_k^{\max})^2 \right]_{\bar{\mu}_k}^+ \quad (5.6g)$$

$$\dot{\nu}_{kl} := \alpha \left[(U^T \mathbf{Y}_{kl} U)^2 + (U^T \bar{\mathbf{Y}}_{kl} U)^2 - (S_{kl}^{\max})^2 \right]_{\nu_{kl}}^+ \quad (5.6h)$$

for all $k \in \mathcal{N}$ and $(k, l) \in \mathcal{L}$. The constant parameter $\alpha > 0$ in (5.6a) – (5.6h) is used for tuning the convergence speed without affecting its locally asymptotic stability. By default, we choose $\alpha = 1$. Simulations show that a large α fastens the convergence of dynamics (5.6a) – (5.6h).

5.2.2 A Distributed OPF Structure

We are interested in solving OPF problem (5.3a) – (5.3e) via the optimization dynamics approach, since dynamics (5.6a) – (5.6h) unveils a distributed structure of the OPF problem.

Let us view each bus in the power network as an individual computing agent. Suppose that each agent k , for all $k \in \mathcal{N}$, stores and manages the following constants and variables

- coefficient matrices: $\mathbf{Y}_k, \bar{\mathbf{Y}}_k, \mathbf{M}_k, \mathbf{Y}_{kl}, \bar{\mathbf{Y}}_{kl}$, for all $l \in \mathcal{N}(k)$
- load demands and operational limits: $P_k^d, Q_k^d, V_k^{\min}, V_k^{\max}, S_{kl}^{\max}$, for all $l \in \mathcal{N}(k)$
- generation parameters: $c_{k2}, c_{k1}, c_{k0}, P_k^{\min}, P_k^{\max}, Q_k^{\min}, Q_k^{\max}$, if $k \in \mathcal{G}$
- Lagrange multipliers: $\underline{\lambda}_k, \bar{\lambda}_k, \underline{\gamma}_k, \bar{\gamma}_k, \underline{\mu}_k, \bar{\mu}_k, \nu_{kl}$, for all $l \in \mathcal{N}(k)$
- voltage variables: U_k and U_{k+n}

where U_k and U_{k+n} denote the k -th and $(k+n)$ -th element in vector U , respectively, and $\mathcal{N}(k)$ denotes the set that contains all the neighboring buses of bus k . If bus k is connected with bus l in the power network, i.e., $l \in \mathcal{N}(k)$ or $k \in \mathcal{N}(l)$, then we allow their corresponding agents to communicate with each other.

Before we move on, let us introduce a lemma that characterizes the sparsity of coefficient matrices \mathbf{Y}_k , $\bar{\mathbf{Y}}_k$, \mathbf{M}_k , \mathbf{Y}_{kl} , and $\bar{\mathbf{Y}}_{kl}$ in dynamics (5.6a) – (5.6h).

Lemma 5. *For all $k \in \mathcal{N}$ and $(k, l) \in \mathcal{L}$, \mathbf{Y}_k , $\bar{\mathbf{Y}}_k$, \mathbf{M}_k , \mathbf{Y}_{kl} , and $\bar{\mathbf{Y}}_{kl}$ are sparse matrices:*

- (1) *All the entries of \mathbf{M}_k are zeros, except two 1 entries on diagonal positions (k, k) and $(k+n, k+n)$.*
- (2) *Besides the two diagonal positions (k, k) and $(k+n, k+n)$, both \mathbf{Y}_k and $\bar{\mathbf{Y}}_k$ only have non-zero entries on positions (k, l) , $(k, l+n)$, $(k+n, l)$, and $(k+n, l+n)$, for $l \in \mathcal{N}(k)$.*
- (3) *Both \mathbf{Y}_{kl} and $\bar{\mathbf{Y}}_{kl}$ only have non-zero entries on positions (k, k) , $(k+n, k+n)$, (k, l) , (l, k) , $(k+n, l+n)$, $(l+n, k+n)$, $(k, l+n)$, $(l+n, k)$, $(k+n, l)$, and $(l, k+n)$.*

Proof of Lemma 5. This is a direct result following from definitions of these matrices. \square

Theorem 21. *According to dynamics (5.6a) – (5.6h), each bus only uses the local information from neighbors to compute its gradients of voltage variables and Lagrange multipliers.*

Proof of Theorem 21. Without loss of generality, let us consider bus k in the power network. By Lemma 5, we know that the Lagrangian multipliers' dynamics (5.6b) – (5.6h) only depend on U_k , U_{k+n} , U_l , and U_{l+n} , for all $l \in \mathcal{N}(k)$.

Moreover, we note that the $\mathbf{B}(U, \lambda, \gamma, \mu, \nu)$ matrix in (5.6a) is a linear combination of \mathbf{Y}_k , $\bar{\mathbf{Y}}_k$, \mathbf{M}_k , \mathbf{Y}_{kl} , and $\bar{\mathbf{Y}}_{kl}$. Again, by Lemma 5, we can easily check that the computation of both dynamics \dot{U}_k and \dot{U}_{k+n} only involves the terms U_k , U_{k+n} , λ_k , γ_k , μ_k , U_l , U_{l+n} , λ_l , γ_l , and ν_{kl} , for all $l \in \mathcal{N}(k)$. Here, we need to explain more about the reference bus 1 because of the extra term $-2\alpha (e_{n+1} e_{n+1}^T) U$. Since all the entries of $e_{n+1} e_{n+1}^T$ are zeros except a only 1 entry on the $(n+1, n+1)$ position, we are in fact subtracting $2\alpha U_{n+1}$ from dynamics \dot{U}_{n+1} . Hence, the distributed OPF structure will not be affected. This completes the proof. \square

Theorem 21 shows that dynamical system (5.6a) – (5.6h) has fully exploited a distributed OPF structure into the bus level, so our optimization dynamics approach can be topologically suitable for the physical settings of power networks. A fundamental reason for this distributed OPF structure lies in the sparsity of power networks. Our result suggests that intelligent buses suffice to cooperate with each other making global OPF decisions via a localized information flow, which, as far as we know, has long been missed in literature.

Example 4. Let us consider a four-bus power network as shown in Fig. 5.2, where bus 1 is a generator bus and others are load buses. The generator bus has a voltage magnitude constraint. Besides, each load bus has a pair of active and reactive power generation constraints.

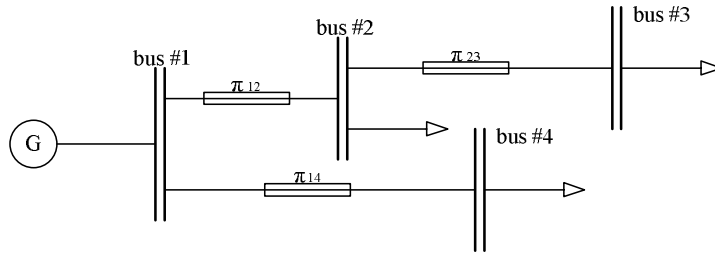


Figure 5.2 A four-bus power network

Example 4 is adopted from Lavaei and Low (2012). Since we are only using this example to illustrate the distributed OPF structure, the detailed problem settings are omitted here.

Let μ be the Lagrange multiplier associated with the voltage magnitude constraint of bus 1. For each load bus k , $2 \leq k \leq 4$, let λ_k and γ_k be the Lagrange multipliers associated with the active and reactive power generation constraints, respectively. Then we can implement our optimization dynamics for this example via the MATLAB Simulink toolbox, see Fig. 5.3.

Let us take bus 1 as an example to illustrate the distributed OPF structure. Since bus 1 is connected with buses 2 and 4 in the power network, agent 1 uses the voltage variables and Lagrange multipliers from agents 2 and 4 as its inputs, and it also outputs its own voltage variables to those two agents. Moreover, agent 1 has no communication with agent 3 because there is no connection between their corresponding buses. Moreover, the same situation holds for all the other buses. To sum up, we conclude that the computation structure of this Simulink implementation mimics the same connection topology of the original power network.

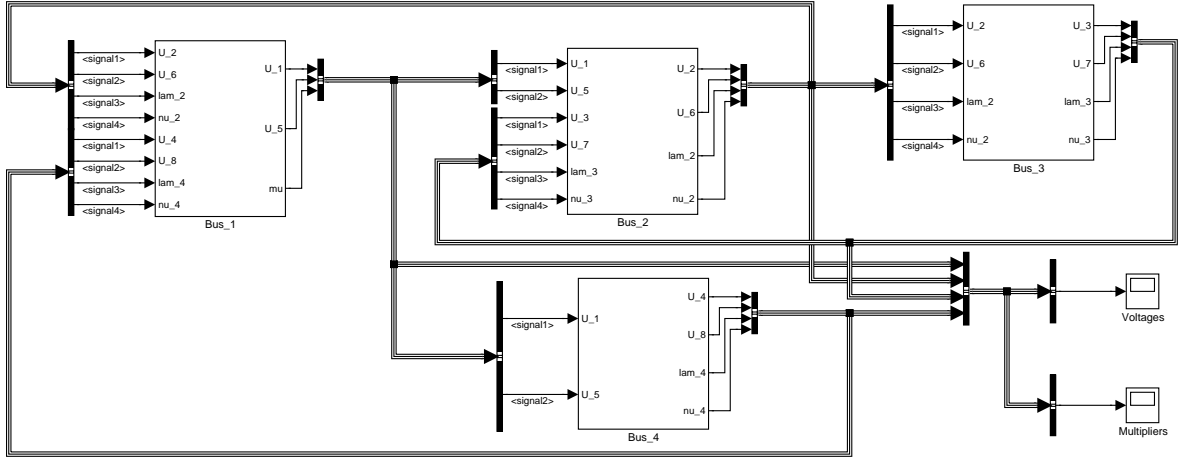


Figure 5.3 The Simulink implementation of the four-bus OPF

5.3 A Sufficient Characterization for Global Optimality

A key point involved in this chapter is to characterize the saddle-points for OPF problems using the equilibrium of the associated optimization dynamics. We have already known that any equilibrium point $(U^*, \lambda^*, \gamma^*, \mu^*, \nu^*)$ of dynamics (5.6a) – (5.6h) is a KKT point for OPF problem (5.3a) – (5.3e). However, due to the non-convexity of OPF problems, a KKT point may not necessarily be a saddle-point. Therefore, a natural question one would ask is: under what conditions the KKT point obtained from dynamics (5.6a) – (5.6h) can be determined as a saddle-point for OPF problem (5.3a) – (5.3e)? To begin with, we provide a sufficient condition to characterize saddle-points for the Lagrangian (5.4).

Lemma 6. *Suppose that OPF problem (5.3a) – (5.3e) has one KKT point $(U^*, \lambda^*, \gamma^*, \mu^*, \nu^*)$. Then, it is also a saddle-point for the Lagrangian (5.4) if the difference*

$$P(U) := L(U, \lambda^*, \gamma^*, \mu^*, \nu^*) - L(U^*, \lambda^*, \gamma^*, \mu^*, \nu^*)$$

can be written as a sum-of-squares (SOS) polynomial in U .

Proof of Lemma 6. Because $(U^*, \lambda^*, \gamma^*, \mu^*, \nu^*)$ is a KKT point, we know that (i) U^* is primal feasible, i.e., U^* satisfies all of the inequality constraints (5.3b) – (5.3e); (ii) $(\lambda^*, \gamma^*, \mu^*, \nu^*)$ is dual feasible, i.e., $\lambda^* \geq 0$, $\gamma^* \geq 0$, $\mu^* \geq 0$, and $\nu^* \geq 0$; and (iii) the complementary slackness

condition holds. Using statements (i) – (iii), it is easy to show that for all $\lambda \geq 0$, $\gamma \geq 0$, $\mu \geq 0$, and $\nu \geq 0$, we have

$$L(U^*, \lambda^*, \gamma^*, \mu^*, \nu^*) \geq L(U^*, \lambda, \gamma, \mu, \nu). \quad (5.7)$$

Next, because $P(U)$ is an SOS polynomial in U , we have $P(U)$ always non-negative. That is, for all $U \in \mathbb{R}^{2n}$

$$L(U^*, \lambda^*, \gamma^*, \mu^*, \nu^*) \leq L(U, \lambda^*, \gamma^*, \mu^*, \nu^*). \quad (5.8)$$

Combining inequalities (5.7) and (5.8), by Definition 8 we conclude that $(U^*, \lambda^*, \gamma^*, \mu^*, \nu^*)$ is a saddle-point for the Lagrangian (5.4). \square

Now we are ready to develop an easier sufficient condition for checking saddle-points using the equilibrium of dynamics (5.6a) – (5.6h).

Theorem 22. *Suppose that optimization dynamics (5.6a) – (5.6h) converges to an equilibrium $(U^*, \lambda^*, \gamma^*, \mu^*, \nu^*)$ with $\mathbf{B}(U^*, \lambda^*, \gamma^*, \mu^*, \nu^*)U^* = 0$. If the matrix $\mathbf{B}(U^*, \lambda^*, \gamma^*, \mu^*, \nu^*) \succeq 0$, then $(U^*, \lambda^*, \gamma^*, \mu^*, \nu^*)$ is a saddle-point for the Lagrangian (5.4).*

Proof of Theorem 22. Each equilibrium $(U^*, \lambda^*, \gamma^*, \mu^*, \nu^*)$ of dynamics (5.6a) – (5.6h) with $\mathbf{B}(U^*, \lambda^*, \gamma^*, \mu^*, \nu^*)U^* = 0$ satisfies all KKT conditions for OPF problem (5.3a) – (5.3e). To prove that $(U^*, \lambda^*, \gamma^*, \mu^*, \nu^*)$ is also a saddle-point for the Lagrangian (5.4), by Lemma 6 we only need to show that $P(U)$ is an SOS polynomial in U .

Neglecting all the constant terms in the Lagrangian (5.4), we define the function

$$\begin{aligned} h(U, \lambda, \gamma, \mu, \nu) := & \sum_{l \in \mathcal{G}} \left[c_{l2}(U^T \mathbf{Y}_l U)^2 + 2c_{l2} P_l^d U^T \mathbf{Y}_l U + c_{l1} U^T \mathbf{Y}_l U \right] \\ & + \sum_{k \in \mathcal{N}} \left(\lambda_k U^T \mathbf{Y}_k U + \gamma_k U^T \bar{\mathbf{Y}}_k U + \mu_k U^T \mathbf{M}_k U \right) \\ & + \sum_{(k,l) \in \mathcal{L}} \nu_{kl} \left[(U^T \mathbf{Y}_{kl} U)^2 + (U^T \bar{\mathbf{Y}}_{kl} U)^2 \right] + (e_{n+1}^T U)^2. \end{aligned}$$

Then the difference polynomial $P(U)$ can be given by

$$\begin{aligned} P(U) &= L(U, \lambda^*, \gamma^*, \mu^*, \nu^*) - L(U^*, \lambda^*, \gamma^*, \mu^*, \nu^*) \\ &= h(U, \lambda^*, \gamma^*, \mu^*, \nu^*) - h(U^*, \lambda^*, \gamma^*, \mu^*, \nu^*). \end{aligned} \quad (5.9)$$

On the one hand, we notice that

$$\begin{aligned}
h(U, \lambda^*, \gamma^*, \mu^*, \nu^*) &= U^T \mathbf{B}(U^*, \lambda^*, \gamma^*, \mu^*, \nu^*) U + \sum_{l \in \mathcal{G}} c_{l2} \left[(U^T \mathbf{Y}_l U)^2 - 2(U^{*T} \mathbf{Y}_l U^*)(U^T \mathbf{Y}_l U) \right] \\
&\quad + \sum_{(k,l) \in \mathcal{L}} \nu_{kl}^* \left[(U^T \mathbf{Y}_{kl} U)^2 - 2(U^{*T} \mathbf{Y}_{kl} U^*)(U^T \mathbf{Y}_{kl} U) \right] \\
&\quad + \sum_{(k,l) \in \mathcal{L}} \nu_{kl}^* \left[(U^T \bar{\mathbf{Y}}_{kl} U)^2 - 2(U^{*T} \bar{\mathbf{Y}}_{kl} U^*)(U^T \bar{\mathbf{Y}}_{kl} U) \right] + (e_{n+1}^T U)^2. \quad (5.10)
\end{aligned}$$

On the other hand, since $\mathbf{B}(U^*, \lambda^*, \gamma^*, \mu^*, \nu^*) U^* = 0$ we must have $e_{n+1}^T U^* = 0$ and

$$h(U^*, \lambda^*, \gamma^*, \mu^*, \nu^*) = - \sum_{l \in \mathcal{G}} c_{l2} \left[(U^{*T} \mathbf{Y}_l U^*)^2 \right] - \sum_{(k,l) \in \mathcal{L}} \nu_{kl}^* \left[(U^{*T} \mathbf{Y}_{kl} U^*)^2 + (U^{*T} \bar{\mathbf{Y}}_{kl} U^*)^2 \right]. \quad (5.11)$$

Substituting (5.10) and (5.11) into (5.9) yields

$$\begin{aligned}
P(U) &= U^T \mathbf{B}(U^*, \lambda^*, \gamma^*, \mu^*, \nu^*) U + (e_{n+1}^T U)^2 + \sum_{l \in \mathcal{G}} c_{l2} \left[(U^T \mathbf{Y}_l U) - (U^{*T} \mathbf{Y}_l U^*) \right]^2 \\
&\quad + \sum_{(k,l) \in \mathcal{L}} \nu_{kl}^* \left\{ \left[(U^T \mathbf{Y}_{kl} U) - (U^{*T} \mathbf{Y}_{kl} U^*) \right]^2 + \left[(U^T \bar{\mathbf{Y}}_{kl} U) - (U^{*T} \bar{\mathbf{Y}}_{kl} U^*) \right]^2 \right\}. \quad (5.12)
\end{aligned}$$

Because $c_{l2} > 0$ for all $l \in \mathcal{G}$, $\nu_{kl}^* \geq 0$ (by the dual feasibility), and $\mathbf{B}(U^*, \lambda^*, \gamma^*, \mu^*, \nu^*) \succeq 0$, the polynomial $P(U)$ is now expressed in terms of a sum of squares. \square

We can only derive a sufficient saddle-point condition here because the Lagrangian (5.4) is a multivariate, quartic polynomial. Hence, the equivalence result between the sum of squares condition and polynomials' non-negativity (Theorem 4) cannot be applied.

5.4 Comparisons with the SDP Dual Relaxation Approach

This section compares the applicability of the proposed optimization dynamics approach with the existing SDP dual relaxation approach for solving OPF problems. We show that our optimization dynamics can find global OPF solutions under more general conditions.

5.4.1 The SDP Dual Relaxation Approach

An efficient approach for solving the OPF problem is to study its SDP dual relaxation, see [Lavari and Low \(2012\)](#). Different from our work, the SDP dual relaxation is developed from

the original OPF problem (5.2a) – (5.2e). By the change of variable $W = UU^T$, an equivalent form to OPF formulation (5.2a) – (5.2e) is given by

$$\underset{\alpha, U, W}{\text{minimize}} \quad \sum_{l \in \mathcal{G}} \alpha_l \quad (5.13a)$$

subject to

$$P_k^{\min} - P_k^d \leq \text{Tr}\{\mathbf{Y}_k W\} \leq P_k^{\max} - P_k^d \quad \forall k \in \mathcal{N} \quad (5.13b)$$

$$Q_k^{\min} - Q_k^d \leq \text{Tr}\{\bar{\mathbf{Y}}_k W\} \leq Q_k^{\max} - Q_k^d \quad \forall k \in \mathcal{N} \quad (5.13c)$$

$$(V_k^{\min})^2 \leq \text{Tr}\{\mathbf{M}_k W\} \leq (V_k^{\max})^2 \quad \forall k \in \mathcal{N} \quad (5.13d)$$

$$\mathbf{L}_{kl} \preceq 0 \quad \forall (k, l) \in \mathcal{L} \quad (5.13e)$$

$$\mathbf{C}_l \preceq 0 \quad \forall l \in \mathcal{G} \quad (5.13f)$$

$$W = UU^T \quad (5.13g)$$

where we define

$$\mathbf{L}_{kl} := \begin{bmatrix} -(S_{kl}^{\max})^2 & \text{Tr}\{\mathbf{Y}_{kl} W\} & \text{Tr}\{\bar{\mathbf{Y}}_{kl} W\} \\ \text{Tr}\{\mathbf{Y}_{kl} W\} & -1 & 0 \\ \text{Tr}\{\bar{\mathbf{Y}}_{kl} W\} & 0 & -1 \end{bmatrix}$$

$$\mathbf{C}_l := \begin{bmatrix} c_{l1} \text{Tr}\{\mathbf{Y}_l W\} + c_{l1} P_l^d + c_{l0} - \alpha_l & \sqrt{c_{l2}} (\text{Tr}\{\mathbf{Y}_l W\} + P_l^d) \\ \sqrt{c_{l2}} (\text{Tr}\{\mathbf{Y}_l W\} + P_l^d) & -1 \end{bmatrix}.$$

Let $\underline{\rho}_k, \bar{\rho}_k, \underline{\xi}_k, \bar{\xi}_k, \underline{\zeta}_k$, and $\bar{\zeta}_k, \forall k \in \mathcal{N}$, respectively, be the scalar Lagrange multipliers associated with the inequality constraints (5.13b) – (5.13d). Also let symmetric matrices

$$\mathbf{H}_{kl} := \begin{bmatrix} h_{kl}^1 & h_{kl}^2 & h_{kl}^3 \\ h_{kl}^2 & h_{kl}^4 & h_{kl}^5 \\ h_{kl}^3 & h_{kl}^5 & h_{kl}^6 \end{bmatrix} \quad \text{and} \quad \mathbf{R}_l := \begin{bmatrix} 1 & r_l^1 \\ r_l^1 & r_l^2 \end{bmatrix}$$

be the matrix Lagrange multipliers associated with LMI's (5.13e) and (5.13f), respectively.

Define the bold Greek variables

$$\boldsymbol{\rho}_k := \bar{\rho}_k - \underline{\rho}_k, \quad \boldsymbol{\xi}_k := \bar{\xi}_k - \underline{\xi}_k, \quad \boldsymbol{\zeta}_k := \bar{\zeta}_k - \underline{\zeta}_k, \quad \forall k \in \mathcal{N}.$$

Furthermore, define the following functions

$$d := \sum_{k \in \mathcal{N}} \left[\underline{\rho}_k P_k^{\min} - \bar{\rho}_k P_k^{\max} + \rho_k P_k^d + \underline{\xi}_k Q_k^{\min} - \bar{\xi}_k Q_k^{\max} + \xi_k Q_k^d + \underline{\zeta}_k (V_k^{\min})^2 - \bar{\zeta}_k (V_k^{\max})^2 \right] \\ + \sum_{l \in \mathcal{G}} \left[(2\sqrt{c_{l2}} r_l^1 + c_{l1}) P_l^d + c_{l0} - r_l^2 \right] - \sum_{(k,l) \in \mathcal{L}} \left[(S_{kl}^{\max})^2 h_{kl}^1 + h_{kl}^4 + h_{kl}^6 \right] \quad (5.14)$$

$$\mathbf{A} := \sum_{k \in \mathcal{N}} \left(\rho_k \mathbf{Y}_k + \xi_k \bar{\mathbf{Y}}_k + \zeta_k \mathbf{M}_k \right) + \sum_{l \in \mathcal{G}} \left(2\sqrt{c_{l2}} r_l^1 + c_{l1} \right) \mathbf{Y}_l + \sum_{(k,l) \in \mathcal{L}} 2 \left(h_{kl}^2 \mathbf{Y}_{kl} + h_{kl}^3 \bar{\mathbf{Y}}_{kl} \right) \quad (5.15)$$

and then the Lagrange dual relaxation to problem (5.13a) – (5.13g) can be formulated as

$$\text{maximize } d \quad (5.16a)$$

subject to

$$\mathbf{A} \succeq 0, \mathbf{H}_{kl} \succeq 0, \mathbf{R}_l \succeq 0 \quad (5.16b)$$

$$\rho_k \geq 0, \bar{\rho}_k \geq 0, \xi_k \geq 0, \bar{\xi}_k \geq 0, \zeta_k \geq 0, \bar{\zeta}_k \geq 0. \quad (5.16c)$$

Since the Lagrange dual problem (5.16a) – (5.16c) is an SDP, it is convex and can be solved efficiently. Based on the optimal dual solution, [Lavaei and Low \(2012\)](#) has derived a sufficient condition under which strong duality holds between the primal OPF (5.13a) – (5.13g) and its SDP dual relaxation (5.16a) – (5.16c). This result is summarized below.

Theorem 23. [[Lavaei and Low \(2012\)](#) Theorem 5] *Strong duality holds for (5.13a) – (5.13g) provided that the SDP dual relaxation (5.16a) – (5.16c) has an optimal solution such that the positive semi-definite matrix \mathbf{A}^{opt} has a zero eigenvalue of multiplicity two.*

If there is no optimal duality gap between problems (5.13a) – (5.13g) and (5.16a) – (5.16c), an optimal solution to OPF (5.13a) – (5.13g) can be easily recovered from the dual optimum. [Lavaei and Low \(2012\)](#) has also concluded that strong duality holds for many practical OPF problems. In other words, the SDP dual relaxation approach is widely applicable.

5.4.2 Comparisons with the SDP Dual Relaxation

Our next result builds a connection between the optimization dynamics approach and the SDP dual relaxation approach. We show that, under the conditions of [Theorem 22](#), these two approaches are equivalent to each other.

Theorem 24. *The SDP dual relaxation (5.16a) – (5.16c) has a zero optimal duality gap with OPF problem (5.13a) – (5.13g) if and only if optimization dynamics (5.6a) – (5.6h) has an equilibrium $(U^*, \lambda^*, \gamma^*, \mu^*, \nu^*)$ with $\mathbf{B}(U^*, \lambda^*, \gamma^*, \mu^*, \nu^*)U^* = 0$ and $\mathbf{B}(U^*, \lambda^*, \gamma^*, \mu^*, \nu^*) \succeq 0$. In this case, we also have $\mathbf{B}(U^*, \lambda^*, \gamma^*, \mu^*, \nu^*) = \mathbf{A}^{opt}$.*

Proof of Theorem 24. This proof is quite long so we have moved it into the Appendix. \square

Combining Theorems 22 and 24 reveals the fact that, if there exists a zero optimal duality gap between OPF problem (5.13a) – (5.13g) and its SDP dual relaxation (5.16a) – (5.16c), then strong duality holds for OPF problem (5.2a) – (5.2e). In this case, we can utilize optimization dynamics (5.6a) – (5.6h) to seek a saddle-point for the associated Lagrangian (5.4). To sum up, the proposed optimization dynamics can be applied to all OPF problems for which the SDP dual relaxation approach has zero optimal duality gaps. As noted in Lavaei and Low (2012), this class of OPF problems is quite large in practice.

Moreover, we discover that optimization dynamics (5.6a) – (5.6h) may still converge to a saddle-point for the Lagrangian (5.4) even when the SDP dual relaxation fails to provide a zero optimal duality gap. This will be shown by Example 6 in the next section. Therefore, we conclude that the proposed optimization dynamics approach is more applicable than the SDP dual relaxation approach.

5.4.3 Two Three-Bus OPF Examples

Let us consider the three-bus power network as shown in Fig. 5.4. This example is adopted from Lesieutre et al. (2011) with a 100 MVA base. The parameters of the network's Π model as well as the power demand constraints are given by Tables 5.1 and 5.2, respectively. In Table 5.2, the numerical values $P_k^d + iQ_k^d$ indicate the active and reactive power demands in MW and MVAR. Moreover, there are no limits on the active and reactive power outputs for generator buses 1 and 2, but generator 3 is assumed to be a synchronous condenser, that is, $P_3^g = 0$. The coefficients of the quadratic power generation costs for generators 1 and 2 are given in Table 5.3. The voltage magnitudes at all buses are constrained to the range from 0.95 to 1.1 PU. Finally, we enforce a line flow limit of 60 MVA on the transmission line between buses 2 and 3.

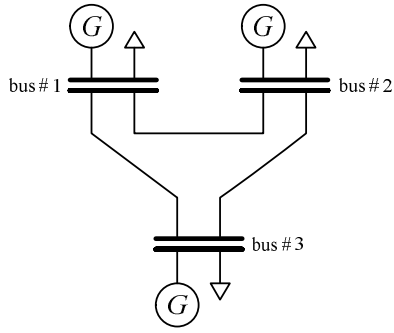


Figure 5.4 A three-bus power network

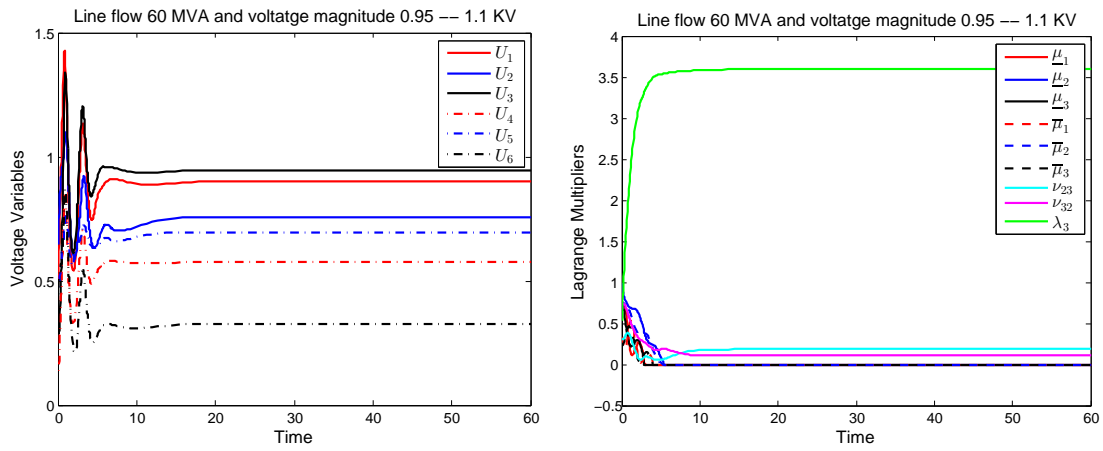


Figure 5.5 Convergence of the three-bus OPF with a line-flow limit 60 MVA

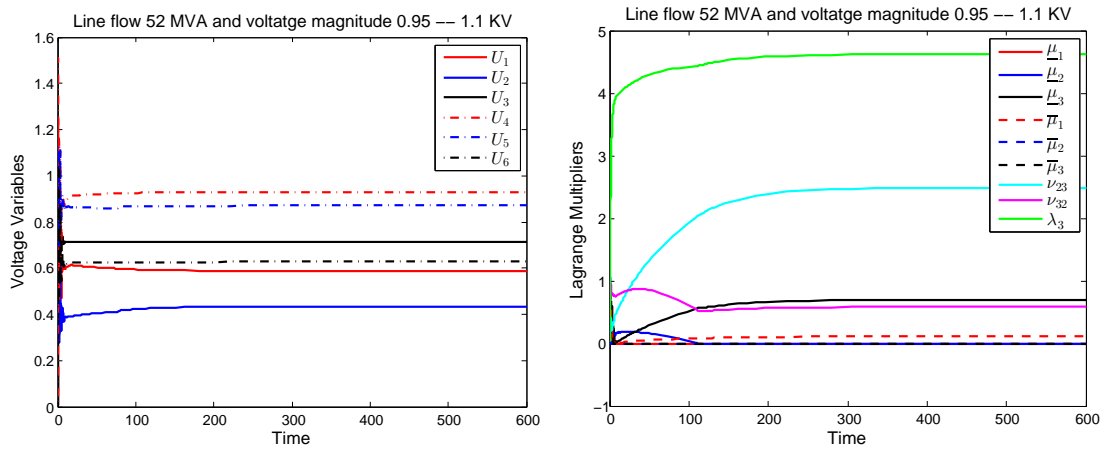


Figure 5.6 Convergence of the three-bus OPF with a line-flow limit 52 MVA

Table 5.1 Parameters of the three-bus power network

From Bus	To Bus	R	X	b
1	3	0.065	0.620	0.450
3	2	0.025	0.750	0.700
1	2	0.042	0.900	0.300

Table 5.2 Power demands of the three-bus OPF

$P_1^d + jQ_1^d$	$P_2^d + jQ_2^d$	$P_3^d + jQ_3^d$
$110 + j40$	$110 + j40$	$95 + j50$

Table 5.3 Generation costs of the three-bus OPF

Generator	c_2	c_1	c_0
1	\$0.11 per MWh ²	\$5 per MWh	\$0
2	\$0.085 per MWh ²	\$1.2 per MWh	\$0

Table 5.4 A global solution to the three-bus OPF with a line-flow limit 60 MVA

V_1	V_2	V_3
$1.069 \angle 0.000^\circ$	$1.028 \angle 9.916^\circ$	$1.001 \angle -13.561^\circ$

Table 5.5 A global solution to the three-bus OPF with a line-flow limit 52 MVA

V_1	V_2	V_3
$1.100 \angle 0.000^\circ$	$0.973 \angle 5.739^\circ$	$0.950 \angle -16.417^\circ$

Example 5. Consider the OPF formulation (5.17a) – (5.17e). We have scaled down the cost function by 1000.

$$\underset{U \in \mathbb{R}^6}{\text{minimize}} \quad f_1(U) + f_2(U) \quad (5.17a)$$

$$\text{subject to} \quad U^T \mathbf{Y}_3 U + 0.95 = 0 \quad (5.17b)$$

$$0.95^2 \leq U^T \mathbf{M}_k U \leq 1.1^2 \quad \forall k = 1, 2, 3 \quad (5.17c)$$

$$(U^T \mathbf{Y}_{23} U)^2 + (U^T \bar{\mathbf{Y}}_{23} U)^2 \leq 0.6^2 \quad (5.17d)$$

$$(U^T \mathbf{Y}_{32} U)^2 + (U^T \bar{\mathbf{Y}}_{32} U)^2 \leq 0.6^2 \quad (5.17e)$$

where

$$f_1(U) = 1.1(U^T \mathbf{Y}_1 U + 1.1)^2 + 0.5(U^T \mathbf{Y}_1 U + 1.1)$$

$$f_2(U) = 0.85(U^T \mathbf{Y}_2 U + 1.1)^2 + 0.12(U^T \mathbf{Y}_2 U + 1.1).$$

We apply the optimization dynamics approach to solve problem (5.17a) – (5.17e). In our simulation, we randomly choose an initial condition $(U^0, \lambda^0, \mu^0, \nu^0)$ with ℓ_∞ norm less than 1 and $U^0 \neq 0$. We find that the associated optimization dynamics converges to an equilibrium $(U^*, \lambda^*, \mu^*, \nu^*)$ with cost \$5707.1. The trajectories are plotted in Fig. 5.5. When represented in the standard polar coordinates with bus 1 as the reference, we can recover the same set of optimal voltages yielded by the MATPOWER toolbox, see Table 5.4.

When we substitute the equilibrium $(U^*, \lambda^*, \mu^*, \nu^*)$ back to verify the optimality conditions in Theorem 22, we obtain a positive semi-definite matrix $\mathbf{B}(U^*, \lambda^*, \mu^*, \nu^*)$ with eigenvalues 0, 0, 0.342, 0.342, 1.339, and 1.339. Therefore, we can guarantee the voltages shown in Table 5.4 are exactly the optimal solutions for Example 5.

When we check the strong duality conditions in Theorem 23, we find that they are satisfied and hence there exists no duality gap between this OPF example and its SDP dual relaxation. Moreover, we have $\mathbf{A}^{\text{opt}} = \mathbf{B}(U^*, \lambda^*, \mu^*, \nu^*)$. Hence, Theorem 24 has also been verified.

Example 6. Consider the same OPF formulation (5.17a) – (5.17e) with a minor change of parameters. We give a new line flow limit between buses 2 and 3 as 52 MVA.

For this example, we discover that the optimization dynamics converges to an equilibrium $(U^*, \lambda^*, \mu^*, \nu^*)$ with cost \$5807.9. The trajectories as well as the voltage solutions are shown

in Fig. 5.6 and Table 5.5, respectively. However, when we check the optimality conditions in Theorem 22, we get an in-definite $\mathbf{B}(U^*, \lambda^*, \mu^*, \nu^*)$ and hence Theorem 22 cannot be applied.

Again, we use both the MATPOWER toolbox and the SDP dual relaxation approach to compare with our result, but the situation is more interesting. First, the MATPOWER toolbox yields a solution that coincides with our optimization dynamics approach. Secondly, the SDP dual approach yields a different solution with cost \$5771.95, which is less than our cost \$5807.9. When we check the strong duality conditions in Theorem 23, we find that they are not satisfied either, because the matrix \mathbf{A}^{opt} has a null space of dimension four.

We can numerically prove here that the set of bus voltages in Table 5.5 is indeed a globally optimal solution and that \$5807.9 is exactly the optimal cost for Example 6. Specifically, we employ the MATLAB-based SOSTOOLS toolbox to numerically show that

$$P(U) = L(U, \lambda^*, \mu^*, \nu^*) - L(U^*, \lambda^*, \mu^*, \nu^*) \succeq_{SOS} 0.$$

Then the global optimality follows from Lemma 6. Readers may refer to Ma and Elia (2014a) for more details. When we go back to check the optimal cost computed by the SDP dual relaxation approach, we find that it fails to maintain strong duality because $5807.9 - 5771.95 > 0$.

The counterexample 6 implies the following facts. First, when compared with the sufficient conditions given in Lavaei and Low (2012), we conclude that strong duality holds for a larger class of OPF problems. Secondly, the Lagrange dual to OPF problem (5.3a) – (5.3e) must be stronger than the SDP dual relaxation (5.16a) – (5.16c). In fact, they are only equivalent to each other under the conditions of Theorem 24. Finally, the optimization dynamics approach proposed in this work can find global OPF solutions under more general conditions.

5.5 Convergence Analysis

This section provides a convergence analysis for optimization dynamics (5.6a) – (5.6h). We show that a saddle-point for the Lagrangian (5.4) is locally asymptotically stable with respect to dynamics (5.6a) – (5.6h) if the conditions of Theorem 24 hold. Specifically, we would like to apply the general convergence result in Theorem 10 to the dynamical system (5.6a) – (5.6h).

To begin with, we notice that the Hessian of the Lagrangian (5.4) with respect to U and evaluated at $(U^*, \lambda^*, \gamma^*, \mu^*, \nu^*)$ is given by

$$\mathbf{H}^* := 2\mathbf{B}(U^*, \lambda^*, \gamma^*, \mu^*, \nu^*) + 8\mathbf{C}(U^*, \nu^*) + 2e_{n+1}e_{n+1}^T \quad (5.18)$$

where we define

$$\mathbf{C}(U^*, \nu^*) := \sum_{l \in \mathcal{G}} c_{l2} \mathbf{Y}_l U^* U^{*T} \mathbf{Y}_l + \sum_{(k,l) \in \mathcal{L}} \nu_{kl}^* \left(\mathbf{Y}_{kl} U^* U^{*T} \mathbf{Y}_{kl} + \bar{\mathbf{Y}}_{kl} U^* U^{*T} \bar{\mathbf{Y}}_{kl} \right) \succeq 0.$$

Our next lemma characterizes the positive definiteness of \mathbf{H}^* .

Lemma 7. *Suppose that the conditions of Theorem 24 hold. Then \mathbf{H}^* is positive definite.*

Proof of Lemma 7. Under the conditions of Theorem 24, the matrix $\mathbf{B}(U^*, \lambda^*, \gamma^*, \mu^*, \nu^*) \succeq 0$ is equivalent to the \mathbf{A}^{opt} matrix yielded by the SDP dual relaxation approach, which has a two-dimensional null space. Then the set $\{U^*, \bar{U}^*\}$ must be a basis of this null space, because (i) $\mathbf{B}(U^*, \lambda^*, \gamma^*, \mu^*, \nu^*)U^* = 0$ and (ii) $\mathbf{B}(U^*, \lambda^*, \gamma^*, \mu^*, \nu^*)\bar{U}^* = 0$, where (ii) follows from the second statement of Lemma 3.

To prove that \mathbf{H}^* is positive definite, we need to show $x^T \mathbf{H}^* x > 0$ for all non-zero $x \in \mathbb{R}^{2n}$. First of all, given any $x \neq 0$ which does not lie in the null space of $\mathbf{B}(U^*, \lambda^*, \gamma^*, \mu^*, \nu^*)$, we have $x^T \mathbf{B}(U^*, \lambda^*, \gamma^*, \mu^*, \nu^*) x > 0$. Because both matrices $\mathbf{C}(U^*, \nu^*)$ and $e_{n+1}e_{n+1}^T$ are positive semi-definite, we must have $x^T \mathbf{H}^* x > 0$.

Next, we consider the vectors in the null space of $\mathbf{B}(U^*, \lambda^*, \gamma^*, \mu^*, \nu^*)$. If we choose $x = U^* \neq 0$, then we have

$$U^{*T} \mathbf{H}^* U^* = 8U^{*T} \mathbf{C}(U^*, \nu^*) U^* > 0 \quad (5.19)$$

where we have applied Assumption 4, saying that at least for one generator bus $l \in \mathcal{G}$

$$c_{l2} (U^T \mathbf{Y}_l U)^2 = c_{l2} (P_l^g - P_l^d)^2 > 0.$$

On the other hand, if we choose $x = \bar{U}^* \neq 0$, then we have

$$\bar{U}^{*T} \mathbf{H}^* \bar{U}^* = 2\bar{U}^{*T} (e_{n+1}e_{n+1}^T) \bar{U}^* = 2(V_1^{\min})^2 > 0 \quad (5.20)$$

since we require $V_k^{\min} > 0$ for all bus $k \in \mathcal{G}$. We need to mention that neither inequality (5.19) nor (5.20) is a purely mathematical derivation. In contrast, they are both obtained from the physical conditions and requirements for OPF problems. According to the discussions above we conclude that $\mathbf{H}^* \succ 0$. This completes the proof. \square

Combining Lemma 7 and Theorem 10 yields the final result of this chapter, which presents the locally asymptotic stability of optimization dynamics (5.6a) – (5.6h).

Theorem 25. *Suppose that the conditions of Theorem 24 hold. Also suppose that equilibrium $(U^*, \lambda^*, \gamma^*, \mu^*, \nu^*)$ is a strictly complementary saddle-point for the Lagrangian (5.4) and U^* is regular. Then there is a small neighborhood around $(U^*, \lambda^*, \gamma^*, \mu^*, \nu^*)$ such that*

- *Optimization dynamics (5.6a) – (5.6h) has a unique solution within this neighborhood;*
- *Any trajectory within this neighborhood converges to $(U^*, \lambda^*, \gamma^*, \mu^*, \nu^*)$ asymptotically.*

Proof of Theorem 25. Applying Lemma 7 to Theorem 10 proves Theorem 25. \square

5.6 Simulation Results

This section verifies by simulations the effectiveness of the continuous-time optimization dynamics approach for solving large-scale OPF problems. We do not study how to discretize our algorithm at present. In contrast, we just use simulation results to describe the evolution and convergence of our optimization dynamics, as if it were physically implemented. We will discuss in details about digital implementations of the optimization dynamics in Chapter 6.

Now we apply the optimization dynamics approach to solve OPF problems over the IEEE 14-, 57-, and 118-bus benchmark systems. All these OPF problems include active and reactive power demand constraints, voltage magnitude limits at all buses, as well as line-flow limits on all transmission lines. All system parameters and problem data used here are extracted from the archives of the MATPOWER toolbox. To obtain a faster convergence, we choose a large scaling constant $\alpha = 100$.

We employ the Matlab ODE solver `ode15s` to run our simulations. Simulation results show that the optimization dynamics converges to saddle-points within 5 seconds (simulation time)

for all IEEE benchmark systems above. Here, we only plot below in Fig. 5.7 the trajectories of the IEEE 57-bus OPF test case. We can see that the proposed optimization dynamics approach works well, even although the IEEE 57-bus network is known as a sensitive test case.

Remark 10. *Although we have only shown the locally asymptotic stability of the saddle-point for the Lagrangian associated with the OPF problem, from simulations we can see that its domain of attraction is quite large.*

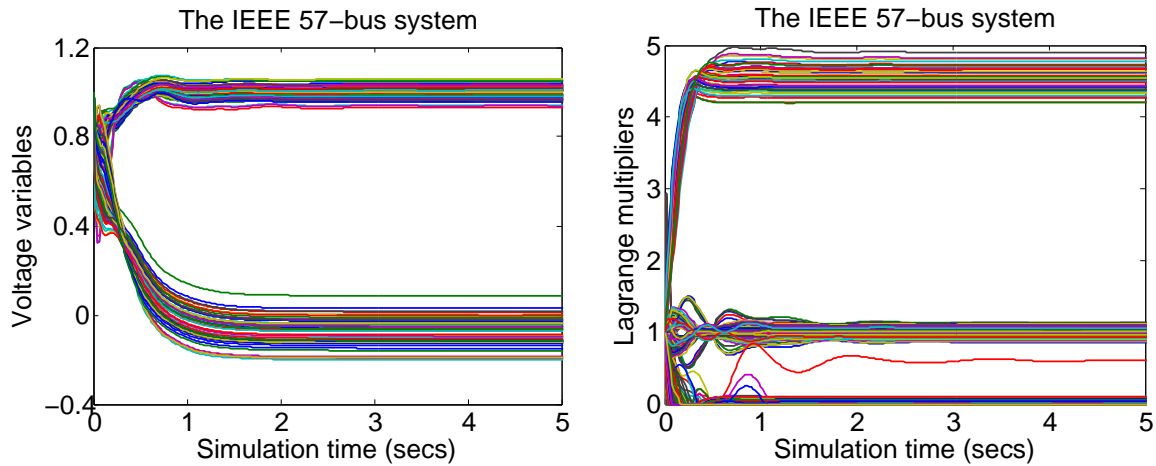


Figure 5.7 Convergence of the IEEE 57-bus OPF test case

5.7 Summary

In this chapter, we have applied the continuous-time optimization dynamics approach for solving optimal power flow problems. The proposed optimization dynamics has fully exploited a distributed OPF structure at the bus level, and hence is suitable for the physical settings of power networks. We have derived a sufficient condition that characterizes the saddle-point for the Lagrangian associated with the OPF problem. Under mild conditions, we have proved the locally asymptotic stability of the saddle-point with respect to the optimization dynamics. Besides, we have discovered that our optimization dynamics approach has a wider applicability than the existing SDP dual relaxation approach. Future research will focus on how to merge the proposed continuous-time OPF solution within the physical layer of power networks.

CHAPTER 6. SOLVERS FOR THE OPTIMIZATION DYNAMICS

This chapter discusses about discrete-time implementations of our optimization dynamics. Knowing from the convergence analysis in Chapter 3 that optimization dynamics (3.1a) – (3.1c) is locally asymptotically stable under mild conditions, we naturally ask: How to seek a stable KKT equilibrium by dynamics (3.1a) – (3.1c) in a distributed and efficient way?

Because (3.1a) – (3.1c) is a continuous-time dynamical system, one possible method is to implement it via analog computing. Analog computation best maintains the distributedness of the optimization dynamics, and hence it is an ideal method to meet our purposes. Aside from analog computation, we are still curious about whether we can search stable KKT equilibrium points by distributed, discrete-time implementations.

There are two different discretized methods to seek the stable KKT equilibrium. The first choice is to solve dynamics (3.1a) – (3.1c) directly via the ordinary differential equation (ODE) solvers (e.g., MATLAB `ode45` or `ode15s`), and we can obtain a stable KKT equilibrium after the dynamical system converges. Alternatively, we may set dynamics (3.1a) – (3.1c) equal to zero and compute an equilibrium from those equations, say, via the Newton-Raphson method.

The latter transforms solving ODEs into solving a set of non-linear equations, so it costs less. However, due to the possible existence of multiple KKT points for non-convex problems, this method highly relies on our initial conditions. If, unluckily, we feed the non-linear equation solver with an initial condition which is far from the stable KKT equilibrium, then the non-linear equation solver may yield an unstable KKT solution or even may not converge to anywhere.

On the other hand, if we directly solve dynamics (3.1a) – (3.1c) using the ODE solvers, we need to be careful for choosing the ODE solvers. Generally speaking, explicit ODE solvers are good choices for non-stiff dynamical systems, whereas implicit ODE solvers perform better to deal with stiff dynamical systems.

From our simulations, for instance, we discover that those optimization dynamical systems associated with phase recovery problems are non-stiff systems; but, in contrast, for most OPF problems their associated optimization dynamical systems are stiff systems.

This numerical issue of stiffness leads us to the following dilemma: If we employ an explicit ODE solver (e.g., `ode45`) that maintains the distributed structure of the optimization dynamics, we usually need a tiny step size to guarantee the convergence of the optimization dynamical system. Hence, it will take a long time for simulation. If we prefer a faster simulation, we should choose those implicit ODE solvers (e.g., `ode15s`), which, however, may destroy the distributed structure of the optimization dynamics since they require matrix inversions in their algorithms.

To deal with the dilemma above, we write an implicit ODE solver by ourselves for dynamics (3.1a) – (3.1c) in this chapter. To be specific, we adopt the implicit ODE algorithm and make the solver more robust to large step sizes. Meanwhile, instead of direct matrix inversions, we apply several distributed, iterative methods for solving linear equations.

After different trials to apply digital solvers for our optimization dynamics, the contribution of this chapter is the discovery of limitations in passing from continuous-time to discrete-time computing approaches. Specifically, if we prefer to digitally solve an ODE with high accuracy and efficiency, then we should employ higher-order explicit or implicit ODE solvers. However, these solvers will usually destroy the distributed structure of the original ODE. On the other hand, if we prefer to best maintain the original ODE's distributed structure, then we should choose the first-order explicit method but with low accuracy and efficiency.

In Section 6.1, we briefly introduce those explicit ODE solvers. We show that the first-order Euler solver best maintains the distributed structure of our optimization dynamics, while all higher-order solvers destroy the distributed structure somehow because they need to use the network multiple times at each update. Then Section 6.2 applies the explicit Euler's method to solve the optimization dynamics associated with phase recovery problems. In Section 6.3, we write a backward Euler ODE solver for stiff dynamical systems. To maintain a distributed computing structure, we also utilize several iterative algorithms to compute solutions to linear systems. Section 6.4 presents simulation results to show that our backward Euler ODE solver can be successfully applied to seek global OPF solutions.

6.1 Explicit ODE Solvers

Let us consider the dynamical system in a general form

$$\dot{x} = f(x) \quad (6.1)$$

where $x \in \mathbb{R}^n$ and $f : \mathbb{R}^n \rightarrow \mathbb{R}^n$ is a continuously differentiable function. We assume that given any initial condition $x^0 \in \mathbb{R}^n$, there is a unique solution to dynamical system (6.1).

If dynamics (6.1) is non-stiff, then we can apply explicit ODE methods to solve it. These methods include the Euler method (first-order), bilinear method (second-order), Runge-Kutta method (fourth-order), and etc. In general, the higher order an explicit ODE solver has, the more accurate it will be.

Next we start our presentation from the simplest one, the so-called explicit Euler method. Suppose that we discretize dynamics (6.1) with a step size T and that we use $x^k \in \mathbb{R}^n$ to denote the evaluation of $x(t)$ at time instant $t = kT$. Then the explicit Euler method updates the state variable x according to the following rule

$$x^{k+1} := x^k + Tf(x^k). \quad (6.2)$$

From (6.2) we can see that we only need x^k and the given step size T to compute x^{k+1} . Since x^k and T are both known, so we call this update rule as an explicit method. Moreover, we just evaluate the vector field $f(\cdot)$ once in each update step.

When the optimization dynamics (3.1a) – (3.1c) is non-stiff, we can easily apply algorithm (6.2) to solve it. Furthermore, if optimization (2.4a) – (2.4c) is defined over a network and its associated optimization dynamics (3.1a) – (3.1c) has a distributed computation structure, then the evaluation of the vector field does not destruct it at all. Also because we just evaluate the vector field once, we only use the network once in each update. Therefore, algorithm (6.2) maintains the distributed computation structure.

In comparison, those higher order explicit ODE solvers require to evaluate the vector field several times in each update. We will employ the second-order bilinear method to illustrate this point. The explicit bilinear method updates the state variable x according to

$$x^{k+1} := x^k + \frac{T}{2}f(x^k) + \frac{T}{2}f\{x^k + Tf(x^k)\} \quad (6.3)$$

where we can easily see that vector field $f(\cdot)$ is evaluated twice. Consequently, if the associated optimization problem (2.4a) – (2.4c) is defined over a network, then we have to use the network twice in each update by implementing the explicit bilinear method. This multiple use of the network finally impairs the original distributed computation structure. After our comparison, we conclude that the explicit Euler method maintains the distributed computation structure best among all explicit ODE algorithms.

6.2 Simulations for Phase Recovery Problems

In this section we apply the explicit Euler method (6.2) to solve the optimization dynamics (4.30a) – (4.30b) associated with phase recovery problem (4.27a) – (4.27b). The explicit Euler method works here because we find that dynamical system (4.30a) – (4.30b) is non-stiff.

Here we define the size of the complex-valued signal x as $n = 128K$ with $m = 3\lceil n \log(n) \rceil$ measurements, where $K = 1, 2, 4, 8, 16$ respectively and $\lceil \cdot \rceil$ represents the ceiling function. Then the coefficient matrix $A \in \mathbb{C}^{m \times n}$ is chosen as a random Gaussian matrix with an appropriate size. According to Theorem 18, it is highly probable that relaxation (4.26a) – (4.26c) is exact.

We run twenty experiments in total for each constant integer K . In each experiment, we first employ the fast algorithm proposed by Netrapalli et al. (2015) to solve the phase recovery problem (4.27a) – (4.27b). In Netrapalli et al. (2015), the authors have invented a fast phase retrieval algorithm by alternating minimizations. Starting from a carefully chosen initial point, this algorithm converges to the phase recovery solution with a fast speed. Then we apply the explicit Euler method starting from random initial conditions to seek a saddle-point equilibrium for optimization dynamics (4.30a) – (4.30b), and finally we compare the average performances between these two approaches.

We notice that the coefficient matrices in the phase recovery problem are not sparse, and hence optimization dynamics (4.30a) – (4.30b) does not possess a distributed structure. In our simulations, we fix the step size as $T = 10^{-5}$ s and, moreover, we choose the stopping criterion as $\varepsilon = 10^{-4}$ for the explicit Euler method.

Our comparison between these two approaches is plotted in Fig. 6.1. We see that for small size phase recovery problems ($K \leq 6$) the fast alternating minimization algorithm proposed

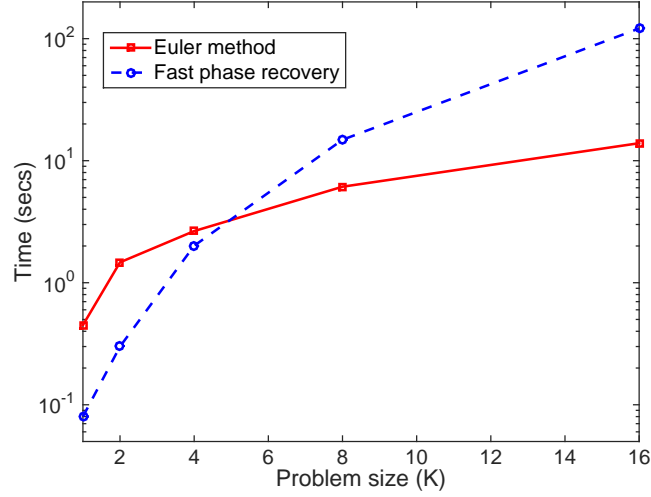


Figure 6.1 A performance comparison between our explicit Euler method and the fast phase retrieval approach proposed by [Netrapalli et al. \(2015\)](#)

by [Netrapalli et al. \(2015\)](#) is faster than our approach. However, when the problem size grows large, the algorithm proposed by [Netrapalli et al. \(2015\)](#) requires to spend more time finding the phase recovery solution. Actually, the fast phase recovery algorithm proposed in [Netrapalli et al. \(2015\)](#) spends some time for its initialization step as the problem size grows large, but in contrast, our algorithm does not have any special requirements for initial conditions.

6.3 The Backward Euler ODE Solver

6.3.1 The Backward Euler's Method

Different from what we have done in the last section, now we start to develop an implicit ODE solver for dynamics (3.1a) – (3.1b) in case it is a stiff system. As mentioned earlier, we find that the optimization dynamical systems associated with OPF problems are stiff systems and, therefore, explicit ODE solvers are not appropriate for them.

Let us reconsider the general dynamical system (6.1). To implicitly compute an integration for dynamics (6.1), we choose the backward Euler's method for the state update

$$x^{k+1} := f(x^k) + Tf(x^{k+1}) \quad (6.4)$$

which gives a system of non-linear equations involving x^{k+1} . Next we can apply the iterative, Newton-Raphson method to solve the state update x^{k+1} from (6.4).

We may rewrite equation (6.4) as

$$Tf(x^{k+1}) - x^{k+1} + f(x^k) = 0 \quad (6.5)$$

and we apply the Newton-Raphson method to solve the non-linear equation (6.5).

Let the following infinite series

$$\{x_1^{k+1}, x_2^{k+1}, \dots\} \rightarrow x^{k+1}$$

denote the state solutions yielded by the Newton-Raphson algorithm. Also suppose that at the $(i + 1)$ -th Newton-Raphson iteration ($i \geq 1$) for time instant $t = kT$, both x^k and x_i^{k+1} are known to us. Then we make an update x_{i+1}^{k+1} according to the following rules

$$F_i := Tf(x_i^{k+1}) - x_i^{k+1} + x^k \quad (6.6)$$

$$H_i := \left. \frac{\partial f(x)}{\partial x} \right|_{x=x_i^{k+1}} \quad (6.7)$$

$$x_{i+1}^{k+1} := x_i^{k+1} - (TH_i - I_n)^{-1}F_i \quad (6.8)$$

where I_n in (6.8) denotes the $n \times n$ identity matrix. We repeat procedures (6.6) – (6.8) until $\|x_{i+1}^{k+1} - x_i^{k+1}\|$ is less than some given tolerance ε . At that time, we believe that the infinite series $\{x_1^{k+1}, x_2^{k+1}, \dots\}$ has already converged to x^{k+1} .

We would like to point out that the backward Euler's method is robust to large step sizes. For example, if dynamics (6.1) is of the form $\dot{x} = Ax$ (linear system) with A Hurwitz, i.e., all eigenvalues of A are strictly on the left half plane, then the backward Euler is unconditionally stable, no matter how large the step size T we take, see Butcher (2008).

Applying (6.4) and (6.6) – (6.8) to the dynamical system (3.1a) – (3.1c), we can write a discretized solver for dynamics (3.1a) – (3.1c), as shown in Algorithm 1.

Algorithm 1 in fact contains two loops, including an outer loop (steps 1 – 4) and an inner loop (steps 2.1 – 2.7). Specifically, the inner loop updates the state according to the backward Euler's method, whereas the outer loop checks when the optimization dynamics converges.

Note that both steps 2.2 and 2.6 in Algorithm 1 are special for the optimization dynamical system (3.1a) – (3.1c), because dynamics (3.1b) employs the positive projection to keep each Lagrange multiplier associated with inequality constraint (2.4b) from leaving the non-negative orthant. To be specific, step 2.2 implements the positive projection on the evaluation of the vector field (3.1b) at each backward Euler iteration, and step 2.6 guarantees no updates for those Lagrange multipliers whose positive projections are active.

Algorithm 1 A backward Euler ODE solver for optimization dynamics (3.1a) – (3.1c)
given initial conditions $x^0 \in \mathbb{R}^n$, $\lambda^0 \in \mathbb{R}_+^p$, and $\nu^0 \in \mathbb{R}^q$, an error tolerance $\varepsilon > 0$, and a step size $T > 0$, **initialize** $k \leftarrow 0$

repeat

1 assign $(x^{k+1}, \lambda^{k+1}, \nu^{k+1}) \leftarrow (x^k, \lambda^k, \nu^k)$

2 **repeat**

2.1 evaluate the vector field (3.1a) – (3.1c) at $(x^{k+1}, \lambda^{k+1}, \nu^{k+1})$ without projections and assign this evaluation to f

2.2 **for all** i such that $1 \leq i \leq p$ **check**

if $f_{n+i} \leq 0$ and $\lambda_i^{k+1} \leq 0$

then $f_{n+i} \leftarrow 0$ and $\lambda_i^{k+1} \leftarrow 0$

end for

2.3 compute $F \leftarrow Tf - (x^{k+1}, \lambda^{k+1}, \nu^{k+1}) + (x^k, \lambda^k, \nu^k)$

2.4 evaluate the Jacobian of (3.1a) – (3.1c) at $(x^{k+1}, \lambda^{k+1}, \nu^{k+1})$ without projections and assign this evaluation to H

2.5 compute $D \leftarrow (TH - I_{n+p+q})^{-1}F$

2.6 **for all** i such that $1 \leq i \leq p$ **check**

if $f_{n+i} = 0$ and $\lambda_i^{k+1} = 0$

then $D_{n+i} \leftarrow 0$

end for

2.7 update $(x^{k+1}, \lambda^{k+1}, \nu^{k+1}) \leftarrow (x^{k+1}, \lambda^{k+1}, \nu^{k+1}) - D$

quit until the stopping criterion $\|D\| \leq \varepsilon$ is satisfied

3 evaluate $E \leftarrow (x^{k+1}, \lambda^{k+1}, \nu^{k+1}) - (x^k, \lambda^k, \nu^k)$

4 update $k \leftarrow k + 1$

quit until the stopping criterion $\|E\| \leq \varepsilon$ is satisfied

6.3.2 Centralized Computing

In Algorithm 1, step 2.5 needs to solve a system of linear equations $(TH - I_{n+p+q})D = F$. Generally speaking, we have two ways to solve linear equations: We can either invert a matrix directly, or approximate the matrix inversion by an infinite number of iterations. We note that the former definitely requires a centralized computing, whereas the latter is more amenable to be implemented in a distributed manner. In this subsection, we discuss about the centralized computing first.

Assumption 5. *In what follows, we assume that matrix $(TH - I_{n+p+q})$ is invertible.*

Notice that the Jacobian H of dynamics (3.1a) – (3.1c) can be generally expressed as

$$H = \begin{bmatrix} -B & -C \\ C^T & \mathbf{0} \end{bmatrix}$$

where $B \in \mathbb{S}^n$ and $C \in \mathbb{R}^{n \times (p+q)}$. Hence we have

$$TH - I_{n+p+q} = - \begin{bmatrix} I_n + TB & TC \\ -TC & I_{p+q} \end{bmatrix}. \quad (6.9)$$

Due to the special structure of $(TH - I_{n+p+q})$, we can reduce the computational complexity for inverting this matrix. If we further assume that $(I_n + TB)$ is invertible, then applying the matrix inversion lemma

$$\begin{bmatrix} A & B \\ C & D \end{bmatrix}^{-1} = \begin{bmatrix} (A - BD^{-1}C)^{-1} & -A^{-1}B(D - CA^{-1}B)^{-1} \\ -(D - CA^{-1}B)^{-1}CA^{-1} & (D - CA^{-1}B)^{-1} \end{bmatrix} \quad (6.10)$$

to matrix (6.9) yields the following result

$$(TH - I_{n+p+q})^{-1} = - \begin{bmatrix} Q^{-1} & -TP^{-1}CR \\ TRC^T P^{-1} & R \end{bmatrix} \quad (6.11)$$

where the blocks in (6.11) are respectively defined by

$$P := I_n + TB \quad (6.12a)$$

$$Q := I_n + TB + T^2CC^T \quad (6.12b)$$

$$R := I_{p+q} - T^2C^TQ^{-1}C. \quad (6.12c)$$

Because we have assumed that $P = I_n + TB$ is invertible, the matrix $Q = I_n + TB + T^2CC^T$ must be invertible, too. Thus, instead of computing the inversion of a $(n + p + q) \times (n + p + q)$ matrix $(TH - I_{n+p+q})$, based on (6.11) and (6.12a) – (6.12c) now we only need to compute two $n \times n$ matrix inversions for P and Q . When $p + q > n$, equation (6.11) can greatly reduce the computational complexity.

6.3.3 Distributed Computing

In order to maintain a distributed structure of Algorithm 1, we can try iterative methods to compute the matrix inversion. In other words, we would like to replace the matrix inversion step 2.5 by another loop procedure that iteratively solves $(TH - I_{n+p+q})D = F$.

How to solve a system of linear equations in an iterative fashion is a well studied topic, and numerous algorithms have been proposed up to now. We list below several candidate methods that can be applied to Algorithm 1.

For the simplicity of presentation, consider a system of linear equations $Au = b$, where both $A \in \mathbb{R}^{n \times n}$ and $b \in \mathbb{R}^n$ are given, and $u \in \mathbb{R}^n$ is the unknown. We assume that A is invertible so that $Au = b$ has a unique solution u^* .

[Bertsekas and Tsitsiklis \(1989\)](#) has introduced several classical methods, including the Jacobi algorithm, the Gauss-Seidel algorithm, the conjugate gradient method, and etc. All of these methods can be implemented in a distributed manner if the A matrix is sparse, and the reader may refer to [Bertsekas and Tsitsiklis \(1989\)](#) for more details.

Let $\{u_1, u_2, \dots\}$ be an infinite series that is generated by an iterative algorithm for solving the linear equation $Au = b$. Different algorithms require different conditions on the A matrix, in order to guarantee that the series $\{u_1, u_2, \dots\}$ converges to the correct solution u^* .

Convergence of the Jacobi algorithm requires that the A matrix should be row diagonally dominant, that is, $|a_{ii}| > \sum_{j \neq i} |a_{ij}|$, for all $i = 1, \dots, n$. In comparison, both the conjugate gradient method and the Gauss-Seidel method require that the A matrix should be symmetric and positive definite. If the A matrix is not symmetric, then we can apply both algorithms to solve the equivalent equation $A^T Au = A^T b$, where we must have $A^T A \succ 0$ since we have assumed that A is invertible.

Besides those classical algorithms presented in Bertsekas and Tsitsiklis (1989), some new iterative methods have also been developed recently. For example, Shental et al. (2008) has proposed a Gaussian belief propagation algorithm for solving the linear equations, which allows for a distributed message passing implementation. Similar to the Jacobi method, the Gaussian belief propagation solver needs a diagonally dominant A matrix to guarantee its convergence.

Moreover, Mou et al. (2013) has developed a distributed linear equation solver via the consensus scheme. Wang and Elia (2014) has equivalently transformed the problem of solving linear equations into a linear equality constrained least square problem, and employed the optimization dynamics to solve it. Both approaches are distributable, and neither of them has a strict requirement on the coefficient matrix A .

6.4 Simulations for OPF Problems

This section presents simulations on searching saddle-point equilibria for the optimization dynamics (5.6a) – (5.6h) associated with OPF problems via the backward Euler solver described in Algorithm 1. We show that our implicit ODE algorithm works efficiently and effectively.

First of all, Lemma 7 in Chapter 5 has shown that the Hessian of the Lagrangian (5.4) associated with OPF (5.3a) – (5.3e) is positive definite when evaluated at a saddle-point.

Since the Lagrangian associated with OPF problem (5.3a) – (5.3e) is a quartic polynomial in the voltage variables and linear in the Lagrange multipliers, the Hessian of the Lagrangian (5.4) must be continuous with respect to those variables. Moreover, by the continuity of eigenvalues Horn and Johnson (1987), we know that eigenvalues of the Lagrangian's Hessian should not change too much within a small neighborhood of the OPF saddle-point.

Due to the locally asymptotic stability of the OPF saddle-point (Theorem 25), we are able to find an initial condition for dynamics (5.6a) – (5.6h) within the OPF saddle-point's domain of attraction, so that the Lagrangian's Hessian is always positive definite at every point along the convergent trajectory of dynamics (5.6a) – (5.6h).

As mentioned before, the backward Euler ODE solver is unconditionally stable for a linear system $\dot{x} = Ax$ with matrix A Hurwitz. Based on our analysis above about the positive definite Hessian of the Lagrangian (5.4), Lemma 1 tells us that the Jacobian associated with dynamics

(5.6a) – (5.6h) must be Hurwitz in a small neighborhood of the OPF saddle-point. Therefore, Algorithm 1 will be robust to large step sizes with a well chosen starting point.

Moreover, we notice that the Jacobian associated with dynamics (5.6a) – (5.6h) is sparse. However, it is neither symmetric nor row diagonally dominant, so the Jacobi and the Gaussian belief propagation methods cannot be applied to solve (5.6a) – (5.6h) via Algorithm 1. If we would like to apply the conjugate gradient or the Gauss-Seidel method, then we need to solve the equivalent linear equation $(TH - I_{n+p+q})^T(TH - I_{n+p+q})D = (TH - I_{n+p+q})^T F$, where H denotes the Jacobian associated with dynamics (5.6a) – (5.6h).

From those simulations for large-scale OPF problems (see the simulation section next), we find that $(TH - I_{n+p+q})^T(TH - I_{n+p+q})$ is still a sparse matrix and hence both the conjugate gradient and the Gauss-Seidel algorithms are distributable. Nevertheless, these discrete-time implementations will destroy to some extent the distributed OPF structure.

We have also attempted to utilize the approaches proposed in [Mou et al. \(2013\)](#) and [Wang and Elia \(2014\)](#) to solve dynamics (5.6a) – (5.6h) via Algorithm 1. However, neither of them works well. The drawback of [Mou et al. \(2013\)](#) is that it requires too much information change during each iteration. As for [Wang and Elia \(2014\)](#), it suffers from the same numerical issue of stiffness, and it usually takes a long time for simulating large-scale OPF problems.

Now we are ready to report our simulations results for large-scale OPF problems. We make comparisons with standard MATLAB solvers, such as `ode15s` and `CVX`. All simulations provided below are carried out using the 2.4GHz Intel Core i5 processor with a 4GB RAM.

We consider the IEEE 14-bus benchmark system. This 14-bus power network example is taken from the IEEE test case archive and uses a 100 MVA base. All system data are extracted from the library of the MATPOWER toolbox, see [Zimmerman et al. \(2011\)](#).

In the 14-bus system, buses 1, 2, 3, 6, and 8 are generators. All power demands are shown in Table 6.1. The coefficients of the quadratic generation costs as well as the generation limits are given in Table 6.2. Finally, all voltage magnitudes are constrained from 0.94 to 1.06 PU.

It has been shown in [Lavaei and Low \(2012\)](#) that strong duality holds for the IEEE 14-bus benchmark system. In other words, there exists a saddle-point for the dynamics (5.6a) – (5.6h) and hence our optimization dynamics approach applies.

We first use MATLAB ODE solvers `ode45` and `ode15s` to simulate dynamics (5.6a) – (5.6h). Here, we pick the default accuracy parameter $\text{RelTol} = 10^{-3}$. We will start at the initial point at all ones and simulate the dynamics for 64 seconds.

The optimization dynamics (5.6a) – (5.6h) associated with the 14-bus OPF example contains 112 variables in total, including 28 voltage variables as well as 84 Lagrange multipliers. It costs `ode45` more than 30 minutes (CPU time) to finish the simulation. In comparison, the `ode15s` solver spends 2.5 minutes for the simulation, as is shown in Fig. 6.2. Obviously, simulating a stiff dynamical system requires a long time.

Then we use our backward Euler solver (Algorithm 1) to simulate dynamics (5.6a) – (5.6h). To get a fair comparison, we start at the same initial point with the same tolerance and simulate for the same long time. We fix the step size $T = 2\text{s}$ to achieve a faster simulation.

The simulation obtained from our own solver is plotted in Fig. 6.3. When represented in the standard polar coordinates, the globally optimal voltages are given in Table 6.3. They are identical to those solved by `ode15s`.

Comparing Fig. 6.2 with Fig. 6.3, we may discover that in the former figure trajectories of dynamics (5.6a) – (5.6h) have experienced a period of oscillation before convergence. This is also the true simulation, and MATLAB ODE solvers have spent a lot of time for computing this oscillation part before yielding the global OPF solution.

When the same dynamics is solved by our own ODE solver, because we have used a quite large step size, our simulation smooths that oscillation and converges to the same saddle-point with a faster speed. Such a distortion of the simulation does not matter too much, since we only care about the final value of the saddle-point rather than those trajectories.

The performances of our solvers for simulating the 14-bus OPF example are listed in Table 6.4. If we employ direct matrix inversions, then it takes 331 iterations with the shortest CPU time 0.45s to finish the simulation. When we use the conjugate gradient or the Gauss-Seidel method instead, it seems that the Gauss-Seidel method costs more than the conjugate gradient one. It requires 1,042,173 iterations and spends 9.95s.

Table 6.1 Power demands of the IEEE 14-bus OPF

$P_1^d + iQ_1^d$	$P_2^d + iQ_2^d$	$P_3^d + iQ_3^d$	$P_4^d + iQ_4^d$	$P_5^d + iQ_5^d$	$P_6^d + iQ_6^d$	$P_7^d + iQ_7^d$
$0 + i0$	$21.7 + i12.7$	$94.2 + i19$	$47.8 - i3.9$	$7.6 + i1.6$	$11.2 + i7.5$	$0 + i0$
$P_8^d + iQ_8^d$	$P_9^d + iQ_9^d$	$P_{10}^d + iQ_{10}^d$	$P_{11}^d + iQ_{11}^d$	$P_{12}^d + iQ_{12}^d$	$P_{13}^d + iQ_{13}^d$	$P_{14}^d + iQ_{14}^d$
$0 + i0$	$29.5 + i16.6$	$9 + i5.8$	$3.5 + i1.8$	$6.1 + i1.6$	$13.5 + i5.8$	$14.9 + i5$

Table 6.2 Generation costs and constraints of the IEEE 14-bus OPF

Generators	c_{l2}	c_{l1}	c_{l0}	P_l^{\min}	P_l^{\max}	Q_l^{\min}	Q_l^{\max}
$l = 1$	\$0.043 per MWh ²	\$20 per MWh	\$0	0	332.4	0	10
$l = 2$	\$0.25 per MWh ²	\$20 per MWh	\$0	0	140	-40	50
$l = 3$	\$0.01 per MWh ²	\$40 per MWh	\$0	0	100	0	40
$l = 6$	\$0.01 per MWh ²	\$40 per MWh	\$0	0	100	-6	24
$l = 8$	\$0.01 per MWh ²	\$40 per MWh	\$0	0	100	-6	24

Table 6.3 A global solution to the IEEE 14-bus OPF

V_1^*	V_2^*	V_3^*	V_4^*	V_5^*	V_6^*	V_7^*
$1.06 \angle 0.0^\circ$	$1.04 \angle -4.0^\circ$	$1.02 \angle -9.9^\circ$	$1.01 \angle -8.7^\circ$	$1.02 \angle -7.4^\circ$	$1.06 \angle -12.7^\circ$	$1.05 \angle -11.2^\circ$
V_8^*	V_9^*	V_{10}^*	V_{11}^*	V_{12}^*	V_{13}^*	V_{14}^*
$1.06 \angle -10.4^\circ$	$1.04 \angle -13.0^\circ$	$1.04 \angle -13.2^\circ$	$1.05 \angle -13.1^\circ$	$1.05 \angle -13.5^\circ$	$1.04 \angle -13.6^\circ$	$1.02 \angle -14.3^\circ$

Table 6.4 Performance Comparisons on the IEEE 14-bus OPF

	ode15s	CVX	Backward Euler (Centralized)	Backward Euler (Conjugate Gradient)	Backward Euler (Gauss-Seidel)
Iterations	—	27	331	45,547	1,042,173
CPU Time	2.5min	3.03s	0.45s	1.28s	9.95s

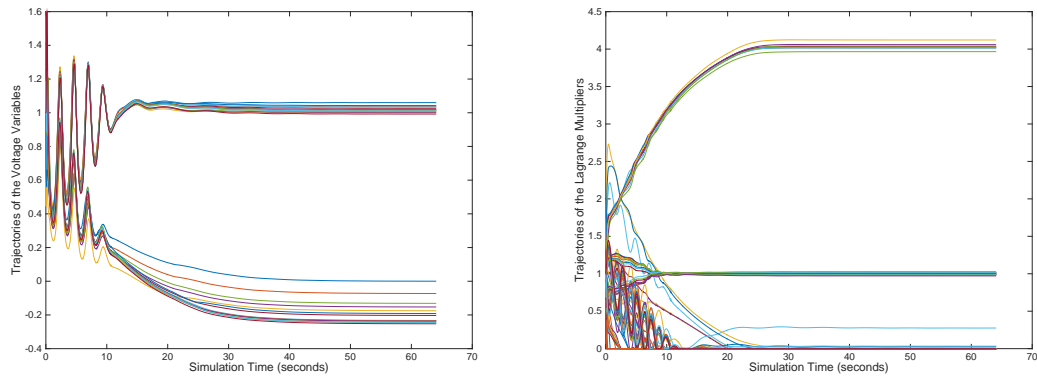


Figure 6.2 The IEEE 14-bus OPF solved by MATLAB ODE solver `ode15s`

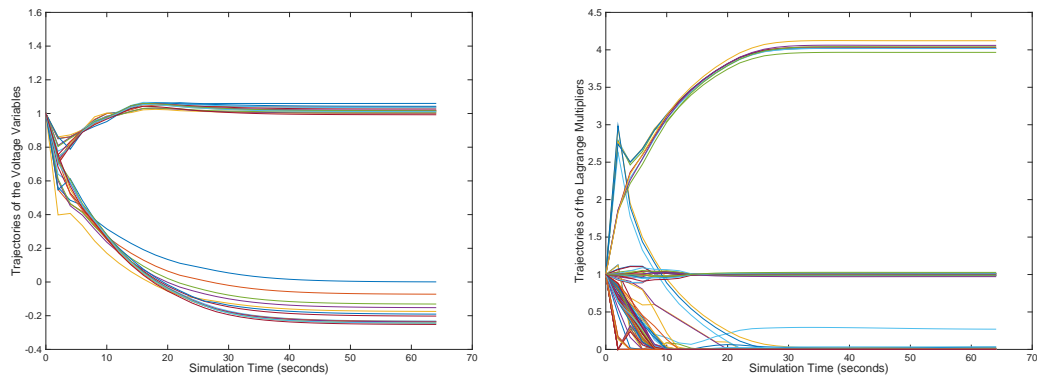


Figure 6.3 The IEEE 14-bus OPF solved by our ODE solver with step size $T = 2s$

Furthermore, we also employ the convex optimization software *CVX* to solve the SDP dual relaxation associated with the IEEE 14-bus OPF example. Of course, this SDP dual relaxation is solved in a centralized manner. We notice that the *CVX* software takes 27 iterations and about 3.03s to finish the computation. When compared with our centralized backward Euler solver, we find that our solver is much faster since it only spends 0.45s to yield the OPF solution.

From the above OPF example we summarize two points. Firstly, the solver which employs the conjugate gradient or the Gauss-Seidel method requires to use the network multiple times in each backward Euler iteration, so the intrinsic distributed OPF structure is somehow destroyed and the computation speed is slow. Secondly, it suggests that our centralized backward Euler solver is faster than the *CVX* software solving associated SDP dual relaxations.

6.5 Summary

This chapter has developed numerical ODE solvers for our continuous-time optimization dynamics approach. We have first applied explicit Euler method to the optimization dynamics associated with phase recovery problems. The explicit Euler method not only performs very fast but also best maintains the distributed computation structure. Next, based on the backward Euler's method and iterative matrix inversions, we have successfully written an implicit Euler solver for the optimization dynamical systems associated with large-scale OPF problems.

When implemented in a centralized manner, simulations show that our implicit solver is faster than the MATLAB ODE solver `ode15s`. When implemented with those iterative matrix inversion algorithms, on the other hand, we have noticed that our implicit solver still maintains a distributed computation structure, but at the expense of using the network multiple times for each backward Euler iteration.

Although the discretization methods for ODEs presented in this chapter are rudimentary, our simulation results are promising for both of the phase recovery and OPF problems. At the same time, these simulations help us reveal some limitations in transforming continuous-time computing approaches into discrete-time algorithms.

CHAPTER 7. OPF PROBLEMS REVISITED: A CONSENSUS-BASED DECOMPOSED SDP RELAXATION APPROACH

We would like to revisit the non-convex OPF problems in this chapter. As mentioned in Chapter 5, for many cases OPF problems can be convexified and hence be efficiently solved by the SDP relaxation approach. However, one major drawback of the standard SDP relaxation lies in the problem size, which does not scale nicely as the size of the power network expands. As a consequence, the SDP relaxations are cumbersome when applied to large-scale problems.

Recent works [Molzahn et al. \(2013\)](#) and [Madani et al. \(2015\)](#) have given new algorithms to address the issue above. Using recent technologies derived in the matrix completion theory, [Molzahn et al. \(2013\)](#) has developed a matrix combination algorithm that shortens the OPF solver's computation time. By the same matrix completion technologies, [Madani et al. \(2015\)](#) has designed a fast OPF solver based on the so-called “tree decomposition” for power networks.

Different from those works, in this chapter we continue to exploit the natural sparsity of power networks to obtain a distributed and efficient OPF solution. Specifically, we decompose the standard SDP relaxation into a bunch of smaller size SDPs. Then each bus in the power network should locally solve its own decomposed SDP relaxation and meanwhile a global OPF solution can be achieved by running a consensus over the whole power network.

We can show that the size of our decomposed SDP relaxation scales linearly as the power network expands and hence it greatly fastens the OPF computation speed. When compared with [Molzahn et al. \(2013\)](#) and [Madani et al. \(2015\)](#), the decomposed SDP relaxation approach is even faster for large-scale OPF problems.

In Section 7.1, we briefly review the SDP relaxations for OPF problems. Then we formulate the decomposed OPF in Section 7.2 and present the decomposed SDP relaxation approach in Section 7.3. Discussions and simulations are, respectively, provided in Sections 7.4 and 7.5.

7.1 Review of the SDP Relaxation

Recall from Chapter 5 that an OPF problem can be formulated as

$$\underset{U \in \mathbb{R}^{2n}}{\text{minimize}} \quad \sum_{l \in \mathcal{G}} f_l(U^T \mathbf{Y}_l U + P_l^d) \quad (7.1a)$$

subject to

$$P_k^{\min} - P_k^d \leq U^T \mathbf{Y}_k U \leq P_k^{\max} - P_k^d \quad \forall k \in \mathcal{N} \quad (7.1b)$$

$$Q_k^{\min} - Q_k^d \leq U^T \bar{\mathbf{Y}}_k U \leq Q_k^{\max} - Q_k^d \quad \forall k \in \mathcal{N} \quad (7.1c)$$

$$(V_k^{\min})^2 \leq U^T \mathbf{M}_k U \leq (V_k^{\max})^2 \quad \forall k \in \mathcal{N} \quad (7.1d)$$

$$(U^T \mathbf{Y}_{kl} U)^2 + (U^T \bar{\mathbf{Y}}_{kl} U)^2 \leq (S_{kl}^{\max})^2 \quad \forall (k, l) \in \mathcal{L} \quad (7.1e)$$

$$U_{n+1} = 0 \quad (7.1f)$$

where we have imposed a new constraint (7.1f) to select bus 1 as the reference bus. Then, by changing all quadratic terms $U^T \mathbf{Y} U$ in (7.1a) – (7.1e) into $\text{Tr}\{\mathbf{Y}W\}$ with $W = UU^T$, problem (7.1a) – (7.1f) can be equivalently rewritten as an epigraph form

$$\underset{\alpha, W}{\text{minimize}} \quad \sum_{l \in \mathcal{G}} \alpha_l \quad (7.2a)$$

subject to

$$P_k^{\min} - P_k^d \leq \text{Tr}\{\mathbf{Y}_k W\} \leq P_k^{\max} - P_k^d \quad \forall k \in \mathcal{N} \quad (7.2b)$$

$$Q_k^{\min} - Q_k^d \leq \text{Tr}\{\bar{\mathbf{Y}}_k W\} \leq Q_k^{\max} - Q_k^d \quad \forall k \in \mathcal{N} \quad (7.2c)$$

$$(V_k^{\min})^2 \leq \text{Tr}\{\mathbf{M}_k W\} \leq (V_k^{\max})^2 \quad \forall k \in \mathcal{N} \quad (7.2d)$$

$$\mathbf{L}_{kl} \preceq 0 \quad \forall (k, l) \in \mathcal{L} \quad (7.2e)$$

$$\mathbf{C}_l \preceq 0 \quad \forall l \in \mathcal{G} \quad (7.2f)$$

$$W \succeq 0 \quad (7.2g)$$

$$Wz = 0 \quad (7.2h)$$

$$\text{rank}(W) = 1 \quad (7.2i)$$

where matrices \mathbf{L}_{kl} and \mathbf{C}_l , for all $(k, l) \in \mathcal{L}$ and $l \in \mathcal{G}$, have been defined in Section 5.4. In constraint (7.2h), moreover, $z \in \mathbb{R}^{2n}$ is a vector of all zeros except the $(n+1)$ -th entry is one.

OPF formulations (7.1a) – (7.1f) and (7.2a) – (7.2i) are equivalent non-convex problems. We also notice that the rank-one constraint (7.2i) is the only non-convex constraint in OPF problem (7.2a) – (7.2i). We could drop constraint (7.2i) and thus (7.2a) – (7.2h) becomes a convex SDP relaxation for OPF problem (7.1a) – (7.1f). If we solve (7.2a) – (7.2h) and obtain a rank-one solution, then we can recover an optimal U^* for OPF problem (7.1a) – (7.1f) with bus 1 as the reference.

Although SDP relaxation (7.2a) – (7.2h) is convex, it has one obvious drawback that the problem size grows in n^2 when the power network size expands, because the decision variable W is a $2n \times 2n$ symmetric matrix. This will certainly slow down the computation speed when it is applied to large-scale OPF problems.

To overcome this drawback, we propose a decomposed SDP relaxation approach for OPF problems. Our approach assigns each bus in the power network to solve a local, smaller SDP relaxation, whose problem size grows linearly with the number of neighboring buses, and at the same time all buses in the power network coordinate with each other to obtain the global OPF solution via a consensus scheme.

7.2 The Decomposed OPF Problem

Let us start our derivation from OPF problem (7.1a) – (7.1f). To begin with, we need to assign each bus with its own local voltage variables. Recall that in problem (7.1a) – (7.1f), the only optimization variable is a $2n$ -dimensional, real voltage vector

$$U := [U_1 \cdots U_n \ U_{n+1} \cdots U_{2n}]^T$$

with its first n elements U_1, \dots, U_n being the real parts of the corresponding complex-valued bus voltages and its last n elements U_{n+1}, \dots, U_{2n} being the corresponding imaginary parts. Now we ask each bus in the power network to duplicate a copy of U for itself. The duplicated voltage vector associated with bus k is denoted by

$$\bar{U}^k := [U_1^k \cdots U_n^k \ U_{n+1}^k \cdots U_{2n}^k]^T \in \mathbb{R}^{2n}.$$

Further, for each bus k , we define the local voltage variable $U^k \in \mathbb{R}^{2(|\mathcal{N}(k)|+1)}$ by deleting the elements U_j^k and U_{n+j}^k from \bar{U}^k , for all indices $j \neq k$ and $j \notin \mathcal{N}(k)$.

For each transmission line $(k, l) \in \mathcal{L}$ that connects bus k and bus l ($k < l$), we define

$$U^{(k,l)} := \left[U_k^k \ U_l^k \ U_{n+k}^k \ U_{n+l}^k \right]^T \in \mathbb{R}^4$$

using the elements from U^k . Moreover, because the power network considered in this work is modeled as a undirected graph, we know that $(l, k) \in \mathcal{L}$, too. However, this time we use the elements from U^l to define

$$U^{(l,k)} := \left[U_k^l \ U_l^l \ U_{n+k}^l \ U_{n+l}^l \right]^T \in \mathbb{R}^4.$$

Of course, vectors $U^{(k,l)}$ and $U^{(l,k)}$ are two different local voltage variables that respectively belong to bus k and bus l .

To make the above definitions clear, let us give a simple example below illustrating how to assign these local voltage variables to each bus in the power network.

Example 7. *Let us reconsider the four-bus power network as shown in Fig. 5.2. This network topologically has a tree structure, and each bus has at most two neighboring buses. Following the definitions above, we can assign the local voltage variables for each bus as*

Bus 1:

$$U^1 = [U_1^1 \ U_2^1 \ U_4^1 \ U_5^1 \ U_6^1 \ U_8^1]^T, \quad U^{(1,2)} = [U_1^1 \ U_2^1 \ U_5^1 \ U_6^1]^T, \quad U^{(1,4)} = [U_1^1 \ U_4^1 \ U_5^1 \ U_8^1]^T$$

Bus 2:

$$U^2 = [U_1^2 \ U_2^2 \ U_3^2 \ U_5^2 \ U_6^2 \ U_7^2]^T, \quad U^{(2,1)} = [U_1^2 \ U_2^2 \ U_5^2 \ U_6^2]^T, \quad U^{(2,3)} = [U_2^2 \ U_3^2 \ U_6^2 \ U_7^2]^T$$

Bus 3:

$$U^3 = [U_2^3 \ U_3^3 \ U_6^3 \ U_7^3]^T, \quad U^{(3,2)} = [U_2^3 \ U_3^3 \ U_6^3 \ U_7^3]^T$$

Bus 4:

$$U^4 = [U_1^4 \ U_4^4 \ U_5^4 \ U_8^4]^T, \quad U^{(4,1)} = [U_1^4 \ U_4^4 \ U_5^4 \ U_8^4]^T.$$

We next focus on the sparsity of coefficient matrices \mathbf{Y}_k , $\bar{\mathbf{Y}}_k$, \mathbf{M}_k , \mathbf{Y}_{kl} , and $\bar{\mathbf{Y}}_{kl}$. According to Lemma 5, we know that these matrices have a bunch of zero rows and columns. Hence, by deleting the corresponding zero rows and columns from \mathbf{Y}_k , $\bar{\mathbf{Y}}_k$, \mathbf{M}_k , \mathbf{Y}_{kl} , and $\bar{\mathbf{Y}}_{kl}$, we obtain

a series of new coefficient matrices \mathbf{Y}_k^D , $\bar{\mathbf{Y}}_k^D$, \mathbf{M}_k^D , \mathbf{Y}_{kl}^D , and $\bar{\mathbf{Y}}_{kl}^D$ such that

$$U^T \mathbf{Y}_k U = (U^k)^T \mathbf{Y}_k^D U^k \quad \forall k \in \mathcal{N} \quad (7.3a)$$

$$U^T \bar{\mathbf{Y}}_k U = (U^k)^T \bar{\mathbf{Y}}_k^D U^k \quad \forall k \in \mathcal{N} \quad (7.3b)$$

$$U^T \mathbf{M}_k U = (U^k)^T \mathbf{M}_k^D U^k \quad \forall k \in \mathcal{N} \quad (7.3c)$$

$$U^T \mathbf{Y}_{kl} U = [U^{(k,l)}]^T \mathbf{Y}_{kl}^D U^{(k,l)} \quad \forall (k,l) \in \mathcal{L} \quad (7.3d)$$

$$U^T \bar{\mathbf{Y}}_{kl} U = [U^{(k,l)}]^T \bar{\mathbf{Y}}_{kl}^D U^{(k,l)} \quad \forall (k,l) \in \mathcal{L}. \quad (7.3e)$$

Then using equations (7.3a) – (7.3e), we can formulate the decomposed OPF problem as

$$\underset{U^k, \forall k \in \mathcal{N}}{\text{minimize}} \quad \sum_{l \in \mathcal{G}} f_l \left[(U^l)^T \mathbf{Y}_l^D U^l + P_l^d \right] \quad (7.4a)$$

subject to

$$P_k^{\min} - P_k^d \leq (U^k)^T \mathbf{Y}_k^D U^k \leq P_k^{\max} - P_k^d \quad \forall k \in \mathcal{N} \quad (7.4b)$$

$$Q_k^{\min} - Q_k^d \leq (U^k)^T \bar{\mathbf{Y}}_k^D U^k \leq Q_k^{\max} - Q_k^d \quad \forall k \in \mathcal{N} \quad (7.4c)$$

$$(V_k^{\min})^2 \leq (U^k)^T \mathbf{M}_k^D U^k \leq (V_k^{\max})^2 \quad \forall k \in \mathcal{N} \quad (7.4d)$$

$$\left\{ [U^{(k,l)}]^T \mathbf{Y}_{kl}^D U^{(k,l)} \right\}^2 + \left\{ [U^{(k,l)}]^T \bar{\mathbf{Y}}_{kl}^D U^{(k,l)} \right\}^2 \leq (S_{kl}^{\max})^2 \quad \forall (k,l) \in \mathcal{L} \quad (7.4e)$$

$$U_{n+1}^1 = 0 \quad (7.4f)$$

$$U^{(k,l)} = U^{(l,k)} \quad \forall (k,l) \in \mathcal{L}. \quad (7.4g)$$

Note that, in the above OPF problem, the cost and constraints (7.4a) – (7.4f) are all equivalent to (7.1a) – (7.1f). Because we have decoupled OPF problem (7.1a) – (7.1f) by duplicating the voltage variables, we require an extra constraint (7.4g) to reach a consensus on voltages over all neighboring buses.

Theorem 26. *The decomposed OPF problem (7.4a) – (7.4g) is equivalent to OPF problem (7.1a) – (7.1f).*

Proof of Theorem 26. First suppose that U^* is an optimal solution to problem (7.1a) – (7.1f). Following the duplications presented before, we can always construct a series of $(U^k)^*$, $\forall k \in \mathcal{N}$, as a solution to problem (7.4a) – (7.4g). Thus, the optimal cost of (7.4a) – (7.4g) is no more than that of (7.1a) – (7.1f).

On the other hand, if we get a series of $(U^k)^*$, $\forall k \in \mathcal{N}$, as an optimal solution to problem (7.4a) – (7.4g), due to the consensus constraint (7.4g), we are able to recover a U^* satisfying all constraints (7.1b) – (7.1f). Hence, the optimal cost of (7.1a) – (7.1f) is no more than that of (7.4a) – (7.4g), either. Therefore, the two problems are equivalent to each other. \square

7.3 The Decomposed SDP Relaxation Approach

Similarly, we would like to make the following change of variables

$$\begin{aligned} W^k &:= U^k (U^k)^T \in \mathbb{R}^{2(|\mathcal{N}(k)|+1) \times 2(|\mathcal{N}(k)|+1)} & \forall k \in \mathcal{N} \\ E^{(k,l)} &:= U^{(k,l)} [U^{(k,l)}]^T \in \mathbb{R}^{4 \times 4} & \forall (k,l) \in \mathcal{L}. \end{aligned}$$

We need to clarify that $E^{(k,l)}$ is part of W^k due to our previous definitions of U^k and $U^{(k,l)}$.

Then we can rewrite the decomposed OPF problem (7.4a) – (7.4g) equivalently as

$$\underset{\alpha, W^k, \forall k \in \mathcal{N}}{\text{minimize}} \quad \sum_{l \in \mathcal{G}} \alpha_l \quad (7.5a)$$

subject to

$$P_k^{\min} - P_k^d \leq \text{Tr}\{\mathbf{Y}_k^D W^k\} \leq P_k^{\max} - P_k^d \quad \forall k \in \mathcal{N} \quad (7.5b)$$

$$Q_k^{\min} - Q_k^d \leq \text{Tr}\{\bar{\mathbf{Y}}_k^D W^k\} \leq Q_k^{\max} - Q_k^d \quad \forall k \in \mathcal{N} \quad (7.5c)$$

$$(V_k^{\min})^2 \leq \text{Tr}\{\mathbf{M}_k^D W^k\} \leq (V_k^{\max})^2 \quad \forall k \in \mathcal{N} \quad (7.5d)$$

$$\bar{\mathbf{L}}_{kl} \preceq 0 \quad \forall (k,l) \in \mathcal{L} \quad (7.5e)$$

$$\bar{\mathbf{C}}_l \preceq 0 \quad \forall l \in \mathcal{G} \quad (7.5f)$$

$$W^k \succeq 0 \quad \forall k \in \mathcal{N} \quad (7.5g)$$

$$W^1 z^1 = 0 \quad (7.5h)$$

$$E^{(k,l)} \succeq 0 \quad \forall (k,l) \in \mathcal{L} \quad (7.5i)$$

$$E^{(k,l)} = E^{(l,k)} \quad \forall (k,l) \in \mathcal{L} \quad (7.5j)$$

$$\text{rank}(W^k) = 1 \quad \forall k \in \mathcal{N} \quad (7.5k)$$

$$\text{rank}[E^{(k,l)}] = 1 \quad \forall (k,l) \in \mathcal{L} \quad (7.5l)$$

where we define

$$\bar{\mathbf{L}}_{kl} := \begin{bmatrix} -(S_{kl}^{\max})^2 & \text{Tr}\{\mathbf{Y}_{kl}^D E^{(k,l)}\} & \text{Tr}\{\bar{\mathbf{Y}}_{kl}^D E^{(k,l)}\} \\ \text{Tr}\{\mathbf{Y}_{kl}^D E^{(k,l)}\} & -1 & 0 \\ \text{Tr}\{\bar{\mathbf{Y}}_{kl}^D E^{(k,l)}\} & 0 & -1 \end{bmatrix}$$

$$\bar{\mathbf{C}}_l := \begin{bmatrix} c_{l1} \text{Tr}\{\mathbf{Y}_l^D W^l\} - \alpha_l + a_l & \sqrt{c_{l2}} \text{Tr}\{\mathbf{Y}_l^D W^l\} + b_l \\ \sqrt{c_{l2}} \text{Tr}\{\mathbf{Y}_l^D W^l\} + b_l & -1 \end{bmatrix}.$$

Moreover, $z^1 \in \mathbb{R}^{2(|\mathcal{N}(1)|+1)}$ is a vector of all zeros except the $(|\mathcal{N}(1)| + 2)$ -th entry is one. If we drop the two rank-one constraints (7.5k) and (7.5l), then problem (7.5a) – (7.5j) becomes a convex SDP relaxation for the decomposed OPF formulation (7.4a) – (7.4g).

Theorem 27. *The relaxation between problems (7.4a) – (7.4g) and (7.5a) – (7.5j) is tight if and only if (7.5a) – (7.5j) has a set of rank-one optimal solutions.*

Proof of Theorem 27. Necessity (\Rightarrow): Let us suppose that $(U^k)^*$ and $[U^{(k,l)}]^*$, for all $k \in \mathcal{N}$ and $(k, l) \in \mathcal{L}$, are optimal solutions to (7.4a) – (7.4g). Then, by definition, we can construct

$$(W^k)^* := (U^k)^* [(U^k)^*]^T \quad \forall k \in \mathcal{N}$$

$$[E^{(k,l)}]^* := [U^{(k,l)}]^* \{[U^{(k,l)}]^*\}^T \quad \forall (k, l) \in \mathcal{L}$$

as a set of rank-one solutions to (7.5a) – (7.5j). Also, this solution set must be optimal because the relaxation is tight between (7.4a) – (7.4g) and (7.5a) – (7.5j).

Sufficiency (\Leftarrow): Conversely, let us suppose that (7.5a) – (7.5j) has a set of rank-one optimal solutions $(W^k)^*$ and $[E^{(k,l)}]^*$, for all $k \in \mathcal{N}$ and $(k, l) \in \mathcal{L}$. We know that the optimal cost of (7.5a) – (7.5j) evaluated with $(W^k)^*$ and $[E^{(k,l)}]^*$ is no more than that of (7.4a) – (7.4g), because (7.5a) – (7.5j) is only a relaxation. Moreover, since $(W^k)^*$ and $[E^{(k,l)}]^*$ are rank-one matrices, from which we can recover $(U^k)^*$ and $[U^{(k,l)}]^*$ as a solution set for (7.4a) – (7.4g). So the optimal cost of (7.4a) – (7.4g) is no more than that of (7.5a) – (7.5j), either. Thus, we conclude that the relaxation between (7.4a) – (7.4g) and (7.5a) – (7.5j) is tight. \square

Corollary 4. *If the decomposed SDP relaxation (7.5a) – (7.5j) has a rank-one optimal solution, then we recover an optimal voltage vector U^* for OPF problem (7.1a) – (7.1f).*

Proof of Corollary 4. This result directly follows from Theorems 27 and 26. \square

7.4 Discussions on the Decomposed SDP Relaxation

This section discusses in details about the decomposed SDP relaxation (7.5a) – (7.5j).

7.4.1 The Problem Size

We prefer to solve OPF problems via the decomposed SDP relaxation (7.5a) – (7.5j) since its problems size grows nicely when the size of the power network n increases.

Let us make a comparison with the SDP relaxation (7.2a) – (7.2h). As we know, the matrix variable W in (7.2a) – (7.2h) is of size $2n \times 2n$. Since W is symmetric, in fact we have totally $(2n + 1)n = 2n^2 + n$ variables there.

Now let us have a look at the decomposed SDP relaxation (7.5a) – (7.5j). Here, we have assigned each bus k a symmetric matrix variable $W^k \in \mathbb{R}^{2(|\mathcal{N}(k)|+1) \times 2(|\mathcal{N}(k)|+1)}$, where we recall that $|\mathcal{N}(k)|$ denotes the number of neighboring buses of bus k , for all $k \in \mathcal{N}$.

Due to the sparsity of power networks, we assume that the average number of neighboring buses over the whole network is given by μ , and usually this average is no more than 4. Thus, for each W^k we have $c := (2\mu + 3)(\mu + 1) = 2\mu^2 + 5\mu + 3 \leq 55$ variables. Summing them up for all $k \in \mathcal{N}$, problem (7.5a) – (7.5j) should have no more than $55n$ variables, which is much less than $2n^2 + n$ when $n \geq 50$.

The decomposed SDP relaxation (7.5a) – (7.5j) not only cuts down the number of variables, but it also reduces the largest size of LMI constraints. In problem (7.2a) – (7.2h) the largest LMI constraint (7.2g) is of a size $2n \times 2n$. In contrast, the size of constraint (7.5g) is no greater than 10×10 on average. We believe that this will be another factor which helps fasten the computation speed for solving OPF problems.

At the expense of reducing the number of variables and the largest size of LMI constraints, the decomposed SDP relaxation (7.5a) – (7.5j) introduces an extra constraint (7.5j), known as the consensus constraint, for each transmission line. Nevertheless, because power networks are sparsely connected, the number of the consensus constraints can be estimated by $\mu n / 2 \leq 2n$. Fortunately, this upper bound also grows linearly as the size of power network expands.

7.4.2 A Distributed Structure

We would also like to point out that the decomposed SDP relaxation (7.5a) – (7.5j) has a distributed structure. Indeed, the objective function (7.5a) is distributable, and, moreover, all the constraints (7.5b) – (7.5i) are completely decoupled for each bus.

As a consequence, we could view (7.5a) – (7.5i) as a collection of decoupled, smaller SDP relaxations, each of which can be assigned to a corresponding bus in the power network. Then, each bus k solves its own SDP relaxation based on those local coefficient matrices \mathbf{Y}_k^D , $\bar{\mathbf{Y}}_k^D$, \mathbf{M}_k^D , \mathbf{Y}_{kl}^D , and $\bar{\mathbf{Y}}_{kl}^D$, and yields one locally optimal solution $(W^k)^*$. Meanwhile, the consensus constraint (7.5j) takes charge of coordinating all the locally optimal solutions over the whole power network, finally reaching a consensus at a global OPF solution.

7.4.3 Rank-One Solutions

It has been shown in Lavaei and Low (2012), Molzahn et al. (2013), and Madani et al. (2015) that when applied to solve large-scale OPF problems, the SDP relaxation (7.2a) – (7.2h) may not provide a rank-one optimal solution. To address this issue, people have figured out several methods to force the optimal solution of problem (7.2a) – (7.2h) to be as close to rank-one as possible.

We have two methods that may improve rank-one solutions for large-scale OPF problems. The first adds a little resistance (10^{-5} PU) to every transformer in the power network, such that the resulting resistive graph of the network becomes strongly connected, see Lavaei and Low (2012) as a reference. The second one, as is proposed by Madani et al. (2015), is using extra penalizations that force problem (7.2a) – (7.2h) to yield rank-one solutions. These penalty terms include the total reactive power and apparent power losses.

Applying these methods respectively to the decomposed SDP relaxation (7.5a) – (7.5j), we find that the latter one works better for large-scale OPF problems. Therefore, in the following simulation section, we will change our previous cost function (7.5a) to be

$$\sum_{l \in \mathcal{G}} \alpha_l + \varepsilon_q \sum_{l \in \mathcal{G}} \text{Tr}\{\bar{\mathbf{Y}}_l^D W^l\} \quad (7.6)$$

and study (7.6) and (7.5b) – (7.5j) as a modified version of our decomposed SDP relaxation.

7.5 Simulations

In this section, we report our simulation results. We solve six OPF test cases over the IEEE benchmark 14, 30, 57, 118, 300, and the Polish 2383WP bus systems, respectively.

System data of these power networks are extracted from the archives of the MATPOWER toolbox. The OPF constraints include the voltage magnitude limits, active and reactive power demands at every bus, as well as apparent power constraints for every transmission lines.

We run all simulations on a computer that has a 2.4 GHz Intel Core i5 CPU and a 4 GB RAM. We employ the MATLAB based CVX toolbox for implementing the decomposed SDP relaxations, and we choose the SDPT3 4.0 as our SDP solver.

In our simulations, we set a threshold 10^{-3} for checking the rank-one condition. In other words, if the second largest eigenvalue of a solution matrix we have obtained is less than 10^{-3} , then we believe that this solution matrix is of rank-one.

Our simulation results are listed in Table 7.3, which shows that the proposed decomposed SDP relaxation can really fasten the computation speed for solving large-scale OPF problems. To illustrate this point, we compare the solution time of our algorithm with the OPF solvers that are proposed by [Molzahn et al. \(2013\)](#) and [Madani et al. \(2015\)](#).

In the both works [Molzahn et al. \(2013\)](#) and [Madani et al. \(2015\)](#), the authors have used computers with Intel i7 quad-core CPU at 3.4 GHz and 16 GB RAM to run their simulations. We need to notice that their computer configurations have a performance about two to three times better than ours. Their solution time are listed, respectively, in Tables 7.1 and 7.2.

Table 7.1 Performance of the OPF solver proposed by [Molzahn et al. \(2013\)](#)

Power Systems	118-Bus	300-Bus	Polish 2383-Bus WP
Solution Time (secs)	2.1	5.7	730

Table 7.2 Performance of the OPF solver proposed by [Madani et al. \(2015\)](#)

Power Systems	30-Bus	57-Bus	118-Bus	300-Bus	Polish 2383-Bus WP
Solution Time (secs)	≤ 5	≤ 5	≤ 5	13.9	529

From the comparisons of Tables 7.1, 7.2, and 7.3, we can see that for small networks which have less than 300 buses the performance of our OPF algorithm is fairly comparable with theirs (taking into account the difference of computer configurations). However, for large networks, taking the Polish 2383-bus WP system for example, our approach is the fastest when compared with both OPF solvers proposed by Molzahn et al. (2013) and Madani et al. (2015).

We also observe that for larger power networks, we need a greater parameter ε_q to keep optimal solutions close to rank-one. Let us take a look at the IEEE 300-bus benchmark system as an example. Although we have already chosen a large $\varepsilon_q = 100$, we still cannot obtain an exact rank-one solution. There are three buses ($k = 97, 99, 245$) whose solution matrices are not rank-one. Nevertheless, we believe that it is close enough to a rank-one solution, because all the second largest eigenvalues associated with those problematic buses are less than 0.1.

7.6 Summary

Different from what we have done in Chapter 5, in this chapter we have proposed another consensus-based decomposed SDP relaxation approach to solve OPF problems.

This new approach also exploits the sparsity structure of the power network. Consequently, the distributed power flow structure enables us to assign each bus in the power network with a decomposed SDP relaxation, and, more importantly, the total problem size scales linearly as the power network expands. Meanwhile, the final OPF solution can be reached by running a consensus over all the buses in the power network. Due to these reasons, our consensus-based decomposed SDP relaxation approach can greatly fasten the computation speed for solving large-scale OPF problems.

Finally, we would like to point out that the decomposed SDP relaxation approach proposed in this chapter is not restrict exclusively to solve OPF problems, but can be also applied to other rank-one SDP relaxations with similar sparse structures.

Table 7.3 Solving IEEE benchmark OPF tests via decomposed SDP relaxations

Test Systems	Optimal Costs	CPU Time (secs)	ε_q	Problematic Buses	The Second Largest Eigenvalues
14-Bus	8081.51	1.24	0	None	Less than 10^{-3}
30-Bus	576.90	1.96	4	None	Less than 10^{-3}
57-Bus	41737.85	3.64	33	None	Less than 10^{-3}
118-Bus	129662.82	7.89	41	None	Less than 10^{-3}
300-Bus	719792.38	23.70	100	97, 99, 245	0.004, 0.072, 0.066
Polish 2383-Bus WP	1875191.44	245.40	5000	35, 183	0.007, 0.007

CHAPTER 8. CONCLUSIONS

This dissertation has proposed a continuous-time optimization dynamics approach to study those non-convex optimizations. The basic idea of this approach is to seek a KKT equilibrium as the dynamical system evolves. We have proved in Chapter 3 that if there exists a strictly complementary KKT point at which the evaluated Hessian of the associated Lagrangian with respect to the primal variable is positive definite, then the optimization dynamics locally has a unique solution which converges asymptotically to the desired KKT point.

As for general optimization problems, we notice that KKT conditions are only necessary for local optimality. Thus, when the optimization dynamics associated with a non-convex problem converges to a KKT equilibrium, we have to further check whether the obtained KKT point is globally optimal or not. So in Chapter 4 we have studied the non-convex QCQPs as a specific class of general optimizations, presenting a necessary and sufficient global optimality condition for those problems. Our result has shown that a KKT point is globally optimal for a non-convex QCQP if and only if it has a positive semi-definite Hessian of the Lagrangian. Moreover, if the associated optimization dynamics has a KKT equilibrium with a positive definite Hessian of the Lagrangian, then, by the convergence analysis developed in Chapter 3, this KKT equilibrium is locally asymptotically stable with respect to the optimization dynamics.

Next we have employed the optimization dynamics to search global solutions for a special class of networked non-convex QCQPs, namely, the OPF problems. We have discovered that the associated optimization dynamics possesses an intrinsic distributed computation structure. Specifically, the optimization dynamics treats each bus in the power network as an intelligent computing agent, which only uses the local information from neighboring buses to update its own decision variables. When compared with the popular SDP dual relaxation approach, the optimization dynamics can find global OPF solutions under more general conditions.

In Chapter 6 we have attempted several methodologies to implement our continuous-time optimization dynamics in a discretized fashion. To maintain the robustness and the distributed structure, we have utilized the backward Euler's method and iterative matrix inversions to write our discrete-time ODE solvers. In simulations, we have successfully applied our ODE solvers to the optimization dynamics associated with large-scale OPF and phase recovery problems. Due to the limitations of discretization, nevertheless, our distributed ODE solvers also require to use the network multiple times at each backward Euler iteration.

We have revisited OPF problems in Chapter 7. Different from Chapter 5, we have proposed a consensus-based, decomposed SDP relaxation approach to solve large-scale OPF problems. This new approach, by fully exploiting the natural sparsity of the power network, decomposes the standard SDP relaxation into a bunch of smaller SDPs. Consequently, the problem size of the decomposed SDP relaxation scales linearly as the power network expands, and it greatly fastens the computation speed for solving large-scale OPF problems.

In future research, we should focus more on investigating the analog implementation of our optimization dynamics, since it will best maintain the distributed computation structure and will be more compatible to real physics. Taking the OPF problem for example, the distributed computation and the suitability for real physics are the exact challenges we need to meet for developing the next-generation smart grids. To achieve an efficient analog implementation, we should further explore the physical meanings of the optimization dynamics, which will help us embed our optimization dynamics into the physical layer of networked systems.

APPENDIX PROOF OF THEOREM 24

Proof of Theorem 24. (Sufficiency \Leftarrow) Suppose that optimization dynamics (5.6a) – (5.6h) has an equilibrium $(U^*, \lambda^*, \gamma^*, \mu^*, \nu^*)$ which satisfies the conditions $\mathbf{B}(U^*, \lambda^*, \gamma^*, \mu^*, \nu^*)U^* = 0$ and $\mathbf{B}(U^*, \lambda^*, \gamma^*, \mu^*, \nu^*) \succeq 0$. Hence, by Theorem 11, $(U^*, \lambda^*, \gamma^*, \mu^*, \nu^*)$ is a saddle-point for the Lagrangian (5.4). Then the optimal cost for OPF problem (5.2a) – (5.2e) is given by

$$\begin{aligned}
p^* &= L(U^*, \lambda^*, \gamma^*, \mu^*, \nu^*) \\
&= \sum_{l \in \mathcal{G}} \left[c_{l2}(P_l^d)^2 - c_{l2}(U^{*T} \mathbf{Y}_l U^*)^2 + c_{l1}P_l^d + c_{l0} \right] \\
&\quad + \sum_{k \in \mathcal{N}} \left[\underline{\lambda}_k^* P_k^{\min} - \bar{\lambda}_k^* P_k^{\max} + \lambda_k^* P_k^d + \underline{\gamma}_k^* Q_k^{\min} - \bar{\gamma}_k^* Q_k^{\max} + \gamma_k^* Q_k^d + \underline{\mu}_k^* (V_k^{\min})^2 - \bar{\mu}_k^* (V_k^{\max})^2 \right] \\
&\quad - \sum_{(k,l) \in \mathcal{L}} \nu_{kl}^* \left[(S_{kl}^{\max})^2 + (U^{*T} \mathbf{Y}_{kl} U^*)^2 + (U^{*T} \bar{\mathbf{Y}}_{kl} U^*)^2 \right]
\end{aligned}$$

where at the first step we have used the complementary slackness, and at the second step we have applied the equality $\mathbf{B}(U^*, \lambda^*, \gamma^*, \mu^*, \nu^*)U^* = 0$. Since OPF problem (5.13a) – (5.13g) is equivalent to (5.2a) – (5.2e), it has the same optimal cost p^* .

Based on this equilibrium $(U^*, \lambda^*, \gamma^*, \mu^*, \nu^*)$, we can construct a solution for the SDP dual relaxation (5.16a) – (5.16c) as follows

$$\begin{aligned}
\underline{\rho}_k^* &= \underline{\lambda}_k^*, \quad \bar{\rho}_k^* = \bar{\lambda}_k^*, \quad \underline{\xi}_k^* = \underline{\gamma}_k^*, \quad \bar{\xi}_k^* = \bar{\gamma}_k^*, \quad \underline{\zeta}_k^* = \underline{\mu}_k^*, \quad \bar{\zeta}_k^* = \bar{\mu}_k^* \\
(h_{kl}^1)^* &= \nu_{kl}^*, \quad (h_{kl}^2)^* = \nu_{kl}^* (U^{*T} \mathbf{Y}_{kl} U^*), \quad (h_{kl}^3)^* = \nu_{kl}^* (U^{*T} \bar{\mathbf{Y}}_{kl} U^*) \\
(h_{kl}^4)^* &= \nu_{kl}^* (U^{*T} \mathbf{Y}_{kl} U^*)^2, \quad (h_{kl}^6)^* = \nu_{kl}^* (U^{*T} \bar{\mathbf{Y}}_{kl} U^*)^2 \\
(h_{kl}^5)^* &= \nu_{kl}^* (U^{*T} \mathbf{Y}_{kl} U^*) (U^{*T} \bar{\mathbf{Y}}_{kl} U^*) \\
(r_l^1)^* &= \sqrt{c_{l2}} (U^{*T} \mathbf{Y}_l U^* + P_l^d), \quad \text{and} \quad (r_l^2)^* = c_{l2} (U^{*T} \mathbf{Y}_l U^* + P_l^d)^2. \tag{A.1}
\end{aligned}$$

We can verify the dual feasibility of solution (A.1). That is, $\mathbf{A}^{\text{opt}} = \mathbf{B}(U^*, \lambda^*, \gamma^*, \mu^*, \nu^*) \succeq 0$,

and

$$\mathbf{H}_{kl}^* = \nu_{kl}^* \begin{bmatrix} 1 & (U^{*T} \mathbf{Y}_{kl} U^*) & (U^{*T} \bar{\mathbf{Y}}_{kl} U^*) \\ (U^{*T} \mathbf{Y}_{kl} U^*) & (U^{*T} \mathbf{Y}_{kl} U^*)^2 & (U^{*T} \mathbf{Y}_{kl} U^*) (U^{*T} \bar{\mathbf{Y}}_{kl} U^*) \\ (U^{*T} \bar{\mathbf{Y}}_{kl} U^*) & (U^{*T} \mathbf{Y}_{kl} U^*) (U^{*T} \bar{\mathbf{Y}}_{kl} U^*) & (U^{*T} \bar{\mathbf{Y}}_{kl} U^*)^2 \end{bmatrix} \succeq 0$$

$$\mathbf{R}_l^* = \begin{bmatrix} 1 & \sqrt{c_{l2}} (U^{*T} \mathbf{Y}_l U^* + P_l^d) \\ \sqrt{c_{l2}} (U^{*T} \mathbf{Y}_l U^* + P_l^d) & c_{l2} (U^{*T} \mathbf{Y}_l U^* + P_l^d)^2 \end{bmatrix} \succeq 0.$$

When substitute solution (A.1) into the SDP dual cost (5.14), we obtain $d^* = p^*$. Therefore, we conclude that strong duality holds between OPF problem (5.13a) – (5.13g) and its SDP dual relaxation (5.16a) – (5.16c).

(Necessity \Rightarrow) Conversely, let us suppose that the SDP dual relaxation (5.16a) – (5.16c) has a zero optimal duality gap with OPF problem (5.13a) – (5.13g). Let (α^*, U^*) denote the optimal primal solution and $(\rho^*, \xi^*, \zeta^*, \mathbf{R}^*, \mathbf{H}^*)$ denote the optimal dual solution, respectively. Then we have $\alpha_l^* \geq c_{l2} (U^{*T} \mathbf{Y}_l U^* + P_l^d)^2 + c_{l1} (U^{*T} \mathbf{Y}_l U^* + P_l^d) + c_{l0}$, $\mathbf{A}^{\text{opt}} \succeq 0$, and $\mathbf{A}^{\text{opt}} U^* = 0$, because Lavaei and Low (2012) has shown that U^* must lie in the null space of \mathbf{A}^{opt} . Furthermore, complementary slackness holds

$$\begin{aligned} \underline{\rho}_k^* (P_k^{\min} - P_k^d - U^{*T} \mathbf{Y}_k U^*) &= 0, & \bar{\rho}_k^* (U^{*T} \mathbf{Y}_k U^* - P_k^{\max} + P_k^d) &= 0, & \forall k \in \mathcal{N} \\ \underline{\xi}_k^* (Q_k^{\min} - Q_k^d - U^{*T} \bar{\mathbf{Y}}_k U^*) &= 0, & \bar{\xi}_k^* (U^{*T} \bar{\mathbf{Y}}_k U^* - Q_k^{\max} + Q_k^d) &= 0, & \forall k \in \mathcal{N} \\ \underline{\zeta}_k^* [(V_k^{\min})^2 - U^{*T} \mathbf{M}_k U^*] &= 0, & \bar{\zeta}_k^* [U^{*T} \mathbf{M}_k U^* - (V_k^{\max})^2] &= 0, & \forall k \in \mathcal{N} \\ \underline{\rho}_k^* \geq 0, & \bar{\rho}_k^* \geq 0, & \underline{\xi}_k^* \geq 0, & \bar{\xi}_k^* \geq 0, & \underline{\zeta}_k^* \geq 0, & \bar{\zeta}_k^* \geq 0, & \forall k \in \mathcal{N} \\ \mathbf{R}_l^* \succeq 0, & \mathbf{tr}\{\mathbf{C}_l(\alpha^*, U^*) \mathbf{R}_l^*\} &= 0, & \forall l \in \mathcal{G} \\ \mathbf{H}_{kl}^* \succeq 0, & \mathbf{tr}\{\mathbf{L}_{kl}(U^*) \mathbf{H}_{kl}^*\} &= 0, & \forall (k, l) \in \mathcal{L}. \end{aligned}$$

Firstly, we can choose $\underline{\lambda}_k^* = \underline{\rho}_k^*$, $\bar{\lambda}_k^* = \bar{\rho}_k^*$, $\underline{\gamma}_k^* = \underline{\xi}_k^*$, $\bar{\gamma}_k^* = \bar{\xi}_k^*$, $\underline{\mu}_k^* = \underline{\zeta}_k^*$, and $\bar{\mu}_k^* = \bar{\zeta}_k^*$.

Secondly, we expand the complementary slackness condition $\mathbf{tr}\{\mathbf{C}_l(\alpha^*, U^*) \mathbf{R}_l^*\} = 0$ as

$$c_{l1} (U^{*T} \mathbf{Y}_l U^* + P_l^d) + c_{l0} - \alpha_l^* + 2(r_l^1)^* \sqrt{c_{l2}} (U^{*T} \mathbf{Y}_l U^* + P_l^d) - (r_l^2)^* = 0. \quad (\text{A.2})$$

Due to the primal feasibility of α^* and U^* , we have

$$\alpha_l^* \geq c_{l2} (U^{*T} \mathbf{Y}_l U^* + P_l^d)^2 + c_{l1} (U^{*T} \mathbf{Y}_l U^* + P_l^d) + c_{l0}. \quad (\text{A.3})$$

Substituting inequality (A.3) into (A.2) we get

$$(r_l^2)^* - 2(r_l^1)^* \sqrt{c_{l2}}(U^{*T} \mathbf{Y}_l U^* + P_l^d) + c_{l2}(U^{*T} \mathbf{Y}_l U^* + P_l^d)^2 \leq 0. \quad (\text{A.4})$$

We also note that $(r_l^2)^* \geq [(r_l^1)^*]^2$ because of the dual feasibility condition $\mathbf{R}_l^* \succeq 0$. Replacing the term $(r_l^2)^*$ in inequality (A.4) by a smaller value $[(r_l^1)^*]^2$ yields

$$[(r_l^1)^* - \sqrt{c_{l2}}(U^{*T} \mathbf{Y}_l U^* + P_l^d)]^2 \leq 0. \quad (\text{A.5})$$

Since the left-hand side of inequality (A.5) is expressed as a sum of squares, which is always non-negative, we must have

$$[(r_l^1)^* - \sqrt{c_{l2}}(U^{*T} \mathbf{Y}_l U^* + P_l^d)]^2 = 0. \quad (\text{A.6})$$

Then equality (A.6) finally implies that $(r_l^1)^* = \sqrt{c_{l2}}(U^{*T} \mathbf{Y}_l U^* + P_l^d)$.

Thirdly, we expand another complementary slackness condition $\text{tr}\{\mathbf{L}_{kl}(U^*)\mathbf{H}_{kl}^*\} = 0$ as

$$(h_{kl}^1)^*(S_{kl}^{\max})^2 - 2(h_{kl}^2)^*(U^{*T} \mathbf{Y}_{kl} U^*) - 2(h_{kl}^3)^*(U^{*T} \bar{\mathbf{Y}}_{kl} U^*) + (h_{kl}^4)^* + (h_{kl}^6)^* = 0. \quad (\text{A.7})$$

Multiplying both the left- and right-hand sides of equality (A.7) by $(h_{kl}^1)^*$ yields

$$(h_{kl}^1)^* \left[(h_{kl}^1)^*(S_{kl}^{\max})^2 - 2(h_{kl}^2)^*(U^{*T} \mathbf{Y}_{kl} U^*) - 2(h_{kl}^3)^*(U^{*T} \bar{\mathbf{Y}}_{kl} U^*) + (h_{kl}^4)^* + (h_{kl}^6)^* \right] = 0. \quad (\text{A.8})$$

Similarly, according to both the primal and dual feasibility, we have

$$(U^{*T} \mathbf{Y}_{kl} U^*)^2 + (U^{*T} \bar{\mathbf{Y}}_{kl} U^*)^2 \leq (S_{kl}^{\max})^2 \quad (\text{A.9})$$

$$(h_{kl}^1)^*(h_{kl}^4)^* \geq [(h_{kl}^2)^*]^2 \quad \text{and} \quad (h_{kl}^1)^*(h_{kl}^6)^* \geq [(h_{kl}^3)^*]^2 \quad (\text{A.10})$$

where inequality (A.10) is derived from the positive semi-definiteness constraint $\mathbf{H}_{kl}^* \succeq 0$.

Substituting inequalities (A.9) and (A.10) into (A.8) yields

$$\left[(h_{kl}^1)^*(U^{*T} \mathbf{Y}_{kl} U^*) - (h_{kl}^2)^* \right]^2 + \left[(h_{kl}^1)^*(U^{*T} \bar{\mathbf{Y}}_{kl} U^*) - (h_{kl}^3)^* \right]^2 \leq 0. \quad (\text{A.11})$$

Again, since the left-hand side of inequality (A.11) is a sum of squares, we must have

$$\left[(h_{kl}^1)^*(U^{*T} \mathbf{Y}_{kl} U^*) - (h_{kl}^2)^* \right]^2 = 0 \quad \text{and} \quad \left[(h_{kl}^1)^*(U^{*T} \bar{\mathbf{Y}}_{kl} U^*) - (h_{kl}^3)^* \right]^2 = 0 \quad (\text{A.12})$$

which implies

$$(h_{kl}^2)^* = (h_{kl}^1)^*(U^{*T}\mathbf{Y}_{kl}U^*) \quad \text{and} \quad (h_{kl}^3)^* = (h_{kl}^1)^*(U^{*T}\bar{\mathbf{Y}}_{kl}U^*). \quad (\text{A.13})$$

Using (A.13) we can rewrite inequality (A.10) as

$$(h_{kl}^1)^*(h_{kl}^4)^* \geq \left[(h_{kl}^1)^*(U^{*T}\mathbf{Y}_{kl}U^*) \right]^2 \quad \text{and} \quad (h_{kl}^1)^*(h_{kl}^6)^* \geq \left[(h_{kl}^1)^*(U^{*T}\bar{\mathbf{Y}}_{kl}U^*) \right]^2. \quad (\text{A.14})$$

Substituting both (A.13) and (A.14) into inequality (A.8) yields

$$\left[(h_{kl}^1)^* \right]^2 \left[(U^{*T}\mathbf{Y}_{kl}U^*)^2 + (U^{*T}\bar{\mathbf{Y}}_{kl}U^*)^2 - (S_{kl}^{\max})^2 \right] \geq 0. \quad (\text{A.15})$$

On the other hand, from inequality (A.9) we know

$$\left[(h_{kl}^1)^* \right]^2 \left[(U^{*T}\mathbf{Y}_{kl}U^*)^2 + (U^{*T}\bar{\mathbf{Y}}_{kl}U^*)^2 - (S_{kl}^{\max})^2 \right] \leq 0. \quad (\text{A.16})$$

Due to both inequalities (A.15) and (A.16), we must have

$$\left[(h_{kl}^1)^* \right]^2 \left[(U^{*T}\mathbf{Y}_{kl}U^*)^2 + (U^{*T}\bar{\mathbf{Y}}_{kl}U^*)^2 - (S_{kl}^{\max})^2 \right] = 0 \quad (\text{A.17})$$

which further implies

$$(h_{kl}^1)^* \left[(U^{*T}\mathbf{Y}_{kl}U^*)^2 + (U^{*T}\bar{\mathbf{Y}}_{kl}U^*)^2 - (S_{kl}^{\max})^2 \right] = 0. \quad (\text{A.18})$$

Let $\nu_{kl}^* = (h_{kl}^1)^*$. Substituting $(r_l^1)^* = \sqrt{c_{l2}}(U^{*T}\mathbf{Y}_lU^* + P_l^d)$, $(h_{kl}^2)^* = \nu_{kl}^*(U^{*T}\mathbf{Y}_{kl}U^*)$, and $(h_{kl}^3)^* = \nu_{kl}^*(U^{*T}\bar{\mathbf{Y}}_{kl}U^*)$ into (5.15), we obtain $0 \preceq \mathbf{A}^{\text{opt}} = \mathbf{B}(U^*, \lambda^*, \gamma^*, \mu^*, \nu^*)$. Applying the fact that U^* lies in the null space of \mathbf{A}^{opt} , we have $\mathbf{B}(U^*, \lambda^*, \gamma^*, \mu^*, \nu^*)U^* = \mathbf{A}^{\text{opt}}U^* = 0$. This completes the proof of Theorem 24. \square

BIBLIOGRAPHY

- Abido, M. (2002). Optimal power flow using particle swarm optimization. *International Journal of Electrical Power and Energy Systems*, vol. 24, no. 7, pp. 563-571.
- Alsac, O. *et al.* (1990). Further developments in LP-based optimal power flow. *IEEE Trans. on Power Systems*, vol. 5, no. 3, pp. 697-711.
- Arrow, K. and Hurwicz, L. (1958). Gradient method for concave programming I, Local results. *Studies in linear and nonlinear programming*, Stanford University Press, pp. 117-126.
- Baldick, R. *et al.* (1999). A fast distributed implementation of optimal power flow. *IEEE Trans. on Power Systems*, vol. 14, no. 3, pp. 858-864.
- Bertsekas, D. P. (1982). *Constrained optimization and Lagrange multiplier methods*, Academic Press.
- Bertsekas, D. P. and Tsitsiklis, J. N. (1989). *Parallel and distributed computation: Numerical methods*, Prentice Hall Press.
- Bolognani, S. and Zampieri, S. (2013). A distributed control strategy for reactive power compensation in smart microgrids. *IEEE Trans. on Automatic Control*, vol. 58, no. 11, pp. 2818-2833.
- Boyd, S. *et al.* (2011). Distributed optimization and statistical learning via the alternating direction method of multipliers. *Foundations and Trends in Machine Learning*, vol. 3, no. 1, pp. 1-122.
- Boyd, S. and Vandenberghe, L. (2004). *Convex optimization*, Cambridge University Press.

- Bunk, O. *et al.* (2007). Diffractive imaging for periodic samples: Retrieving one-dimensional concentration profiles across micro-fluidic channels. *Acta Crystallographica Section A: Foundation of Crystallography*, vol. 63, no. 4, pp. 306-314.
- Butcher, J. C. (2008). *Numerical methods for ordinary differential equations*, John Wiley & Sons, Ltd.
- Candès, E. J. *et al.* (2011). PhaseLift: Exact and stable signal recovery from magnitude measurements via convex programming. *arXiv:1109.4499*.
- Candès, E. J. *et al.* (2015). Phase retrieval via Wirtinger flow: Theory and algorithms. *arXiv:1407.1065*.
- Carpentier, J. (1962). Contribution to the economic dispatch problem. *Bulletin Societe Fran-coise Electriciens*, vol. 3, no. 8, pp. 431-477.
- Cavraro, G. *et al.* (2014). A distributed control algorithm for the minimization of the power generation cost in smart micro-grid. *the 53rd IEEE Conference on Decision and Control*, pp. 5642-5647.
- Cherukuri, A. *et al.* (2016). Asymptotic convergence of constrained primal-dual dynamics. *Systems and Control Letters*, vol. 87, pp. 10-15.
- Dall'Anese, E. *et al.* (2013). Distributed optimal power flow for smart microgrids. *IEEE Trans. on Smart Grid*, vol. 4, no. 3, pp. 1464-1475.
- d'Aspremont, A. and Boyd, S. (2003). Relaxations and Randomized Methods for Nonconvex QCQPs. *EE392o Class Notes*, Stanford University.
- Dommel, H. and Tinney, W. (1968). Optimal power flow solutions. *IEEE Trans. on Power Apparatus and Systems*, vol. PAS-87, no. 10, pp. 1866-1876.
- Dörfler, F. *et al.* (2014). Breaking the hierarchy: Distributed control & economic optimality in microgrids, version 2. <http://arxiv.org/abs/1401.1767>.

- Erseghe, T. (2014). Distributed optimal power flow using ADMM. *IEEE Trans. on Power Systems*, vol. 29, no. 5, pp. 2370-2380.
- Feijer, D. and Paganini, F. (2010). Stability of primal-dual gradient dynamics and applications to network optimization. *Automatica*, vol. 46, no. 12, pp. 1974-1981.
- Frank, S. *et al.* (2012). Optimal power flow: A bibliographic survey, I: Formulations and deterministic methods. *Energy Systems*, vol. 3, pp. 221-258.
- Frank, S. *et al.* (2012). Optimal power flow: A bibliographic survey, II: Nondeterministic and hybrid methods. *Energy Systems*, vol. 3, pp. 259-289.
- Grant, M. and Boyd, S. (2013). CVX: Matlab software for disciplined convex programming, version 2.0 beta. <http://cvxr.com/cvx>.
- Griffin, D. and Lim, J. (1984). Signal estimation from modified short-time Fourier transform. *IEEE Trans. on Acoustics, Speech and Signal Processing*, vol. 32, no. 2, pp. 236-243.
- Haddad, W. M. and Chellaboina, V. (2008). *Nonlinear dynamical systems and control: A Lyapunov-based approach*, Princeton University Press.
- Han, F. and Lu, Q. (2008). An improved chaos optimization algorithm and its application in the economic load dispatch problem. *International Journal of Computer Mathematics*, vol. 85, no. 6, pp. 969-982.
- Harrison, R. W. (1993). Phase problem in crystallography. *JOSA A*, vol. 10, no. 5, pp. 1046-1055.
- Hartati, R. and El-Hawary, M. (2001). Optimal active power flow solutions using a modified Hopfield neural network. *Canadian Conference on Electrical and Computer Engineering*, vol. 1, pp. 189-194.
- Horn, R. and Johnson, C. (1987). *Matrix Analysis*, Cambridge University Press.

- Hug-Glanzmann, G. and Andersson, G. (2009). Decentralized optimal power flow control for overlapping areas in power systems. *IEEE Trans. on Power Systems*, vol. 24, no. 1, pp. 327-336.
- Josz, C. *et al.* (2015). Application of the moment-SOS approach to global optimization of the OPF problem. *IEEE Trans. on Power Systems*, vol. 30, no. 1, pp. 463-470.
- Kelly, F. *et al.* (1998). Rate control in communication networks: Shadow prices, proportional fairness and stability. *Journal of the Operational Research Society*, vol. 49, no. 3, pp. 237-252.
- Khalil, H. K. (2002). *Nonlinear systems*, Prentice Hall.
- Lam, A. *et al.* (2012). Distributed Algorithms for optimal power flow problem. *The 51st IEEE Conference on Decision and Control*, pp. 430-437.
- Lasserre, J. B. (2010). *Moments, positive polynomials and their applications*, Imperial College Press.
- Lavaei, J. and Low, S. (2012). Zero duality gap in optimal power flow problem. *IEEE Transactions on Power Systems*, vol. 27, no. 1, pp. 92-107.
- Lesieutre, B. *et al.* (2011). Examining the limits of the application of semidefinite programming to power flow problems. *The 49th Annual Allerton Conference*, pp. 1492-1499.
- Li, F. *et al.* (2010). Smart transmission grid: Vision and framework. *IEEE Trans. on Smart Grid*, no. 99, pp. 168-177.
- Low, S. (2014). Convex relaxation of optimal power flow, Part I: Formulations and equivalence. *IEEE Trans. on Control of Network Systems*, vol. 1, no. 1, pp. 15-27.
- Low, S. (2014). Convex relaxation of optimal power flow, Part II: Exactness. *IEEE Trans. on Control of Network Systems*, vol. 1, no. 2, pp. 177-189.
- Lygeros, J. *et al.* (2003). Dynamical properties of hybrid automata. *IEEE Trans. on Automatic Control*, vol. 48, no. 1, pp. 2-17.

- Ma, X. and Elia, N. (2013). A distributed continuous-time gradient dynamics approach for the active power loss minimizations. *The 51st Annual Allerton Conference*, pp. 100-106.
- Ma, X. and Elia, N. (2014). Existence of strong Lagrange duals to certain optimal power flows. *The 22nd Mediterranean Control Conference*, pp. 640-645.
- Ma, X. and Elia, N. (2014). A sufficient saddle point characterization for the Lagrangian associated with general OPF problems. *The 53rd IEEE Conference on Decision and Control*, pp. 1119-1124.
- Ma, X. and Elia, N. (2015). Convergence analysis for the primal-dual gradient dynamics associated with optimal power flow problems. *The 2015 European Control Conference*, pp. 1261-1266.
- Ma, X. and Elia, N. (2016). Seeking saddle-points for non-convex QCQPs via the distributed optimization dynamics approach. Accepted by *the 22nd International Symposium on Mathematical Theory of Networks and Systems*.
- Ma, X. and Elia, N. (2016). Solving optimal power flows via consensus and decomposed semi-definite programming (SDP) relaxations. Submitted to *the 55th IEEE Conference on Decision and Control*.
- Madani, R. *et al.* (2015). Convex relaxation for optimal power flow problem: Mesh networks. *IEEE Trans. on Power Systems*, vol. 30, no. 1, pp. 199-211.
- Mahdad, B. *et al.* (2010). Dynamic strategy based fast decomposed GA coordinated with FACTS devices to enhance the optimal power flow. *Energy Conversion and Management*, vol. 51, no. 7, pp. 1370-1380.
- Mallada, E. *et al.* (2014). Optimal load-side control for frequency regulation in smart grids. *The 52nd Annual Allerton Conference*, pp. 731-738.
- Marshall, A. W. and Olkin, I. (1979). *Inequalities: Theory of majorization and its applications*, Academic Press.

- Miao, J. *et al.* (2008). Extending x-ray crystallography to allow the imaging of non-crystalline materials, cells, and single protein complexes. *Annu. Rev. Phys. Chem.*, vol. 59, pp. 387-410.
- Molzahn, D. *et al.* (2013). Implementation of a large-scale optimal power flow solver based on semidefinite programming. *IEEE Trans. on Power Systems*, vol. 28, no. 4, pp. 3987-3998.
- Mou, S. *et al.* (2013). A distributed algorithm for solving a linear algebraic equation. *The 51st Annual Allerton Conference*, pp. 267-274.
- Nedić, A. and Ozdaglar, A. (2009). Subgradient methods for saddle-point problems. *Journal of Optimization Theory and Applications*, vol. 142, no. 1, pp. 205-228.
- Netrapalli, P. *et al.* (2015). Phase retrieval using alternating minimization. *IEEE Trans. on Signal Processing*, vol. 63, no. 18, pp. 4814-4826.
- Newman, M. (2010). *Networks: An introduction*, Oxford University Press.
- Nogales, F. *et al.* (2003). A decomposition methodology applied to the multi-area optimal power flow problem. *Annals of Operations Research*, no. 120, pp. 99-116.
- Papachristodoulou, A. *et al.* (2013). Sum of squares optimization toolbox for MATLAB: User's guide. <http://www.cds.caltech.edu/sostools/>.
- Rajkumar, R. *et al.* (2010). Cyber-physical systems: The next computing revolution. *The 47th Design Automation Conference*, pp. 731-736, ACM.
- Shental, O. *et al.* (2008). Gaussian belief propagation solver for systems of linear equations. *the IEEE International Symposium on Information Theory*, pp. 1863-1867.
- Shor, N. Z. (1987). Class of global minimum bounds of polynomial functions. *Cybernetics*, vol. 23, no. 6, pp. 731-734.
- Stewart, G. W. and Sun J. G. (1990). *Matrix Perturbation Theory*, Academic Press.
- Sun, D. *et al.* (1984). Optimal power flow by Newton's approach. *IEEE Trans. on Power Apparatus and Systems*, vol. PAS-103, no. 10, pp. 2864-2880.

- Tinney, W. and Hart, C. (1967). Power flow solution by Newton's method. *IEEE Trans. on Power Apparatus and Systems*, vol. PAS-86, no. 11, pp. 1449-1460.
- Tütüncü, R. H. *et al.* (2003). Solving semidefinite-quadratic-linear programs using SDPT3. *Mathematical Programming*, vol. 95, no. 2, pp. 189–217.
- Uzawa, H. (1958). Gradient method for concave programming II, Global stability in the strictly concave case. *Studies in linear and nonlinear programming*, Stanford University Press, pp. 127-132.
- Vidyasagar, M. (2002). *Nonlinear Systems Analysis*, 2nd Edition, Prentice Hall.
- Waldspurger, I. *et al.* (2013). Phase recovery, MaxCut and complex semidefinite programming. *arXiv:1206.0102*.
- Wang, J. and Elia, N. (2011). A control perspective for centralized and distributed convex optimization. *The 50th IEEE Conference on Decision and Control*, pp. 3800-3805.
- Wang, J. and Elia, N. (2014). Solving systems of linear equations by distributed convex optimization in the presence of stochastic uncertainty. *World Congress*, vol. 19, no. 1, pp. 1210-1215.
- Wang, J. and Elia, N. (2016). Control-oriented parallel and distributed continuous-time convex optimization. Submitted to *Automatica*.
- Wei, H. *et al.* (1998). An interior point nonlinear programming for optimal power flow problems with a novel data structure. *IEEE Trans. on Power Systems*, vol. 13, no. 3, pp. 870-877.
- Wu, Y. *et al.* (1994). A direct nonlinear predictor-corrector primal-dual interior point algorithm for optimal power flows. *IEEE Trans. on Power Systems*, vol. 9, no. 2, pp. 876-883.
- Zhao, C. *et al.* (2014). Design and stability of load-side primary frequency control in power systems. *IEEE Trans. on Automatic Control*, vol. 59, no. 5, pp. 1177-1189.

Zimmerman, R. D. *et al.* (2011). MATPOWER: Steady-state operations, planning and analysis tools for power systems research and education. *IEEE Trans. on Power Systems*, vol. 26, no. 1, pp. 12-19.